arXiv:2611.31024v1 [math.DG] 23 Nov 2026

THE KAO–LAI–OSTING CONJECTURE FOR THE SECOND LAPLACE EIGENVALUE ON RIEMANNIAN TWO-TORI

ALEXANDER PIGAZZINI

Abstract. We prove the $k = 2$ case of the Kao–Lai–Osting conjecture for the area-normalized Laplace spectrum of Riemannian two-tori:

$$\sup_g \lambda_2(T^2, g)\,\mathrm{Area}(T^2, g) = \frac{8\pi^2}{\sqrt{3}} + 8\pi,$$

where the supremum is taken over smooth Riemannian metrics. No smooth metric attains this value. It is approached by a sequence in the equilateral conformal class developing a round spherical bubble, and the equilateral class is the only conformal class whose conformal supremum equals the global one. The upper bound follows from spherical folding and a sharp truncated conformal-area inequality for fundamental embeddings into S^5. Normal-curvature and normal-chord estimates yield high-cap area control, with exact elementary estimates on nested high-centre strips. The proof is partly computer-assisted. Rational polynomial inequalities handle the low-weight cap range and the entire residual high-cap region, the latter through exact Bernstein certificates on rational boxes, which are also checked independently in ball arithmetic. The residual product inequality is established by rigorous upper quadratures, with two independent reproducible certificates, in ball and in interval arithmetic, and exact domain-coverage checks.

Contents

1. Introduction 3
1.1. The second eigenvalue problem on a two-torus 3
1.2. Conformal volume, folding, and the remaining moduli 4
1.3. A truncated single-centre conformal-area principle 4
1.4. Analytic geometry and the finite parameter step 5
1.5. Rigidity and the organization of the argument 6
2. The spectral statement and the proof architecture 6
3. The folding implication 8
4. The fundamental embeddings and a one-parameter reduction 10
4.1. Exact normal curvature 11

Date: 23 November 2026.

2020 *Mathematics Subject Classification.* Primary 58J50; Secondary 35P15, 53C42, 65G20.

Key words and phrases. Kao–Lai–Osting conjecture, Laplace–Beltrami eigenvalues, two-tori, spectral geometry, conformal folding, rigidity.

4.2. A global normal-chord estimate 11
4.3. Area density of high caps 12
5. Scalar majorants for the truncated conformal area 14
6. Analytic bounds for small conformal centers 15
6.1. Uniform small-center theorem 16
7. Analytic control of low-weight conformal caps 20
7.1. Quartic Hermite estimates 20
7.2. Exact integration of the cap kernel 21
7.3. Uniform control of the remaining low-weight caps 22
7.4. The intermediate centres, $17/40 \le s \le 149/200$ 23
7.5. The large intermediate centres, $149/200 \le s \le 19/20$ 24
8. Analytic high-centre estimates for conformal caps 25
8.1. Three nested strips 26
8.2. Proof of the three nested strips 26
Case I: $0 \le e \le \delta^2/3$ 27
Case II: $\delta^2/3 \le e < t_0$ 29
8.3. The outer-weight high-centre strip 30
9. Exact rational control of the residual high caps 33
9.1. Cells, thresholds and weight bounds 34
9.2. Direct cells 35
9.3. Quadratic cells 37
9.4. The finite certificate and the proof of Theorem 9.1 39
10. The certified product inequality and proof of the truncation theorem 40
11. The complementary moduli, with an exact endpoint 42
12. Sharpness, nonattainment, and the unique maximizing class 43
13. Concluding remarks 44
Appendix A. Exact rational positivity certificates 45
A.1. Small-center Bernstein comparisons 45
A.2. Quartic Hermite and moment-envelope identities 46
A.3. The intermediate-centre rational sign 47
A.4. The large-intermediate-centre rational sign 47
Appendix B. The product inequality: upper quadratures and certified bounds 48
B.1. The upper chord rule 48
B.2. An exact angular representation 48
B.3. The verification in ball arithmetic 49
B.4. An independent interval certificate 53
Appendix C. The residual high-cap certificate 54
C.1. Cells, bands and boxes 54
C.2. Verification obligations 55
C.3. Arithmetic and execution 56
C.4. A second verification in ball arithmetic 57
Appendix D. Certificate obligations, arithmetic model, and reproducibility 57

D.1. Finite proof obligations 57
D.2. Completed finite verification records 58
D.3. Validated arithmetic and coverage 58
D.4. Source integrity and execution 59
Appendix E. An exact rational check on product strips 60
E.1. Statement and the higher-order mechanism 60
E.2. Quartic product strips 62
E.3. Higher-order two-cosine bounds 66
Statements and Declarations 69
Conflict of interest 69
Data and code availability 69
Funding 69
Use of AI tools 69
References 69

1. Introduction

1.1. **The second eigenvalue problem on a two-torus.** Let (Σ, g) be a closed Riemannian surface. Throughout, the eigenvalues of the nonnegative Laplace–Beltrami operator are enumerated with their multiplicities as $0 = \lambda_0(g) < \lambda_1(g) \le \lambda_2(g) \le \cdots$. In dimension two the quantities $\lambda_k(g)\operatorname{Area}(\Sigma, g)$ are invariant under homothetic rescaling of the metric. Their optimization is therefore governed by an interaction between conformal geometry, the spectrum of the Laplacian, and the possible loss of compactness of a maximizing sequence. The first positive eigenvalue on the sphere was bounded sharply by Hersch [7]; for two-tori, the sharp first-eigenvalue inequality was obtained by Nadirashvili [19], settling Berger's isoperimetric problem. In both cases, conformal transformations and sphere-valued test maps enter essentially. For the second eigenvalue, Nadirashvili [20] proved $\Lambda_2(S^2) = 16\pi$, which Petrides [23] reproved, and Nadirashvili and Penskoi [21] proved $\Lambda_2(\mathbb{RP}^2) = 20\pi$; Karpukhin [11] determined $\Lambda_k(\mathbb{RP}^2)$ for every k, and on the sphere the values $\Lambda_k(S^2) = 8\pi k$ are known for every k [13]. For higher eigenvalues, concentration of area can create spherical components and the corresponding noncompact sequences need not converge to smooth maximizers. This phenomenon is part of the framework developed for conformally maximal metrics by Petrides [22], Karpukhin–Nadirashvili–Penskoi–Polterovich [12], and Karpukhin–Stern [14]. At the level of the second eigenvalue, conformal concentration already changes the expected extremal metric: adding a round sphere to a first-eigenvalue maximizing torus leads to the candidate value $8\pi^2/\sqrt{3} + 8\pi$.

Kao, Lai and Osting [10] studied Laplace–Beltrami eigenvalue maximization on closed surfaces, including extensive conformal and numerical investigations. Their conjecture for the second positive eigenvalue of a two-torus

reads

$$\Lambda_2(T^2) := \sup_g \lambda_2(T^2, g)\,\mathrm{Area}(T^2, g) = \frac{8\pi^2}{\sqrt{3}} + 8\pi. \tag{1}$$

The supremum is over smooth Riemannian metrics. The expected maximizing sequence lives in the conformal class of the equilateral flat torus and develops one spherical bubble. The equality in (1) is a statement about a supremum, not about attainment by a smooth metric.

1.2. **Conformal volume, folding, and the remaining moduli.** The starting point for the upper bound is conformal volume, introduced by Li and Yau [15] and developed for minimal immersions and conformal area by Montiel and Ros [17]. Bryant's explicit treatment of conformal volume for fundamental two-tori [1] provides an unusually concrete and effective bridge between a conformal class and a sphere-valued test map. It makes available precise estimates as the conformal modulus varies and, in suitable ranges, determines the full single-map conformal volume.

For the second eigenvalue one needs trial functions that are orthogonal to both constants and a first eigenfunction. The folding construction, which goes back to Nadirashvili [20] and to Girouard, Nadirashvili and Polterovich [5], and which was combined with conformal volume on surfaces by Karpukhin and Stern [14], Eddaoudi and Girouard [3] and Kang [9], supplies exactly this orthogonality by distributing a test map between two conformally transformed pieces. Kang established new conformal-class bounds for λ_2 and reduced the unproved part of (1) to a compact portion of the usual fundamental domain for flat tori:

$$0 \le a \le \tfrac{1}{2}, \qquad \sqrt{1-a^2} \le b \le \tfrac{44}{25}, \tag{2}$$

where $a + ib$ parametrizes the lattice. This reduction is one of the reasons that a rigorous finite verification is feasible: the remaining conformal classes form an explicitly bounded parameter region. The conformal-volume method alone is not sharp enough on that region; a further estimate is required that tracks the two folded pieces without paying twice for their entire conformal areas.

1.3. **A truncated single-centre conformal-area principle.** Our basic technical quantity is the *truncated conformal area*. Let $F_r : T^2 \to S^5$ be the standard fundamental conformal embedding of the flat torus with weights $r = (r_1, r_2, r_3)$ and induced area $A(r)$. Set

$$A_{\mathrm{eq}} = \frac{4\pi^2}{\sqrt{3}}, \qquad L = A_{\mathrm{eq}} - 4\pi.$$

For $v \in B^6$, write $k_v(F_r)$ for the conformal factor of a Möbius transformation of the target, in the convention defined in Section 2 below. We consider

$$J(r, v) = \int_{T^2} \left(k_v(F_r)^2 - \frac{L}{A(r)} \right)_+ dA_r. \tag{3}$$

The desired one-centre bound is

$$J(r, v) \leq 4\pi. \tag{4}$$

This is stronger than a bound for the total conformal volume, but it is precisely aligned with folding: if two conformal maps are used on complementary pieces, the pointwise inequality

$$\max\{x, y\} \leq c + (x - c)_+ + (y - c)_+$$

with $c = L/A(r)$ bounds their combined energy by $L + 8\pi$. A Rayleigh-quotient argument then yields the right-hand side of (1). The fact that one can treat the two pieces by *separate* truncated energies, without requiring their energies to coincide, is indispensable.

The geometry behind (4) is unexpectedly rigid. The fundamental immersion has an explicit normal-curvature constant, and a global estimate for its normal chords controls the topology of superlevel sets of a height function. Above an explicit threshold these superlevel sets are disks. Flat Gauss–Bonnet then provides a sharp estimate of the distribution of the cap area. Away from these high levels, convexity allows replacement of the three dependent Fourier modes by a two-cosine average. These two estimates are the complementary mechanisms in the proof: a direct product estimate handles the broad middle of the height distribution, while cap geometry controls the concentration near its maximum.

1.4. **Analytic geometry and the finite parameter step.** The conclusion of the paper is the exact value (1), strict inequality for every individual smooth metric, and uniqueness of the equilateral conformal class among those whose conformal supremum attains $\Lambda_2(T^2)$. The theorem follows from geometric estimates, exact polynomial positivity identities and one validated finite inequality on a compact parameter set.

The key inequality is a sharp bound for the truncated conformal area. Three complementary mechanisms establish it. For small conformal centres, Hermite polynomial majorants and Fourier moments give explicit rational comparisons. In the cap regions, the same method is augmented by a monotone geometric cap kernel and exact elementary integration. For low weights and for the entire residual high-weight cap region, all required signs follow from rational Bernstein identities, in the latter case on finitely many explicit rational boxes; that certificate is checked twice, in exact rational arithmetic and, independently, in ball arithmetic. The remaining product region is treated by convex quadrature; its strict inequality is certified on the complete parameter domain, not at sampled points, by two independent programs. The supplement supplies the executable certificates, exact checks of constants and coverage, and the rational positivity checks.

The analytic estimates also cover all centre radii $s \leq 1/4$ or $s \geq 47/50$ and all conformal classes outside the compact moduli region. The proof is computer-assisted: exact rational arithmetic verifies the Bernstein certificates for the small centres, for the low weights and, on 4439 explicit boxes, for the

residual high caps, and validated numerical computation is needed only for the product inequality.

1.5. **Rigidity and the organization of the argument.** Once (4) is known, strictness and the characterization of the maximizing class require separate arguments. The single-centre bound has one equality configuration: the equilateral fundamental torus with zero conformal centre. In the folding construction this configuration cannot saturate the required combined-energy bound. To distinguish the supremum in one *fixed* non-equilateral conformal class, the two-centre quantity must also be controlled when conformal centres tend to the sphere. Such a boundary limit has area at most 4π for a single centre and is strictly separated from the equilateral volume in every other conformal class. Finally, the standard conformal bubbling construction gives the matching lower bound in the equilateral class. Throughout, uniqueness of conformal class is understood modulo diffeomorphisms, not for a fixed marked torus.

Section 2 states the sharp spectral theorem and the truncation principle. The folding argument, the geometry of the fundamental embeddings and the scalar majorants precede the analytic bounds for small centres, low-weight caps and large conformal centres. Section 9 reduces the residual high caps to exact rational positivity on finitely many boxes. The certified product inequality is formulated as a precise lemma in Section 10, where the truncation theorem is completed. The complementary moduli and conformal rigidity are then treated. Appendices A–D supply, respectively, the rational positivity certificates, the product certification, the high-cap certificate and the full reproducibility specification; Appendix E checks the bound $J < 4\pi$ on three substrips of the product domain in exact rational arithmetic, and the product inequality itself on part of them; the proof does not use it.

2. The spectral statement and the proof architecture

We count eigenvalues with multiplicity, beginning with zero:

$$0 = \lambda_0(T^2, g) < \lambda_1(T^2, g) \le \lambda_2(T^2, g) \le \cdots .$$

For a conformal class $\mathcal{C}$, write

$$\Lambda_2(T^2, \mathcal{C}) = \sup_{g \in \mathcal{C}} \lambda_2(T^2, g)\,\mathrm{Area}(T^2, g), \qquad \Lambda_2(T^2) = \sup_{\mathcal{C}} \Lambda_2(T^2, \mathcal{C}).$$

All metrics in these definitions are smooth and positive. Set

$$A_{\mathrm{eq}} = \frac{4\pi^2}{\sqrt{3}}, \qquad L = A_{\mathrm{eq}} - 4\pi, \qquad C_* = 2A_{\mathrm{eq}} + 8\pi.$$

Statements of uniqueness of a conformal class are understood in the moduli space: classes are identified under pullback by diffeomorphisms. No uniqueness of a marked conformal class on a fixed parametrized torus is asserted.

Theorem 2.1. *For every smooth metric g on the torus,*

$$\lambda_2(T^2, g)\,\mathrm{Area}(T^2, g) < C_*.$$

Nevertheless $\Lambda_2(T^2) = C_*$. Moreover,

$$\Lambda_2(T^2, \mathcal{C}) = C_* \quad \Longleftrightarrow \quad \mathcal{C} = [g_{\mathrm{eq}}].$$

The supremum is approached by a sequence of metrics in the equilateral conformal class that develops one round spherical bubble.

The value in Theorem 2.1 is the $k = 2$ case of the Kao–Lai–Osting conjecture [10, 9]. No assertion concerning all higher eigenvalues is made here. Kang [9] reduces the unresolved moduli to

$$\mathcal{K} = \{0 \le a \le 1/2, \quad \sqrt{1-a^2} \le b \le 44/25\}. \tag{5}$$

We also give an explicit rational-endpoint proof for the complementary moduli in Section 11, so the boundary $44/25$ does not depend on rounding a numerical plot.

The proof uses the standard fundamental conformal embedding F_r into S^5, described below. Its area is $A(r)$. For $v \in B^6$ define

$$k_v(y) = \frac{1-|v|^2}{1+|v|^2+2v\cdot y}, \qquad J(r,v) = \int_{T^2}\left(k_v(F_r)^2 - \frac{L}{A(r)}\right)_+ dA_r.$$

Here $x_+ = \max\{x, 0\}$. Orthogonal transformations of the target do not change the area formula; every conformal transformation of S^5 has an area factor of this form after such a transformation.

Theorem 2.2 (Truncated conformal area)**.** *For every fundamental embedding with modulus in $\mathcal{K}$ and every $v \in B^6$,*

$$J(r, v) \le 4\pi. \tag{6}$$

Equality occurs precisely when $r_1 = r_2 = r_3 = 1/3$ and $v = 0$.

The estimate treats every target direction and all conformal densities on the source torus. Its proof is partitioned into the following exhaustive parameter domains, where $R = r_1$, $s = |v|$, $R_* = 1936/2561$, and $\sigma(R) = (2 + 52R - 32R^2)/25$.

Weight range	Center range	Proof component
$1/3 \le R \le R_*$	$0 \le s \le 1/4$	Analytic (Theorem 6.2)
$1/3 \le R \le 7/20$	$1/4 \le s \le 19/20$	Analytic (Theorem 7.6)
$7/20 \le R \le R_*$	$1/4 \le s \le \sigma(R)$	Certified product inequality (Lemma 10.1)
$7/20 \le R \le R_*$	$\sigma(R) \le s < 1$	Exact rational certificate and nested strips (Theorem 9.1)
$1/3 \le R \le R_*$	$47/50 \le s < 1$	Analytic (Section 8)

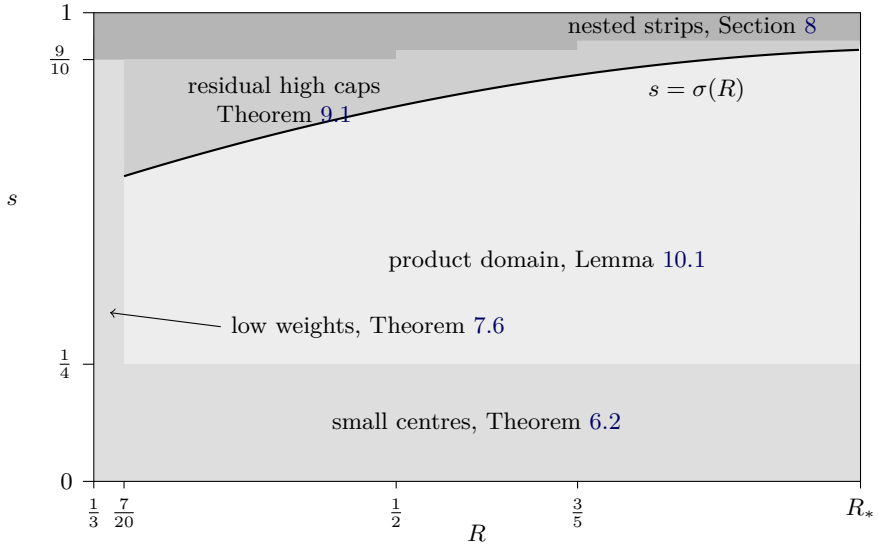

FIGURE 1. The parameter domains of the proof of Theorem 2.2 in the (R, s)-rectangle. The product domain is bounded above by $s = \sigma(R)$; the residual high caps lie between $\sigma(R)$ and $s_{\mathrm{top}}(R)$, the lower edge of the nested strips.

Figure 1 shows these domains. The low-weight bound is established in Section 7, and the nested high-centre estimates in Section 8. Theorem 9.1 covers the residual high caps by an exact rational certificate, which is also verified independently in ball arithmetic. Lemma 10.1 covers the product domain; it is established by two independent certificates, which also cover a slightly larger range of centre radii. The finite verifications bound closed parameter boxes, and their complete verification records appear in Appendix D. Appendix E proves $J < 4\pi$ on three substrips of the product domain in exact rational arithmetic, and the bound of Lemma 10.1 itself on part of them; this independent check is not used in the proof.

3. The folding implication

For a closed spherical cap $C \subset S^n$ let ι_C be the conformal reflection of S^n across the sphere ∂C, and let Fold_C be the map equal to the identity on C and to ι_C on $S^n \setminus C$. The reflection ι_C reverses orientation. A conformal automorphism M of S^n maps closed caps to closed caps and satisfies $M \circ \iota_{M^{-1}(C)} = \iota_C \circ M$; hence

$$\mathrm{Fold}_C \circ M = M \circ \mathrm{Fold}_{M^{-1}(C)},$$

so folding and composition with a conformal automorphism may be performed in either order.

Lemma 3.1 (Conformal folding)**.** *Let $F : T^2 \to S^n$ be a smooth embedding, let g be a smooth metric, and fix a first eigenfunction u_1 of g. There is a conformal automorphism M of S^n such that either $G = M \circ F$, or $G = M \circ \mathrm{Fold}_C \circ F$ for a closed spherical cap C, is a map in $H^1(T^2, S^n)$ whose coordinate functions are orthogonal in $L^2(g)$ to both 1 and u_1. In the second case G agrees with $M \circ F$ on $F^{-1}(C)$ and with $(M \circ \iota_C) \circ F$ on its complement.*

This is the folding lemma of Eddaoudi and Girouard [3, Lemma 2.8], in the form stated and proved in the published paper of Kang [9, Lemma 2.2]. The method goes back to Nadirashvili [20] and to Girouard, Nadirashvili and Polterovich [5]; see also [23]. The same two-piece construction, a conformal dilation composed with a map that is the identity on a cap and a conformal reflection on its complement, gives the bound $\Lambda_2(\Sigma, [g]) \le 4V_c(\Sigma, [g])$ of Karpukhin and Stern [14, Proposition 1.20]. One first conformally balances the push-forward of dA_g. If its correlation with u_1 already vanishes, the first alternative applies. Otherwise one folds across a spherical cap, balances again, and a degree argument over the family of caps yields a cap for which the folded map is orthogonal to u_1. On each piece, the resulting map is a composition of globally defined conformal maps; on the complement of $F^{-1}(C)$ the conformal map applied to F is $M \circ \iota_C$, which reverses orientation when M preserves it. Like every conformal transformation of S^n, it is a conformal dilation followed by an orthogonal transformation, so its area factor is again of the form k_w; this is what (7) uses. We use the lemma's orthogonality conclusion, together with the two separate energy integrals; equality of these integrals is neither assumed nor needed.

Suppose now that F is conformal and write dA_F for its induced area element. The conformal invariance of two-dimensional Dirichlet energy gives

$$\mathcal{E}(M_v \circ F) := \frac{1}{2}\int |d(M_v \circ F)|_g^2 dA_g = \int k_v(F)^2 \, dA_F.$$

For a folded map with pieces D and D^c,

$$\begin{aligned} \mathcal{E}(G) &= \int_D k_v(F)^2 \, dA_F + \int_{D^c} k_w(F)^2 \, dA_F \\ &\le \int \max\{k_v(F)^2, k_w(F)^2\} \, dA_F. \end{aligned} \tag{7}$$

The elementary inequality

$$\max\{x, y\} \le c + (x - c)_+ + (y - c)_+$$

therefore combines with Theorem 2.2 to yield

$$\mathcal{E}(G) \le L + 8\pi = A_{\mathrm{eq}} + 4\pi. \tag{8}$$

If either center has strict inequality in (6), this bound is strict. The only remaining possibility is the equilateral embedding with both centers zero, in which case $\mathcal{E}(G) = A_{\mathrm{eq}}$ and strictness again holds. The single-map case follows by using two identical centers.

Writing $G = (G_1, \dots, G_{n+1})$, the Rayleigh principle gives

$$\lambda_2(g) \int G_i^2 \, dA_g \le \int |dG_i|_g^2 \, dA_g.$$

Summing and using $\sum G_i^2 = 1$ proves

$$\lambda_2(g)\,\mathrm{Area}(g) \le 2\mathcal{E}(G) < 2A_{\mathrm{eq}} + 8\pi = C_* \tag{9}$$

for all moduli in $\mathcal{K}$. Orthogonality to one chosen first eigenfunction is sufficient even when λ_1 is multiple, because the eigenvalues are ordered with multiplicity.

4. The fundamental embeddings and a one-parameter reduction

Let $0 \le a \le \frac{1}{2}$ and $b \ge \sqrt{1-a^2}$. Put

$$d = a(1-a), \qquad D = 1 + b^2 - d, \qquad r_1 = \frac{D-1}{D}, \quad r_2 = \frac{1-a}{D}, \quad r_3 = \frac{a}{D}.$$

The weights satisfy $r_1 \ge r_2 \ge r_3 \ge 0$ and $\sum r_i = 1$. The standard fundamental immersion [1], up to conjugation of one complex coordinate, is

$$F_r(\theta_1, \theta_2) = \big(\sqrt{r_1} e^{i\theta_1}, \sqrt{r_2} e^{i\theta_2}, \sqrt{r_3} e^{-i(\theta_1+\theta_2)}\big) \in S^5.$$

To identify the source modulus, take $\theta_1 = 2\pi y/b$ and $\theta_2 = 2\pi(x - ay/b)$ on $\mathbb{R}^2/\langle (1,0), (a,b)\rangle$. The induced metric is $(4\pi^2/D)(dx^2 + dy^2)$, so this is a homothetic conformal embedding of the torus of modulus $a + ib$. Its induced metric is flat, and its area is

$$A(r) = 4\pi^2 \sqrt{r_1 r_2 + r_1 r_3 + r_2 r_3} = \frac{4\pi^2 b}{D}.$$

These statements continue to hold when $r_3 = 0$: the image is then an embedded product torus in an equatorial S^3.

Write $R = r_1$. For fixed R, the elementary inequality $r_2 r_3 \le (1-R)^2/4$ gives

$$A(r) \le \overline{A}(R) := 2\pi^2 \sqrt{(1-R)(1+3R)} \le A_{\mathrm{eq}}. \tag{10}$$

On the residual moduli region $b \le 44/25$ we have

$$\frac{1}{3} \le R \le R_* := \frac{1936}{2561}. \tag{11}$$

Indeed $D \le 1 + b^2$ and $R = 1 - D^{-1}$. Equality in the upper bound is attained at $a = 0$, $b = 44/25$.

For a unit ambient vector p, set $q = p \cdot F_r$. Fourier orthogonality and the constant induced area element imply

$$\int q \, dA = 0, \qquad \frac{1}{A(r)} \int q^2 \, dA = \frac{1}{2} \sum_{i=1}^{3} r_i |p_i|^2 \le \frac{R}{2}, \tag{12}$$

where p_i are the three complex coordinate components of p.

4.1. **Exact normal curvature.**

Lemma 4.1. *If* II *denotes the spherical second fundamental form of* F_r*, then*

$$\kappa_r := \max_{|X|=1} |\mathrm{II}(X,X)| = \sqrt{D-1} = \sqrt{\frac{R}{1-R}}.$$

Proof. In the flat physical coordinates of the torus, the three directional frequencies for an induced-unit tangent vector making angle ϑ are

$$\ell_1 = \sqrt{D}\,\frac{\sin\vartheta}{b},$$
$$\ell_2 = \sqrt{D}\left(\cos\vartheta - \frac{a\sin\vartheta}{b}\right), \quad \ell_3 = \sqrt{D}\left(\cos\vartheta + \frac{(1-a)\sin\vartheta}{b}\right).$$

Their weighted second moment is one. Direct differentiation therefore gives $|\mathrm{II}(X,X)|^2 = \sum r_i \ell_i^4 - 1$. Writing $c = \cos\vartheta$, $s = \sin\vartheta$, expansion yields

$$\sum r_i \ell_i^4 = D\left[c^4 + \frac{6d}{b^2}c^2s^2 + \frac{4d(1-2a)}{b^3}cs^3 + \frac{b^2-3d^2}{b^4}s^4\right].$$

Subtracting the bracket from $(c^2+s^2)^2$ gives

$$s^2(A_0c^2 - B_0cs + C_0s^2),$$
$$A_0 = 2 - \frac{6d}{b^2}, \qquad B_0 = \frac{4d(1-2a)}{b^3}, \qquad C_0 = 1 - \frac{1}{b^2} + \frac{3d^2}{b^4}.$$

Put $u = b^2 - (1-a^2) \geq 0$. Then $A_0 \geq 0$, since $b^2 - 3d = u + (1-a)(1-2a)$. The numerator of C_0 equals $2a^2(1-a)(1-2a)$ at $u = 0$ and increases with $b^2 \geq 3/4$. Finally,

$$\frac{b^6}{2}\left(A_0C_0 - \frac{B_0^2}{4}\right) = u(u+1-2a)(u+1-a) \geq 0.$$

The quadratic form is nonnegative, proving $\sum r_i\ell_i^4 \leq D$. Equality holds for $\sin\vartheta = 0$. □

4.2. **A global normal-chord estimate.**

Lemma 4.2. *For any two points* F_0, F *of the image,*

$$|\operatorname{proj}_{N_{F_0}} F| \leq \kappa_r(1 - F_0 \cdot F),$$

where N_{F_0} *is the normal space in the sphere. The spherical normal injectivity radius is at least* $\arctan(1/\kappa_r)$*.*

Proof. By homogeneity take $F_0 = F_r(0)$. Initially suppose all weights are positive. Write $\theta_1 + \theta_2 + \theta_3 = 0$ and set

$$x_i = 1 - \cos\theta_i, \quad z = \sum r_i x_i = 1 - F_0 \cdot F, \quad P = \sum \sin\theta_i, \quad S = \sum r_i^{-1}.$$

The trigonometric identities

$$P^2 = (x_1+x_2+x_3)^2 - 2\sum x_i^2 = 2x_1x_2x_3$$

hold because $\theta_1+\theta_2+\theta_3=0$. Identify $\mathbb{C}^3$ with $\mathbb{R}^6$. At $F_0=(\sqrt{r_1},\sqrt{r_2},\sqrt{r_3})$ the tangent vectors are $i(\sqrt{r_j}\,a_j)_j$ with $\sum a_j=0$, so the spherical normal space is

$$N_{F_0}=\Big\{(\xi_j+i\lambda r_j^{-1/2})_j:\ \sum_j \sqrt{r_j}\,\xi_j=0,\ \lambda\in\mathbb{R}\Big\}.$$

The real part $(\sqrt{r_j}\cos\theta_j)_j$ of F projects to $(\sqrt{r_j}(z-x_j))_j$, whose squared length is $\sum r_jx_j^2-z^2$. The imaginary part $(\sqrt{r_j}\sin\theta_j)_j$ projects onto the unit vector $S^{-1/2}(r_j^{-1/2})_j$ with coefficient $P/\sqrt{S}$. Hence

$$|\operatorname{proj}_{N_{F_0}}F|^2=\sum r_ix_i^2-z^2+\frac{P^2}{S}=x^{\mathsf T}M_rx-z^2,$$
$$M_r=\operatorname{diag}(r_i-2/S)+S^{-1}\mathbf{1}\mathbf{1}^{\mathsf T}.$$

The matrix M_r is positive definite. Its scaled matrix SM_r has positive diagonal entries; its principal two-by-two minors are $Sr_ir_j/r_k>0$, and its determinant is 4.

The set

$$\{x:\ r\cdot x=1,\ (\sum x_i)^2\ge 2\sum x_i^2,\ \sum x_i\ge 0\}$$

is a compact elliptical disk, a section of a Lorentz cone. This forward cone is contained in the nonnegative octant. The convex function $x\mapsto x^{\mathsf T}M_rx$ attains its maximum on this compact convex set at an extreme point, hence on the boundary $(\sum x_i)^2=2\sum x_i^2$. This boundary equation is equivalent to $4x_1x_2=(x_3-x_1-x_2)^2$. For a nonnegative solution put $t_1=\sqrt{x_1}$, $t_2=\pm\sqrt{x_2}$ with the sign of $x_3-x_1-x_2$, and $t_3=-t_1-t_2$; then $x_i=t_i^2$, $\sum t_i=0$ and $\sum r_it_i^2=1$, so that $X=i(\sqrt{r_j}\,t_j)_j$ is a unit tangent vector at F_0. On the boundary the last two terms of $x^{\mathsf T}M_rx$ cancel, and the normal-chord quotient is

$$\sum r_it_i^4-1=|\mathrm{II}(X,X)|^2\le\kappa_r^2.$$

Homogeneity in x proves the asserted inequality. The case $r_3=0$ follows by continuity; the limiting torus is still embedded.

For a unit spherical normal n at F_0, put $p=\cos\eta\,F_0+\sin\eta\,n$. The estimate just proved gives

$$p\cdot F\le\cos\eta-(\cos\eta-\kappa_r\sin\eta)(1-F_0\cdot F).$$

If $\eta<\arctan(1/\kappa_r)$, F_0 is the unique maximizer of this height function. This proves the normal injectivity assertion, including uniqueness of the nearest point. □

4.3. **Area density of high caps.**

Lemma 4.3. *Let $q=p\cdot F_r$ and $m=\max q$. If $\sqrt{R}<t<m$, the superlevel $\{q>t\}$ is a disk and its area density satisfies*

$$-\frac{d}{dt}\operatorname{Area}\{q>t\}\le\frac{2\pi(1-R)}{t-Rm-\sqrt{R(1-R)(1-m^2)}}. \tag{13}$$

Proof. We use the flat induced metric g of F_r, with its gradient ∇ and Hessian Hess, the normal connection $\nabla^\perp$ of the normal bundle of F_r in S^5, and we write $\kappa = \kappa_r$. At each point decompose the fixed vector

$$p = q\,F_r + \nabla q + n,$$

where n is normal to F_r in S^5. Differentiating along a tangent vector X and separating tangential and normal components gives

$$\operatorname{Hess} q(X,Y) = -q\langle X,Y\rangle + \langle \mathrm{II}(X,Y), n\rangle, \qquad \nabla^\perp_X n = -\mathrm{II}(X,\nabla q). \tag{14}$$

For a unit normal ν the symmetric form $\langle \mathrm{II}(\cdot,\cdot),\nu\rangle$ satisfies $|\langle \mathrm{II}(X,X),\nu\rangle| \le \kappa|X|^2$, so its eigenvalues lie in $[-\kappa,\kappa]$; hence $|\mathrm{II}(X,Y)| \le \kappa|X||Y|$.

Critical points and topology. Since $|n|^2 = 1 - q^2 - |\nabla q|^2 \le 1 - q^2$, (14) gives

$$-\operatorname{Hess} q \ge (q - \kappa\sqrt{1-q^2})g,$$

and $q-\kappa\sqrt{1-q^2} > 0$ exactly when $q^2 > \kappa^2/(1+\kappa^2) = R$. Thus every critical point of q in $\{q > \sqrt{R}\}$ is a nondegenerate local maximum. At such a point x_0 one has $p = q\,F_r(x_0) + n$, that is, $p = \cos\eta\,F_r(x_0) + \sin\eta\,\nu$ with a unit normal ν and $\cos\eta = q > \sqrt{R}$, so that $\eta < \arctan(1/\kappa)$; by Lemma 4.2, x_0 is the unique global maximum point. Hence, for $\sqrt{R} < t < m$, the only critical point of q in $\{q \ge t\}$ is the maximum point x_m, and every value in $[t,m)$ is regular. Near x_m the superlevel sets are small disks by the Morse lemma, and the flow of $\nabla q/|\nabla q|^2$ carries each level set $\{q = t'\}$ diffeomorphically onto $\{q = t''\}$ for $t \le t' < t'' < m$. Therefore $D_t = \{q \ge t\}$ is a closed disk with smooth boundary $\Gamma_t = \{q = t\}$, and $\{q > t\}$ is its interior.

The normal component. Let $x \in \Gamma_t$ and let γ be the integral curve of $\nabla q/|\nabla q|^2$ through x. Along γ the function q increases with unit speed, and γ tends to x_m as $q \to m$, because D_t contains no other critical point. By (14) the function $|n|$ is Lipschitz along γ, with

$$\Big|\frac{d|n|}{dq}\Big| \le |\nabla^\perp_{\gamma'} n| = |\mathrm{II}(\gamma', \nabla q)| \le \kappa|\gamma'||\nabla q| = \kappa,$$

and $|n| = \sqrt{1-m^2}$ at x_m, where $\nabla q = 0$. Integration from $q = t$ to $q = m$ gives $|n| \le \sqrt{1-m^2} + \kappa(m-t)$ at x.

Curvature of the level curves. Inserting this bound into (14), we obtain on Γ_t

$$-\operatorname{Hess} q \ge \beta(t)\,g, \qquad \beta(t) = (1+\kappa^2)t - \kappa^2 m - \kappa\sqrt{1-m^2}.$$

The function $\mu \mapsto \kappa^2\mu + \kappa\sqrt{1-\mu^2}$ is decreasing for $\mu > \sqrt{R}$, so its value at m is at most its value at t, and $\beta(t) \ge t - \kappa\sqrt{1-t^2} > 0$. Let T be a unit tangent vector of Γ_t and $\nu = \nabla q/|\nabla q|$ the normal pointing into D_t. Differentiating $\langle \nabla q, T\rangle = 0$ along Γ_t shows that the geodesic curvature of Γ_t with respect to ν is $k_g = -\operatorname{Hess} q(T,T)/|\nabla q| \ge \beta(t)/|\nabla q|$.

Gauss–Bonnet and coarea. The metric g is flat, so the Gauss–Bonnet formula for the disk D_t gives $\int_{\Gamma_t} k_g\,ds = 2\pi$, hence $\int_{\Gamma_t} |\nabla q|^{-1} ds \le 2\pi/\beta(t)$.

All values in $(\sqrt{R}, m)$ are regular, and the coarea formula gives

$$-\frac{d}{dt}\operatorname{Area}\{q > t\} = \int_{\Gamma_t} \frac{ds}{|\nabla q|} \le \frac{2\pi}{\beta(t)}.$$

Finally $1+\kappa^2 = 1/(1-R)$, $\kappa^2/(1+\kappa^2) = R$ and $\kappa/(1+\kappa^2) = \sqrt{R(1-R)}$ turn $2\pi/\beta(t)$ into the right-hand side of (13). □

5. Scalar majorants for the truncated conformal area

Table 1 collects the notation that is used throughout the paper.

Symbol	Meaning
$r = (r_1, r_2, r_3)$, $R = r_1$	weights of the fundamental embedding F_r and the largest weight (Section 4)
R_*	1936/2561, the largest value of R on $\mathcal{K}$
$A(r)$, $\overline{A}(R)$	area of F_r and its envelope $2\pi^2\sqrt{(1-R)(1+3R)} \ge A(r)$
A_{eq}, L	$4\pi^2/\sqrt{3}$ and $A_{\mathrm{eq}} - 4\pi$
$c(r)$, $\bar{c}(R)$	truncation levels $L/A(r) \ge L/\overline{A}(R)$
p, v, s	a unit vector, the conformal centre $v = -sp$, and its radius $s = \lvert v\rvert$
q, m	the height $p \cdot F_r$ and its maximum
$k_s(q)$, $f_{R,s}(q)$	$(1-s^2)/(1+s^2-2sq)$ and $\big(k_s(q)^2 - \bar{c}(R)\big)_+$
κ_r	the normal-curvature constant $\sqrt{R/(1-R)}$ (Lemma 4.1)
$J(r, v) = J(r, s, p)$	the truncated conformal area (3)
$\mathcal{P}(R, s, \alpha)$	the product majorant (Proposition 5.1)
$\sigma(R)$, $s_{\mathrm{top}}(R)$	$(2 + 52R - 32R^2)/25$, the upper edge of the product domain, and the lower edge of the nested high-centre strips (Section 9)
t	$s/(1+s^2)$ in Sections 6 and 7 and in Appendices A and E; elsewhere a local parameter
$\overline{R}$	in Section 9, a rational upper bound for R on a box

Table 1. Principal notation.

All other letters, such as x, z, b, B, D, H, K, M, N, P, Q, V and the Greek letters β, γ, δ, η, ρ, τ, χ, ω, denote auxiliary quantities whose meaning is local to the section or proof in which they are introduced.

Put

$$L = A_{\mathrm{eq}} - 4\pi, \quad c(r) = L/A(r), \quad \bar{c}(R) = L/\overline{A}(R),$$
$$k_s(q) = \frac{1-s^2}{1+s^2-2sq}.$$

For $v = -sp$, the desired single-center estimate is

$$J(r, v) := \int \big(k_s(p \cdot F_r)^2 - c(r)\big)_+ \, dA \le 4\pi.$$

Set $f_{R,s}(q) = (k_s(q)^2 - \bar{c}(R))_+$. This is convex in q. The inequality $c(r) \geq \bar{c}(R)$ permits replacing the integrand by $f_{R,s}$.

Proposition 5.1 (Product majorant)**.** *For every center $v = -sp$,*

$$J(r, v) \leq \sup_{0 \leq \alpha \leq 1} \mathcal{P}(R, s, \alpha),$$

where

$$\mathcal{P}(R, s, \alpha) = \frac{\overline{A}(R)}{4\pi^2} \int_0^{2\pi} \int_0^{2\pi} f_{R,s}(\sqrt{R}\alpha \cos u + \sqrt{1-R}\sqrt{1-\alpha^2} \cos w)\, du\, dw.$$

Proof. Separate the first coordinate contribution, with $\alpha = |p_1|$. For fixed u, the other two terms combine into one cosine in w, whose amplitude is at most

$$\sqrt{r_2}|p_2| + \sqrt{r_3}|p_3| \leq \sqrt{1-R}\sqrt{1-\alpha^2}.$$

For every convex function f, the circular average of $f(x + h\cos w)$ is non-decreasing in $h \geq 0$. This follows by pairing opposite cosine values in its derivative, or directly by convex order. The induced area element is constant. Finally replace its total area by the larger $\overline{A}(R)$. □

Proposition 5.2 (Cap plus quadratic majorant)**.** *Choose $t > \sqrt{R}$, $\xi \in \mathbb{R}$, and $C \geq 0$ such that*

$$f_{R,s}(q) \leq Q(q) := C(q - \xi)^2 \qquad (-1 \leq q \leq t).$$

Then $J(r, v)$ is bounded by

$$\mathcal{U}(R, s, m; t, \xi, C) = \overline{A}(R)C(R/2 + \xi^2) + 2\pi(1-R) \int_t^m \frac{[f_{R,s}(q) - C(q-\xi)^2]_+}{q - Rm - \sqrt{R(1-R)(1-m^2)}}\, dq$$

when $m = \max(p \cdot F_r) > t$. If $m \leq t$, the first term alone is a valid upper bound.

Proof. Integrate Q using (12) and $A(r) \leq \overline{A}(R)$. Its positive excess is supported above t, where Lemma 4.3 applies. □

6. Analytic bounds for small conformal centers

In the notation of Sections 4–5, let $\mathrm{d}\mu = \mathrm{d}A/A(r)$ be normalized area measure, $c(R) = L/\overline{A}(R) = \bar{c}(R)$, $f_s(h) = k_s(h)^2$, and $R_* = 1936/2561$. The analytic theorem of this section covers the complete strip $s \leq 1/4$. Its finite coefficient inequalities are statements over $\mathbb{Q}$, stated explicitly in Appendix A; the proof uses no interval rounding or sampling.

The following bounds are elementary Fourier identities followed by AM–GM; they hold for $1/3 \leq R \leq 2/3$:

$$\mathbb{E}_\mu q = 0, \qquad \mathbb{E}_\mu q^2 \leq R/2, \qquad |\mathbb{E}_\mu q^3| \leq R/4, \qquad \mathbb{E}_\mu q^4 \leq 5R^2/8. \tag{15}$$

Indeed, after absorbing phases write $q = \sum_{i=1}^{3} a_i \cos\theta_i$ with $\theta_3 = -\theta_1 - \theta_2 + \phi$, $a_i \geq 0$, $S = \sum a_i^2 \leq R$. Then

$$\mathbb{E}_\mu q^2 = S/2, \quad \mathbb{E}_\mu q^3 = \tfrac{3}{2} a_1 a_2 a_3 \cos\phi, \quad \mathbb{E}_\mu q^4 = \tfrac{3}{4} S^2 - \tfrac{3}{8} \sum_i a_i^4,$$

and $a_1 a_2 a_3 \leq (S/3)^{3/2}$.

Set $t = s/(1+s^2) \in [0, 1/2)$. Since $(1-s^2)^2 = (1+s^2)^2 - 4s^2$, one has $k_s(h)^2 = (1-4t^2)/(1-2th)^2$; we write

$$f_t(h) = \frac{1-4t^2}{(1-2th)^2},$$

and in the quartic construction below every quantity is regarded as a function of t. Fix $x = -1/5$, $y = 1/4$ and $d = y - x = 9/20$. Define

$$u_2 = \frac{f_t(y) - f_t(x) - f_t'(x) d}{d^2},$$
$$u_3 = \frac{f_t'(y) - f_t'(x) - 2u_2 d}{d^2},$$
$$u_4 = \frac{f_t(1) - f_t(x) - f_t'(x)(1-x) - u_2(1-x)^2 - u_3(1-x)^2(1-y)}{(1-x)^2(1-y)^2}$$

and the degree-four polynomial

$$\begin{aligned} H_t(h) &= f_t(x) + f_t'(x)(h-x) + u_2(h-x)^2 \\ &\quad + u_3(h-x)^2(h-y) + u_4(h-x)^2(h-y)^2 = \sum_{j=0}^{4} h_j(t) h^j. \end{aligned} \tag{16}$$

For $0 < t < 1/2$ the fifth derivative of f_t is positive. Hermite's remainder gives

$$f_t(h) - H_t(h) = \frac{f_t^{(5)}(\xi_h)}{5!}(h-x)^2(h-y)^2(h-1) \leq 0 \qquad (-1 \leq h \leq 1).$$

For $t = 0$ the polynomial is constant 1.

Lemma 6.1 (Moment envelope)**.** *Let $1/3 \leq R \leq 2/3$, and suppose that $h_2(t), h_3(t), h_4(t) \geq 0$. Then*

$$\mathbb{E}_\mu H_t(q) \leq B(R,t) := h_0(t) + \left(\frac{h_2(t)}{2} + \frac{h_3(t)}{4}\right) R + \frac{5}{8} h_4(t) R^2. \tag{17}$$

Proof. The linear term vanishes because $\mathbb{E}_\mu q = 0$. The moment bounds (15) and the signs of h_2, h_3, h_4 bound the remaining three terms. □

6.1. **Uniform small-center theorem.**

Theorem 6.2 (Uniform analytic small-center bound)**.** *For all homogeneous fundamental tori with $1/3 \leq R \leq R_*$, all unit directions p and all $0 \leq s \leq 1/4$, one has*

$$\boxed{J(r,s,p) \leq 4\pi.}$$

For $0 \le t \le 4/17$, that is, for $0 \le s \le 1/4$, the Hermite interpolant H_t of (16) is globally bounded below by $1/2$ on $[-1,1]$ and satisfies $h_2, h_3, h_4 \ge 0$. This is established by the exact six-rectangle Bernstein certificates in Appendix A; hence Lemma 6.1 applies to these values of t.

Lemma 6.3 (Small-center rational comparisons)**.** *For $0 \le t \le 4/17$ the following hold.*

(1) If $1/3 \le R \le 5/8$, then

$$B(R,t) \le 1 + \frac{9}{8}(R - 1/3)^2. \tag{18}$$

(2) If $5/8 \le R \le 2/3$ and

$$U(R) = \frac{649}{625} - \frac{21}{25}\left(R - \frac{5}{8}\right),$$

then

$$U(R)\left(B(R,t) - \frac{49}{100}\right) \le \frac{7}{11}. \tag{19}$$

Proof. Both inequalities are exact rational positivity statements: after multiplication by the positive common denominator $D(t) = (2-t)^3(1-2t)(5+2t)^3$ of the coefficients $h_j(t)$ (each $D(t)h_j(t)$ is a polynomial of degree at most 7), their residuals are respectively

$$P_A = D(t)\left[1 + \frac{9}{8}(R - 1/3)^2 - B(R,t)\right],$$
$$P_B = D(t)\left[\frac{7}{11} - U(R)(B(R,t) - 49/100)\right].$$

On the rectangle in (1), P_A is a polynomial of bidegree $(7,2)$; all 24 Bernstein coefficients are nonnegative, four being zero and all other coefficients greater than $1/2$. On the rectangle in (2), P_B is of bidegree $(7,3)$; all 32 coefficients are greater than $1/3$. These coefficients follow from the rational formula and the domain substitutions of Table 3; they are computed in exact rational arithmetic by the supplementary program `small_centre_certificates.py`, and no sampling or roundoff is involved. □

Proof of Theorem 6.2 when $R \le 2/3$. Case I: $1/3 \le R \le 5/8$. We have $c(R) \le c(5/8) < 1/2$. For an elementary strict rational check, use $\sqrt{3} > 265/153$, $\pi < 22/7$ and $\sqrt{69} > 83/10$ to obtain

$$c(5/8) = \frac{8}{\sqrt{69}}\left(\frac{2}{\sqrt{3}} - \frac{2}{\pi}\right) < \frac{80}{83}\left(\frac{306}{265} - \frac{7}{11}\right) = \frac{24176}{48389} < \frac{1}{2}.$$

Since $f_t \le H_t$ and $H_t \ge 1/2 > c(R)$, and since $L/A \ge c(R)$,

$$\left(f_t(q) - \frac{L}{A}\right)_+ \le H_t(q) - c(R).$$

Integrating and invoking Lemma 6.1 gives $J \le \overline{A}(R)B(R,t) - L$. Finally, since

$$\frac{A_{\mathrm{eq}}}{\overline{A}(R)} = \left(1 - \frac{9}{4}(R-1/3)^2\right)^{-1/2} \ge 1 + \frac{9}{8}(R-1/3)^2 \ge B(R,t),$$

we obtain $J \le A_{\mathrm{eq}} - L = 4\pi$.

Case II: $5/8 \le R \le 2/3$. Here $c(R) \ge c(5/8) > 49/100$. Indeed $\sqrt{3} < 26/15$, $\pi > 157/50$ and $\sqrt{69} < 25/3$ imply

$$c(5/8) > \frac{24}{25}\left(\frac{15}{13} - \frac{100}{157}\right) = \frac{5064}{10205} > \frac{49}{100}.$$

Because $H_t \ge 1/2 > 49/100$,

$$\left(f_t(q) - \frac{L}{A}\right)_+ \le H_t(q) - \frac{49}{100}, \quad \text{so} \quad J \le \overline{A}(R)\left(B(R,t) - \frac{49}{100}\right).$$

The positive function $\sqrt{(1-R)(1+3R)}$ is concave. At $R = 5/8$ it is $\sqrt{69}/8 < 649/625$ and has derivative $-7/\sqrt{69} < -21/25$. The second comparison follows from $\sqrt{69} < 25/3$. Thus, by the tangent-line inequality for concave functions,

$$\sqrt{(1-R)(1+3R)} \le U(R) \qquad (5/8 \le R \le 2/3).$$

Lemma 6.3 consequently gives

$$J \le 2\pi^2\, U(R)\left(B(R,t) - \frac{49}{100}\right) \le \frac{14\pi^2}{11} < 4\pi,$$

where the final inequality is precisely $\pi < 22/7$. □

6.1.1. *Quadratic proof for* $2/3 \le R \le R_*$. We use a quadratic Hermite majorant that avoids a larger collection of coefficient inequalities. Let $V = R/2 \in [1/3, R_*/2]$. Denote by $H_{s,V}$ the quadratic Hermite polynomial tangent to f_s at $-V$ and agreeing with f_s at 1. The positivity of f_s''' makes $H_{s,V} \ge f_s$ on $[-1,1]$. Its minimum on the real line can be expressed as

$$\min_{h\in\mathbb{R}} H_{s,V}(h) - \frac{1}{2} = \frac{N(s,V)}{2(1+s^2+2Vs)^3(3s^2+2Vs-4s+3)}, \tag{20}$$

with

$$\begin{aligned} N(s,V) &= 1 + a_7(s+s^7) + a_6(s^2+s^6) + a_5(s^3+s^5) + a_4 s^4 + s^8,\\ a_7 &= 4 - 4V, \quad a_6 = -20 + 8V - 40V^2,\\ a_5 &= 12 - 76V + 48V^2 - 48V^3,\\ a_4 &= -10 + 80V - 112V^2 + 32V^3 - 16V^4. \end{aligned}$$

For $1/6 \le V \le 19/50$ and $0 \le s \le 1/4$, the bounds $a_6 \le -98/5$, $a_5 \le 1$, $a_4 \le 23$, $a_7 \le 4$ imply $N_{ss} < -19$. Furthermore

$$N_V \le -4s + 80s^4 \le -\frac{11}{4}s,$$

because $8 - 80V < 0$, $-76 + 96V - 144V^2 < 0$, and $a_4' \le 80$. Thus N is concave in s and nonincreasing in V, and

$$N(s,V) \ge \min\{1, N(1/4, 19/50)\} = \frac{173885049}{25600000000} > 0. \tag{21}$$

Therefore $H_{s,V} \ge 1/2$.

For $R \ge 2/3$, the threshold obeys

$$c(R) \ge c(2/3) = \frac{2}{\sqrt{3}} - \frac{2}{\pi} > \frac{15}{13} - \frac{20}{31} > \frac{1}{2},$$

using $\sqrt{3} < 26/15$ and $\pi > 31/10$. Hence $J \le A(\int H_{s,V}\,\mathrm{d}\mu - 1/2)$. The positive coefficient of h^2 in $H_{s,V}$ and the moment bound $\int q^2\,\mathrm{d}\mu \le V$ yield

$$\int H_{s,V}\,\mathrm{d}\mu \le F(s,V) := \frac{f_s(-V) + V f_s(1)}{1+V}.$$

An exact simplification gives

$$F(s,V) = 1 + \frac{4s^2 Q(s,V)}{(1-s)^2(1+s^2+2Vs)^2},$$
$$Q(s,V) = (3V-1)(1+s^2) + (4V^2 - 2V + 2)s.$$

For $V \ge 1/3$ all coefficients of Q as a polynomial in s are nonnegative. Moreover

$$\frac{\mathrm{d}}{\mathrm{d}s}\big[(1-s)(1+s^2+2Vs)\big] = 2V - 1 + (2-4V)s - 3s^2 \le -\frac{6}{25} + \frac{1}{6} < 0$$

when $V \le 19/50$ and $s \le 1/4$. Thus $F(s,V)$ increases in $s \in [0, 1/4]$, and

$$F(s, R/2) \le M(R) := F(1/4, R/2) = \frac{450/(17+4R)^2 + 25R/9}{2+R}.$$

A direct differentiation yields

$$M'(R) = \frac{800(4R+35)}{9(4R+17)^3} \le M'(2/3) = \frac{90400}{205379} < \frac{1}{2}.$$

On the other hand

$$\frac{\mathrm{d}}{\mathrm{d}R}\left(\frac{1}{2} + \frac{2}{\pi\sqrt{(1-R)(1+3R)}}\right) = \frac{6R-2}{\pi\big((1-R)(1+3R)\big)^{3/2}} \ge \frac{2}{\pi} > \frac{1}{2} \qquad (R \ge 2/3).$$

The desired comparison therefore reduces to $R = 2/3$, where

$$M(2/3) = \frac{35425}{31329} < \frac{25}{22} < \frac{1}{2} + \frac{2}{\pi}.$$

It follows that

$$J \le \overline{A}(R)(M(R) - 1/2) < 4\pi,$$

proving the final range in Theorem 6.2. The endpoint $s = 0$ follows by continuity, or directly from $J = (A - L)_+ \le 4\pi$.

7. Analytic control of low-weight conformal caps

Let $1/3 \le R \le 7/20$, $s \in [0, 19/20]$, and $q = p \cdot F_r$, with $d\mu = dA_r/A(r)$, and let $c(R) = L/\overline{A}(R)$ as in Section 6. Since $R \le 7/20 < 2/3$, the moment bounds (15) hold.

7.1. **Quartic Hermite estimates.** We use the quartic Hermite interpolant $H_t(h) = \sum_{j=0}^{4} h_j(t)h^j$ of (16), with $t = s/(1+s^2)$, the moment envelope $B(R,t)$ of (17), and the common denominator $D(t) = (2-t)^3(1-2t)(5+2t)^3$ introduced in the proof of Lemma 6.3. For $0 \le t < 1/2$ Hermite's remainder formula gives, as in Section 6,

$$f_t(h) \le H_t(h) \qquad (-1 \le h \le 1). \tag{22}$$

Theorem 7.1. *For every fundamental embedding with $1/3 \le R \le 7/20$, every unit ambient direction p, and every $1/4 \le s \le 17/40$, one has*

$$J(r,s,p) < 4\pi.$$

More precisely, if $1/4 \le s \le 2/5$ then

$$J(r,s,p) \le 4\pi - \frac{3A_{\mathrm{eq}}}{3400}, \tag{23}$$

and if $2/5 \le s \le 17/40$ then

$$J(r,s,p) \le 4\pi - \frac{A_{\mathrm{eq}}}{14000}. \tag{24}$$

Proof. First, $\overline{A}(R)$ is decreasing on $R \ge 1/3$, so $c(R) \le c(7/20)$. Direct simplification gives

$$c(7/20) = \frac{40}{\sqrt{533}}\left(\frac{1}{\sqrt{3}} - \frac{1}{\pi}\right) < \frac{1000}{577}\left(\frac{153}{265} - \frac{7}{22}\right) = \frac{151100}{336391} < \frac{9}{20}.$$

Here one needs only $\sqrt{533} > 577/25$, $\sqrt{3} > 265/153$ and $\pi < 22/7$. The middle strict inequality and final integer comparison are elementary.

We shall use the following exact *rational polynomial inequalities*:

$$H_t(h) + \frac{(1-h)^2}{17} \ge \frac{9}{20}, \qquad B(R,t) \le \frac{93}{100}, \qquad \frac{4}{17} \le t \le \frac{10}{29}, \tag{25}$$

$$H_t(h) + \frac{(1-h)^2}{14} \ge \frac{9}{20}, \qquad B(R,t) \le \frac{229}{250}, \qquad \frac{10}{29} \le t \le \frac{680}{1889}. \tag{26}$$

Both lines hold for $-1 \le h \le 1$ and $1/3 \le R \le 7/20$. Furthermore $h_2, h_3, h_4 \ge 0$ throughout these intervals. The coefficient inequalities are verified exactly in Appendix A.2. No real-parameter sampling or interval floating-point calculation enters these assertions.

Choose $\gamma = 1/17$ in the first strip and $\gamma = 1/14$ in the second. By (22), (25)–(26), and $c(R) < 9/20$, the polynomial

$$Q_t(h) = H_t(h) - c(R) + \gamma(1-h)^2$$

is nonnegative on $[-1,1]$ and bounds $f_t(h) - c(R)$ from above. Consequently,

$$\left(k_s(h)^2 - c(R)\right)_+ \le Q_t(h) \qquad (-1 \le h \le 1).$$

Since $A(r) \le \overline{A}(R)$, the actual truncation level $L/A(r) \ge c(R)$ and hence

$$\begin{aligned} J(r,s,p) &\le A(r)\,\mathbb{E}_\mu Q_t(q) \\ &\le A(r)\left[B(R,t) - c(R) + \gamma\left(1+\frac{R}{2}\right)\right] \\ &\le \overline{A}(R)\left[B(R,t) + \gamma\left(1+\frac{R}{2}\right)\right] - L. \end{aligned}$$

For the second inequality use (15) and $h_2, h_3, h_4 \ge 0$. The bracket in the third inequality is nonnegative, since it bounds the mean of the nonnegative polynomial Q_t.

For $1/4 \le s \le 2/5$, since $R \le 7/20$,

$$B(R,t) + \frac{1}{17}\left(1+\frac{R}{2}\right) \le \frac{93}{100} + \frac{47}{680} = \frac{3397}{3400}.$$

For $2/5 \le s \le 17/40$,

$$B(R,t) + \frac{1}{14}\left(1+\frac{R}{2}\right) \le \frac{229}{250} + \frac{47}{560} = \frac{13999}{14000}.$$

Finally $\overline{A}(R) \le A_{\mathrm{eq}}$ and $L = A_{\mathrm{eq}} - 4\pi$ give (23)–(24), both strictly below 4π. □

7.2. **Exact integration of the cap kernel.** This primitive gives an exact formula for the cap majorant. Let $s > 0$, and let $c > 0$, $C \ge 0$, b and a threshold $T > \sqrt{R}$ be constants; Subsections 7.4–7.5 and Section 9 make specific choices. Put

$$P = 1 - s^2, \qquad B = 1 + s^2, \qquad \psi(q) = \frac{P^2}{(B-2sq)^2} - c - C(q+b)^2.$$

For $T \le m \le 1$ set

$$d = Rm + \sqrt{R(1-R)(1-m^2)}, \qquad D_d = B - 2sd.$$

The underlying cap estimate is $d \le \sqrt{R} < T$, so every denominator is positive. Put

$$A_0 = \frac{P^2}{D_d^2} - c - C(d+b)^2, \qquad E_0 = \frac{2sP^2}{D_d^2}, \qquad F_0 = \frac{2sP^2}{D_d}.$$

Then one has the exact identity

$$\frac{\psi(q)}{q-d} = \frac{A_0}{q-d} + \frac{E_0}{B-2sq} + \frac{F_0}{(B-2sq)^2} - C(q+d+2b).$$

Consequently:

Proposition 7.2. *For $T \le m \le 1$,*

$$\begin{aligned}\int_T^m \frac{\psi(q)}{q-d}\,dq = A_0 \log\frac{m-d}{T-d} + \frac{E_0}{2s}\log\frac{B-2sT}{B-2sm} \\ + \frac{F_0}{2s}\left(\frac{1}{B-2sm} - \frac{1}{B-2sT}\right) \\ - C\left(\frac{m^2-T^2}{2} + (d+2b)(m-T)\right).\end{aligned} \tag{27}$$

Consequently, if $c = \bar{c}(R)$, $f_{R,s} \le C(q+b)^2$ on $[-1,T]$ and $\psi \ge 0$ on $[T,1]$, the bound of Proposition 5.2 with $t = T$ and $\xi = -b$ takes the closed form

$$\frac{J}{4\pi} \le \mathcal{U}(R,s,m) := \frac{\overline{A}(R)}{4\pi} C\left(\frac{R}{2} + b^2\right) + \frac{1-R}{2} \tag{28}$$

the right-hand side of (27). Thus no numerical quadrature is needed to express the cap-bound obligation.

Proof. Integrate the partial fractions termwise; all logarithmic arguments are positive because $d < T \le m$ and $B - 2sq > 0$ for $q \le 1$. The identity is algebraic in d and therefore holds for every constant $d < T$; this is how it is used below with d replaced by the upper bound $\widehat{d}(m)$. □

7.3. **Uniform control of the remaining low-weight caps.** The following rational-algebraic argument covers the full low-weight cap region. Together with Theorems 7.1 and 6.2, this covers every $1/3 \le R \le 7/20$ and $0 \le s \le 19/20$. The two complementary subranges use a common monotonicity principle.

Lemma 7.3 (Monotonicity of the cap kernel)**.** *For $0 < R < 1$, let*

$$d_R(m) = Rm + \sqrt{R(1-R)(1-m^2)}, \qquad m \in [-1,1].$$

Whenever $d_R(m) < q \le m$, one has

$$\frac{\partial}{\partial R}\frac{1-R}{q-d_R(m)} = \frac{m - q + \dfrac{1-R}{2\sqrt{R(1-R)}}\sqrt{1-m^2}}{(q-d_R(m))^2} \ge 0. \tag{29}$$

In particular, for $R \le 7/20$ and $q > \sqrt{7/20}$, the cap density kernel is no larger than that corresponding to $R = 7/20$.

Proof. Differentiate the quotient using

$$\frac{d}{dR}\sqrt{R(1-R)} = \frac{1-2R}{2\sqrt{R(1-R)}}.$$

The numerator simplifies exactly to the numerator of (29). The cap condition $q > d_R(m)$ follows from $q > \sqrt{7/20}$ by Cauchy–Schwarz. □

We will use the fixed rational upper bound

$$\widehat{d}(m) = \frac{7}{20}m + \frac{12}{25}\sqrt{1-m^2} \ge d_{7/20}(m), \qquad \widehat{d}(m) \le \sqrt{\frac{3529}{10000}} < \frac{3}{5}. \tag{30}$$

Indeed $\sqrt{(7/20)(13/20)} = \sqrt{91}/20 < 12/25$. The cap-density estimate of Lemma 4.3, together with Lemma 7.3, now gives the scalar bound

$$\frac{J}{4\pi} \le \frac{A(r)}{4\pi}\,\mathbb{E}_\mu Q(q) + \frac{13}{40}\int_T^m \frac{\psi(q)}{q-\widehat{d}(m)}\,dq \tag{31}$$

whenever $Q \ge 0$ is a quadratic majorant for the nonnegative truncation on $[-1,T]$, and ψ is the nonnegative excess above $T > \sqrt{3529}/100$; by (30), $q - \widehat{d}(m) > 0$ for $T \le q \le m$. An integral with $m \le T$ is omitted.

7.4. **The intermediate centres,** $17/40 \le s \le 149/200$**.** Set, for the rest of this subsection,

$$\tau = \frac{3}{5}, \qquad \beta = \frac{7}{24}, \qquad c_0 = \frac{4}{9},$$
$$P = 1 - s^2, \qquad B = 1 + s^2,$$
$$C(s) = \frac{P^2/(B-2s\tau)^2 - c_0}{(\tau+\beta)^2}.$$

In the stated interval $C(s) > 0$. Put $f_s(q) = (P^2/(B-2sq)^2 - c_0)_+$ and $Q_s(q) = C(s)(q+\beta)^2$. The quotient $f_s(q)/(q+\beta)^2$ is nondecreasing for $q > q_0(s) := (5s^2-1)/(4s)$. Indeed, with $z = B - 2sq$, its derivative has the sign of

$$c_0 z^3 - 2P^2 z + P^2(B + 2s\beta),$$

whose minimum over $z \ge 0$, attained at $z = P\sqrt{2/(3c_0)}$, equals $P^2\big(B+2s\beta - \tfrac{4}{3}\sqrt{2/(3c_0)}\,P\big)$. For $c_0 = 4/9$ the cubic is therefore nonnegative provided

$$B + 2s\beta \ge \frac{2\sqrt{6}}{3}\,P.$$

Since $(49/30)^2 = 2401/900 > 8/3 = (2\sqrt{6}/3)^2$, it suffices that $g(s) = 1 + s^2 + \frac{7}{12}s - \frac{49}{30}(1-s^2) \ge 0$. The function g is increasing for $s \ge 0$, and $g(17/40) = 4331/48000 > 0$. Also $q_0(s) + \beta > 0$ and $q_0(s) < \tau$ throughout this subrange. Therefore $f_s \le Q_s$ on $[-1,\tau]$ and $f_s \ge Q_s$ on $[\tau,1]$. The cap excess there is

$$\psi_s(q) = \frac{P^2}{(B-2sq)^2} - c_0 - C(s)(q+\beta)^2 \ge 0.$$

By the second-moment estimate $\mathbb{E}q = 0$, $\mathbb{E}q^2 \le R/2$,

$$\frac{1}{4\pi}\int Q_s(q)\,dA_r \le \frac{\pi}{\sqrt{3}} C(s)\left(\frac{7}{40} + \beta^2\right) < \frac{363}{200}\frac{749}{2880}C(s).$$

Here $\pi/\sqrt{3} < 363/200$ follows from the classical rational bounds $\pi < 22/7$ and $\sqrt{3} > 265/153$.

For $m \geq \tau$ let $d = \widehat{d}(m)$ and introduce

$$D = B - 2sd, \qquad T = B - 2s\tau, \qquad V = B - 2sm,$$
$$K = P^2/D^2, \qquad A_0 = K - c_0 - C(s)(d+\beta)^2 \leq 0,$$
$$u = \frac{m-\tau}{m+\tau-2d}, \qquad v = \frac{s(m-\tau)}{B - s(m+\tau)}.$$

Thus $0 \leq u, v < 1$. The elementary series $\log \frac{1+h}{1-h} = 2\sum_{k\geq 0} h^{2k+1}/(2k+1)$ implies

(32)
$$\log \frac{m-d}{\tau-d} \geq 2\left(u + \frac{u^3}{3}\right), \qquad \log \frac{B-2s\tau}{B-2sm} \leq 2\left(v + \frac{v^3}{3} + \frac{v^5}{5(1-v^2)}\right).$$

By the primitive (27), Lemma 7.3, and $A_0 \leq 0$, we obtain

$$\frac{J}{4\pi} \leq W_{\mathrm{mid}}(s,y), \qquad m = \frac{1-y^2}{1+y^2}, \quad 0 \leq y \leq \frac{1}{2}, \tag{33}$$

where the following expression is *rational* in s, y:

$$W_{\mathrm{mid}} = \frac{363}{200}\frac{749}{2880}C(s) + \frac{13}{40}\Bigg\{2A_0\left(u + \frac{u^3}{3}\right) + 2K\left(v + \frac{v^3}{3} + \frac{v^5}{5(1-v^2)}\right)$$
$$+ \frac{P^2}{D}\left(\frac{1}{V} - \frac{1}{T}\right) - C(s)\left[\frac{m^2-\tau^2}{2} + (d+2\beta)(m-\tau)\right]\Bigg\}. \tag{34}$$

If $m < \tau$, only the first term is needed, which equals $W_{\mathrm{mid}}(s, 1/2)$ and is controlled by the same inequality.

Lemma 7.4 (Exact rational sign)**.** *For* $17/40 \leq s \leq 149/200$ *and* $0 \leq y \leq 1/2$*,*

$$W_{\mathrm{mid}}(s,y) < 1.$$

Proof. The exact rational positivity certificate, including the denominators and the Bernstein coefficient bounds on rational rectangles, is established in Appendix A.3. □

7.5. **The large intermediate centres,** $149/200 \leq s \leq 19/20$**.** By $c(R) \geq 1 - \sqrt{3}/\pi > 4/9$, the positive truncation is supported where

$$q > q_0(s) = \frac{5s^2-1}{4s}.$$

This threshold increases with s and obeys

$$q_0(s) \geq q_0(149/200) = \frac{14201}{23840} > \frac{\sqrt{3529}}{100} > \sqrt{7/20}.$$

If $m \leq q_0$, then $J = 0$. Otherwise, put $d = \widehat{d}(m)$, $D = B - 2sd$, $V = B - 2sm$, $K = P^2/D^2$,

$$u = \frac{m-q_0}{m+q_0-2d}, \qquad v = \frac{s(m-q_0)}{B - s(m+q_0)}, \qquad A_0 = K - \frac{4}{9} < 0.$$

Again $0 \le u, v < 1$. Since $B - 2sq_0 = 3P/2$, direct integration of the cap density, the bound $\log((1+u)/(1-u)) \ge 2u$, and the upper estimate in (32) with τ replaced by q_0, give

$$\begin{aligned} \frac{J}{4\pi} &\le W_{\mathrm{end}}(s,m) \\ &:= \frac{13}{40}\Bigg\{2A_0u + 2K\left(v + \frac{v^3}{3} + \frac{v^5}{5(1-v^2)}\right) \\ &\qquad + \frac{P^2}{D}\left(\frac{1}{V} - \frac{2}{3P}\right)\Bigg\}. \end{aligned} \tag{35}$$

Set $x = \sqrt{1-s}$ and $y = \sqrt{(1-m)/(1+m)} = xz$. Then $m = (1 - x^2z^2)/(1+x^2z^2)$ and $\sqrt{1-m^2} = 2xz/(1+x^2z^2)$. The inequality $5s^2 - s - 2 \ge 0$ for $s \ge 149/200$ implies $0 \le y \le \sqrt{1-s} = x$. Hence the actual parameter domain is contained in the rational rectangle

$$\frac{1}{5} \le x \le \frac{101}{200}, \qquad 0 \le z \le 1.$$

Here $1/5 < \sqrt{1/20}$ and $(101/200)^2 > 1 - 149/200$. After substitution, W_{end} is a rational function of x, z.

Lemma 7.5 (Exact rational sign)**.** *On the above rectangle one has* $W_{\mathrm{end}}(x,z) < 1$.

Proof. The exact rational positivity certificate, including the denominators and the Bernstein coefficient bounds on rational rectangles, is established in Appendix A.4. □

Theorem 7.6 (Entire low-weight cap domain)**.** *For every fundamental homogeneous torus with* $1/3 \le R \le 7/20$*, every unit direction* p*, and every* $0 \le s \le 19/20$*, one has*

$$J(r,s,p) \le 4\pi,$$

with equality only for $R = 1/3$ *and* $s = 0$*. This assertion uses only geometric estimates, elementary integration, and the explicitly specified rational polynomial-sign comparisons of Theorem 7.1 and Lemmas 7.4–7.5.*

Proof. The analytic small-centre theorem, Theorem 6.2, covers $0 \le s \le 1/4$ with its sharp equality case. Theorem 7.1 covers $1/4 \le s \le 17/40$ strictly. The intermediate-centre argument (33) and Lemma 7.4 cover $17/40 \le s \le 149/200$ strictly. The direct cap argument (35) and Lemma 7.5 cover $149/200 \le s \le 19/20$ strictly. These intervals overlap at their rational endpoints, so no parameter is omitted. □

8. Analytic high-centre estimates for conformal caps

We obtain uniform estimates on nested strips in the largest weight and conformal-centre radius. Write $q = p \cdot F_r$ and $m = \max q$. The cap-density

bound is Lemma 4.3. The estimates below use elementary integration and rational inequalities only. For reference we set

$$A_{\mathrm{eq}} = \frac{4\pi^2}{\sqrt{3}}, \qquad L = A_{\mathrm{eq}} - 4\pi, \qquad k_s(q) = \frac{1-s^2}{1+s^2-2sq},$$
$$J(r,s,p) = \int_{T^2} \left(k_s(q)^2 - \frac{L}{A(r)} \right)_+ dA_r.$$

The universal threshold inequality $L/A(r) \geq 1 - \sqrt{3}/\pi > 4/9$ will be used throughout Subsection 8.1.

8.1. **Three nested strips.**

Theorem 8.1 (Three nested high-centre strips)**.** *For every fundamental torus with modulus in $\mathcal{K}$ and every unit direction p,*

$$J(r,s,p) < 4\pi$$

whenever at least one of the following conditions holds:

$$\begin{aligned} &\frac{1}{3} \leq R \leq \frac{1}{2}, \quad \frac{9}{10} \leq s < 1; \\ &\frac{1}{3} \leq R \leq \frac{3}{5}, \quad \frac{23}{25} \leq s < 1; \\ &\frac{1}{3} \leq R \leq \frac{7}{10}, \quad \frac{47}{50} \leq s < 1. \end{aligned} \tag{36}$$

In particular, the three stated strips require neither interval certificates nor computer algebra.

8.2. **Proof of the three nested strips.**

Proof of Theorem 8.1. We prove all three cases simultaneously. Put $\delta = 1-s$, $h = 1-R$, and $\kappa^2 = R/(1-R)$. Replacing the true truncation level by $4/9$ only enlarges J. The positive part of the new integrand is supported on $q > q_0$ where

$$t_0 = 1 - q_0 = \frac{\delta(6-5\delta)}{4(1-\delta)}. \tag{37}$$

For the three pairs $(\overline{R}, \delta_*)$ in the theorem,

$$(\overline{R}, \delta_*) \in \left\{ \left(\frac{1}{2}, \frac{1}{10}\right), \left(\frac{3}{5}, \frac{2}{25}\right), \left(\frac{7}{10}, \frac{3}{50}\right) \right\},$$

$0 < \delta \leq \delta_*$ implies $q_0 > \sqrt{\overline{R}} \geq \sqrt{R}$. Indeed, at the three endpoints q_0 is respectively $61/72$, $101/115$, and $1709/1880$; their squares are strictly larger than $1/2$, $3/5$, and $7/10$, respectively. Thus (13) applies to the entire support.

Let $e = 1-m$. If $e \geq t_0$ then $J = 0$. Otherwise put

$$a = \delta^2 + 2se, \qquad P_0 = \delta(2-\delta),$$
$$H = h(1 + \kappa^2 e - \kappa\sqrt{2e-e^2}), \quad \phi(t) = \frac{P_0^2}{(\delta^2+2st)^2} - \frac{4}{9}.$$

The cap-density inequality and $q = 1 - t$ give

$$\frac{J}{4\pi} \le \frac{h}{2} \int_e^{t_0} \frac{\phi(t)}{H - t}\, dt. \tag{38}$$

The denominators are positive by $q_0 > \sqrt{R}$. A direct one-variable integration, independent of any numerical quadrature, gives

$$I_0 := \int_e^{t_0} \phi(t)\, dt = \frac{(P_0 - 2a/3)^2}{2sa}, \tag{39}$$

$$I_1 := \int_e^{t_0} t\phi(t)\, dt \le I_1(0),$$

$$I_1(0) = \frac{\delta^2}{72(1-\delta)^2} \left[18(2-\delta)^2 \log \frac{3(2-\delta)}{2\delta} - 108 + 156\delta - 55\delta^2 \right]. \tag{40}$$

Moreover $\phi \ge 0$ on $[e, t_0]$ and $0 \le P_0 - 2a/3 \le P_0$ because $a \le \delta^2 + 2st_0 = 3P_0/2$.

Case I: $0 \le e \le \delta^2/3$**.** For $0 \le t \le t_0$,

$$\frac{1}{H - t} \le \frac{1}{H} + \frac{t}{H(H - t_0)}.$$

Set $x = \sqrt{2se}/\delta$ and $\alpha = \kappa\delta/\sqrt{s}$. Then $H/h \ge 1 - \alpha x + \alpha^2 x^2/2$ and

$$\frac{aH}{\delta^2 h} \ge (1 + x^2) \left(1 - \alpha x + \frac{\alpha^2 x^2}{2} \right) \ge 1 - \alpha x + \frac{x^2}{2} \ge 1 - \frac{\kappa^2 \delta^2}{2s}.$$

If $R \le \overline{R}$ and $k_* = \overline{R}/(1 - \overline{R})$, (39) consequently yields

$$\frac{hI_0}{2H} \le U_0(\delta) := \frac{(2 - 5\delta/3)^2}{4(1-\delta) - 2k_*\delta^2}. \tag{41}$$

The following *integer polynomial comparisons* follow by multiplying out positive denominators. For $\overline{R} = 1/2$ and $0 \le \delta \le 1/10$,

$$(1 - \tfrac{3}{5}\delta)(4(1-\delta) - 2\delta^2) - (2 - 5\delta/3)^2 = \tfrac{\delta}{45}(54\delta^2 - 107\delta + 12) \ge 0.$$

For $\overline{R} = 3/5$ and $0 \le \delta \le 2/25$,

$$(1 - \tfrac{3}{5}\delta)(4(1-\delta) - 3\delta^2) - (2 - 5\delta/3)^2 = \tfrac{\delta}{45}(81\delta^2 - 152\delta + 12) \ge 0.$$

Finally, for $\overline{R} = 7/10$ and $0 \le \delta \le 3/50$,

$$(1 - \tfrac{11}{20}\delta)(4(1-\delta) - \tfrac{14}{3}\delta^2) - (2 - 5\delta/3)^2 = \tfrac{\delta}{90}(231\delta^2 - 472\delta + 42) \ge 0.$$

For the middle line the bracket decreases on the stated interval and equals $224/625 > 0$ at $\delta = 2/25$; the other two brackets are plainly positive using their interval endpoints. Thus

$$U_0(\delta) \le 1 - \eta\delta, \qquad \eta = \begin{cases} 3/5, & \overline{R} = 1/2, 3/5, \\ 11/20, & \overline{R} = 7/10. \end{cases} \tag{42}$$

In the same three ranges, respectively, we have

$$\kappa\sqrt{2e} \le \gamma\delta, \qquad (\gamma, h_*) = (1, \tfrac{1}{2}),\ (1, \tfrac{2}{5}),\ (\tfrac{5}{4}, \tfrac{3}{10}),$$

since $\kappa\sqrt{2/3} \le \gamma$ and $h \ge h_* = 1 - \overline{R}$. Consequently $H/h \ge K := 1 - \gamma\delta$, so

$$\frac{hI_1}{2H(H - t_0)} \le \frac{I_1(0)}{2K(h_*K - t_0)}. \tag{43}$$

All denominators are positive on their stated intervals.

For completeness, these last expressions can be bounded without any symbolic sign checking. Write

$$V(\delta) = \delta\left[18(2-\delta)^2 \log\frac{3(2-\delta)}{2\delta} - 108 + 156\delta - 55\delta^2\right].$$

For $0 < \delta \le 1/10$ the logarithm exceeds 3, since $\frac{3(2-\delta)}{2\delta} \ge 57/2 > e^3$ and $e < 11/4$. Differentiation gives

$$V'(\delta) = 18(2-\delta)(2-3\delta)\log\frac{3(2-\delta)}{2\delta} - 180 + 348\delta - 165\delta^2 > 36 - 84\delta - 3\delta^2 > 0.$$

Since $I_1(0)/\delta = V(\delta)/[72(1-\delta)^2]$, this quotient increases. Meanwhile $2K(h_*K - t_0)$ decreases as δ increases. Its endpoint lower bounds, and the corresponding elementary upper bounds on $I_1(0)/\delta$, are

$\overline{R}$	δ_*	$2K(h_*K - t_0) \ge$	$I_1(0)/\delta <$
1/2	1/10	107/200	1681/7290
3/5	2/25	1416/3125	26492/119025
7/10	3/50	129759/376000	143451/883600

The bounds in the last column use, at the respective endpoints, $\log(57/2) < 7/2$, $\log(36) < 4$, and $\log(97/2) < 4$. These follow from short positive Taylor sums for e^x: for example $e > 8/3$ gives $e^4 > (8/3)^4 > 97/2$, and $e^{7/2} > (8/3)^3(1 + 1/2 + 1/8) > 57/2$. The three ratios of the last two columns are respectively

$$\frac{33620}{78003}, \qquad \frac{827875}{1685394}, \qquad \frac{136620}{290413}, \quad \text{each strictly less than } \frac{1}{2}.$$

Combining (38), (42), and (43) yields

$$\frac{J}{4\pi} < 1 - (\eta - \tfrac{1}{2})\delta < 1. \tag{44}$$

Case II: $\delta^2/3 \le e < t_0$**.** Write $x = \sqrt{e}$ and $A_x = 1 + 2sx^2/\delta^2$. Since $\phi \ge 0$, (38) and (39) imply

$$\frac{J}{4\pi} \le \frac{(2 - \delta - \frac{2\delta}{3}A_x)^2}{4sA_x\,(H - t_0)/h}. \tag{45}$$

For each pair $(\overline{R}, \delta_*)$, the function $1+\kappa^2 e-\kappa\sqrt{2e-e^2}$ is nonincreasing in $0 \le \kappa \le \sqrt{k_*}$ when $e \le t_0 \le t_0(\delta_*)$: indeed $e < 2/(4k_*+1)$, so $2\kappa e \le \sqrt{2e-e^2}$. Using $\sqrt{2} < 3/2$, $\sqrt{3} < 7/4$, and $\sqrt{14/3} < 13/6$, respectively, gives

$$\frac{H - t_0}{h} \ge G(x) := 1 - \beta - a_*x + b_*x^2, \qquad \beta = \frac{t_0}{h_*},$$

where the constants are

$\overline{R}$	a_*	b_*	$\beta \le$	$x <$
1/2	3/2	1	11/36	2/5
3/5	7/4	3/2	7/23	2/5
7/10	13/6	7/3	57/188	1/3

.

In each row $G(x) > 0$ because $G \ge 1 - 1/3 - a_*^2/(4b_*) > 0$. The numerator of (45) decreases with A_x, as it is nonnegative before squaring; see $a \le 3P_0/2$ above. Since $A_x \ge A_* := 1 + 2s/3 = (5 - 2\delta)/3$, we obtain

$$\frac{J}{4\pi} \le \frac{Z(\delta)}{F_\delta(x)}, \quad Z(\delta) := \frac{(2 - \delta - \frac{2\delta}{3}A_*)^2}{4s}, \quad F_\delta(x) := A_xG(x). \tag{46}$$

An exact differentiation shows

$$F_\delta'(x) = -a_* + 2b_*x + \frac{2sx}{\delta^2}\big(2(1-\beta) - 3a_*x + 4b_*x^2\big).$$

The derivative is positive on $\delta/\sqrt{3} \le x \le \sqrt{t_0}$. For the first row, the term in parentheses is at least 13/30 for $x \le 1/5$, and at least 13/75 for $1/5 \le x \le 2/5$; the displayed derivative is positive since $s/\delta \ge 9$. For the second row that term is at least 29/150 on $[0, 2/5]$, so positivity follows from $s/\delta \ge 23/2$. For the third it is at least 11/54 on $[0, 1/3]$, and $s/\delta \ge 47/3$ suffices. In all three cases we have used $x \ge \delta/\sqrt{3} > \delta/2$.

Therefore $F_\delta(x) \ge F_\delta(\delta/\sqrt{3})$. The elementary inequalities

$$\frac{3/2}{\sqrt{3}} < \frac{7}{8}, \qquad \frac{7/4}{\sqrt{3}} < \frac{21}{20}, \qquad \frac{13/6}{\sqrt{3}} < \frac{4}{3}$$

show that

$$F_\delta(x) \ge Y(\delta) := A_*\left(1 - \beta - \mu\delta + \frac{b_*}{3}\delta^2\right), \qquad \mu = \frac{7}{8},\ \frac{21}{20},\ \frac{4}{3},$$

respectively. A direct expansion of $Y - Z$ yields the three *quartic* polynomial identities

$$\overline{R} = \tfrac{1}{2}: \quad Y - Z = \frac{112\delta^4 - 1658\delta^3 + 5101\delta^2 - 4329\delta + 432}{648(1-\delta)},$$
$$\overline{R} = \tfrac{3}{5}: \quad Y - Z = \frac{920\delta^4 - 11278\delta^3 + 32723\delta^2 - 26640\delta + 2160}{3240(1-\delta)},$$
$$\overline{R} = \tfrac{7}{10}: \quad Y - Z = \frac{152\delta^4 - 1624\delta^3 + 4469\delta^2 - 3492\delta + 216}{324(1-\delta)}.$$

Each numerator is strictly decreasing on its stated interval: its derivative is bounded above, respectively, by

$$448(1/10)^3 + 10202(1/10) - 4329 < 0,$$
$$3680(2/25)^3 + 65446(2/25) - 26640 < 0,$$
$$608(3/50)^3 + 8938(3/50) - 3492 < 0.$$

At the right endpoints the three numerators have the strictly positive values

$$\frac{60579}{1250}, \qquad \frac{18163324}{78125}, \qquad \frac{34718103}{1562500}.$$

Thus $F_\delta(x) \geq Y(\delta) > Z(\delta)$ and $J/(4\pi) < 1$ in Case II. This completes the proof of Theorem 8.1. □

8.3. **The outer-weight high-centre strip.**

Theorem 8.2. *For every fundamental torus with*

$$\frac{7}{10} \leq R \leq R_* := \frac{1936}{2561}, \qquad \frac{47}{50} \leq s < 1,$$

and every unit ambient direction p, one has $J(r, s, p) < 4\pi$.

Proof. Write $\delta = 1 - s$, $h = 1 - R$, and $\kappa^2 = R/h$. Thus $0 < \delta \leq 3/50$, $h \geq 625/2561 > 6/25$, and $\kappa^2 \leq 1936/625 < 19/6$. We take the fixed lower truncation ρ^2, with $\rho = 18/25$. It is admissible because

$$\frac{L}{A(r)} \geq \frac{L}{\overline{A}(R)} \geq \frac{L}{\overline{A}(7/10)} = \frac{2}{\sqrt{93/100}}\left(\frac{1}{\sqrt{3}} - \frac{1}{\pi}\right) > \frac{105500}{197977} > \left(\frac{18}{25}\right)^2.$$

The strict rational comparison uses $\sqrt{93/100} < 97/100$, $\sqrt{3} < 26/15$ and $\pi > 157/50$. The positive part with threshold ρ^2 is supported where $q > q_0 = 1 - t_0$, with

$$t_0 = \frac{\delta[2 - (1+\rho)\delta]}{2\rho(1-\delta)}. \tag{47}$$

This function increases for $\delta \in [0, 3/50]$, and $1 - t_0 \geq 25829/28200 > \sqrt{1936/2561} \geq \sqrt{R}$. Consequently Lemma 4.3 applies on the full support. If $m = \max(p \cdot F_r) \leq q_0$, the integral is zero. Otherwise put $e = 1 - m < t_0$ and

$$a = \delta^2 + 2se, \quad P_0 = \delta(2 - \delta), \quad H = 1 - Rm - \sqrt{R(1-R)(1-m^2)}.$$

Let $\phi(t) = P_0^2/(\delta^2 + 2st)^2 - \rho^2$. The cap-density inequality gives

$$\frac{J(r,s,p)}{4\pi} \le \frac{h}{2}\int_e^{t_0} \frac{\phi(t)}{H-t}\,dt, \qquad H > t_0, \quad \phi(t) \ge 0. \tag{48}$$

An elementary integration yields

$$I_0(e) := \int_e^{t_0} \phi(t)\,dt = \frac{(P_0 - \rho a)^2}{2sa}, \tag{49}$$

$$I_1(e) := \int_e^{t_0} t\phi(t)\,dt \le I_1(0),$$

$$I_1(0) = \frac{\delta^2}{8s^2}\left[2(2-\delta)^2 \log\frac{2-\delta}{\rho\delta} - 3(2-\delta)^2 + 4\rho\delta(2-\delta) - \rho^2\delta^2\right]. \tag{50}$$

Case 1: $e \le \delta^2/3$. Since $t \le t_0 < H$, $(H-t)^{-1} \le H^{-1} + t/[H(H-t_0)]$. With $x = \sqrt{2se}/\delta$ and $\alpha = \kappa\delta/\sqrt{s}$, the exact expression for H gives

$$\frac{H}{h} \ge 1 - \alpha x + \frac{\alpha^2 x^2}{2}, \qquad \frac{aH}{\delta^2 h} \ge 1 - \alpha x + \frac{x^2}{2} \ge 1 - \frac{\kappa^2\delta^2}{2s}.$$

Here the middle inequality follows by expanding $(1+x^2)(1-\alpha x + \alpha^2 x^2/2)$, and the last by completing the square. Since $0 \le P_0 - \rho a \le P_0 - \rho\delta^2$,

$$\frac{hI_0(e)}{2H} \le \frac{[2-(1+\rho)\delta]^2}{4s - 2\kappa^2\delta^2} \le U_0(\delta) := \frac{(2-43\delta/25)^2}{4(1-\delta) - 19\delta^2/3}.$$

One checks directly that

$$\begin{aligned}(1-31\delta/50)\,[4(1-\delta) - 19\delta^2/3] - (2-43\delta/25)^2 \\ = \frac{\delta}{3750}(14725\delta^2 - 25544\delta + 1500) > 0.\end{aligned}$$

for $0 < \delta \le 3/50$: the quadratic in parentheses decreases on this interval and is positive at $3/50$. Hence $U_0(\delta) < 1 - 31\delta/50$.

For the remaining term set $K(\delta) = 1 - 73\delta/50$. The inequalities $\kappa\sqrt{2/3} < 73/50$ and $e \le \delta^2/3$ give $H/h \ge K(\delta)$. Also $h \ge 6/25$, so

$$\frac{hI_1(e)}{2H(H-t_0)} \le \frac{I_1(0)}{2K(\frac{6}{25}K - t_0)} < \frac{31}{50}\delta. \tag{51}$$

For the last strict bound, all quantities in the denominator are positive and t_0 increases with δ. Moreover $I_1(0)/\delta$ increases with δ. Indeed, writing $V(\delta)$ for δ times the square bracket in (50), differentiation gives

$$V'(\delta) = 2(2-\delta)(2-3\delta)\log\frac{2-\delta}{\rho\delta} - (\delta(1+\rho) - 2)(\delta(3\rho+9) - 10) > 0.$$

Here the logarithm exceeds 3 on $0 < \delta \le 3/50$, so the first term exceeds $6(97/50)(91/50) > 20$, while the last product is at most 20. Since $(1-\delta)^{-2}$ increases, the formula $I_1(0)/\delta = V(\delta)/[8(1-\delta)^2]$ proves the claim. The denominator of the middle expression in (51) decreases with δ. Thus it

suffices to check the right endpoint, $\delta = 3/50$. There $K = 2281/2500$, $t_0 = 2371/28200$, and

$$\log\frac{2-\delta}{\rho\delta} = \log\frac{2425}{54} < \frac{381}{100};$$

the last inequality follows from the rational Taylor sum $\sum_{j=0}^{10}(381/100)^j/j! > 2425/54$. Substitution into (50) gives

$$\frac{I_1(0)}{2K(\frac{6}{25}K - t_0)} \le \frac{37380651525}{1019571589756} < \frac{31}{50}\cdot\frac{3}{50}.$$

The difference in the last strict comparison is $\frac{171066129351}{318616121798750} > 0$. Combining with the I_0 bound in (48) proves $J/(4\pi) < 1$ in Case 1.

Case 2: $\delta^2/3 \le e < t_0$. Write $x = \sqrt{e}$ and $A_x = 1 + 2sx^2/\delta^2$, so $a = \delta^2 A_x$. Since $t_0 \le 2371/28200 < (29/100)^2$, we have $\delta/\sqrt{3} \le x < 29/100$. Put

$$b_* := \frac{1936}{625}, \quad a_* := \frac{249}{100}, \quad h_* := \frac{625}{2561}, \quad \beta := \frac{t_0}{h_*}.$$

The function $1 + \kappa^2x^2 - \kappa x\sqrt{2-x^2}$ decreases in $\kappa \in [0, \sqrt{b_*}]$ for $0 \le x < 29/100$: $4b_*(29/100)^2 < 2 - (29/100)^2$. As $a_* > \sqrt{2b_*}$, it follows that

$$\frac{H - t_0}{h} \ge G(x) := 1 - \beta - a_*x + b_*x^2 > 0.$$

Indeed $\beta \le 6072131/17625000$, and $G(x) \ge 1 - 6072131/17625000 - a_*^2/(4b_*) = 42334881947/272976000000 > 0$. Using (49) and replacing $(H-t)^{-1}$ by $(H-t_0)^{-1}$,

$$\frac{J}{4\pi} \le \frac{[2 - \delta - \rho\delta A_x]^2}{4sA_xG(x)} \le \frac{Z_*(\delta)}{F_\delta(x)},$$

$$F_\delta(x) = A_xG(x), \qquad Z_*(\delta) = \frac{[2-\delta-\rho\delta A_*]^2}{4s}.$$

where $A_* := 1 + 2s/3 = (5 - 2\delta)/3$. The second inequality holds because $A_x \ge A_*$ and $2 - \delta - \rho\delta A_x \ge 0$. An explicit derivative gives

$$F_\delta'(x) = -a_* + 2b_*x + \frac{2sx}{\delta^2}\left[2(1-\beta) - 3a_*x + 4b_*x^2\right].$$

The bracket decreases on $0 \le x \le 29/100$ and is at least

$$2\left(1 - \frac{6072131}{17625000}\right) - 3a_*\frac{29}{100} + 4b_*\left(\frac{29}{100}\right)^2 = \frac{164526289}{881250000} > \frac{9}{50}.$$

Since $x \ge \delta/\sqrt{3} > \delta/2$ and $s/\delta \ge 47/3$,

$$F_\delta'(x) > -\frac{249}{100} + \frac{47}{3}\frac{9}{50} > 0.$$

Therefore $F_\delta(x) \ge F_\delta(\delta/\sqrt{3})$. Since $a_*/\sqrt{3} < 36/25$, we obtain

$$F_\delta(x) \ge Y_*(\delta) := A_*\left(1 - \beta - \frac{36}{25}\delta + \frac{b_*}{3}\delta^2\right).$$

Straight expansion gives the following one-variable identity:

$$Y_*(\delta) - Z_*(\delta) = \frac{212288\delta^4 - 206015\delta^3 + 540300\delta^2 - 405625\delta + 22500}{33750(1-\delta)}.$$

The numerator decreases on $[0, 3/50]$, since its derivative is bounded above by $4 \cdot 21288(3/50)^3 + 2 \cdot 540300(3/50) - 405625 < 0$. At $\delta = 3/50$ its value is $197989539/3125000 > 0$. Thus $F_\delta(x) \geq Y_*(\delta) > Z_*(\delta)$ and $J(r, s, p) < 4\pi$ in Case 2. □

Corollary 8.3. *For every $1/3 \leq R \leq R_*$, every unit direction p, and every $47/50 \leq s < 1$, the truncated conformal area satisfies $J(r, s, p) < 4\pi$.*

Proof. For $R \leq 7/10$ the first three strips of Theorem 8.1 cover the claimed range, while for $R \geq 7/10$ the conclusion is Theorem 8.2. □

9. Exact rational control of the residual high caps

Throughout this section $R = r_1$ is the largest weight, $R_* = 1936/2561$, $\sigma(R) = (2 + 52R - 32R^2)/25$, $P = 1 - s^2$, $B = 1 + s^2$, $q = p \cdot F_r$ and $m = \max q$. Put

$$s_{\mathrm{top}}(R) = \begin{cases} 9/10, & R \leq 1/2, \\ 23/25, & 1/2 < R \leq 3/5, \\ 47/50, & 3/5 < R \leq R_*. \end{cases}$$

By Theorem 8.1 and Corollary 8.3, $J(r, s, p) < 4\pi$ whenever $s \geq s_{\mathrm{top}}(R)$. The remaining compact high-cap domain is

$$\mathcal{D}_{\mathrm{hi}} = \Big\{ \frac{7}{20} \leq R \leq R_*, \qquad \sigma(R) \leq s \leq s_{\mathrm{top}}(R) \Big\}. \tag{52}$$

It is treated by the mechanism of Subsections 7.4 and 7.5: the cap density estimate with the monotone kernel of Lemma 7.3, the exact primitive of Proposition 7.2, and elementary logarithmic inequalities. Here the constants are adapted to small cells of the parameter domain, and every resulting sign condition is a polynomial inequality with rational coefficients on a rational rectangle, decided by the exact Bernstein expansion (64).

Theorem 9.1 (Residual high caps)**.** *For every fundamental embedding with modulus in $\mathcal{K}$ and $7/20 \leq R \leq R_*$, every unit vector p, and every $\sigma(R) \leq s < 1$,*

$$J(r, s, p) < 4\pi.$$

Two majorants are used. In the upper part of $\mathcal{D}_{\mathrm{hi}}$ the positive part of the integrand lives above the level $\sqrt{R}$, and the cap density estimate applies to its whole support (*direct cells*, as in Subsection 7.5). Near $s = \sigma(R)$ the integrand is split into a quadratic part, controlled by the height moments, and a cap excess (*quadratic cells*, as in Subsection 7.4).

9.1. **Cells, thresholds and weight bounds.** A *cell* consists of an interval $[R_{\mathrm{lo}}, R_{\mathrm{hi}}] \subset [7/20, R_*]$ and a rational number $\rho \in (0,1)$ such that

$$\rho^2 < \bar{c}(R_{\mathrm{lo}}) = \frac{2(1/\sqrt{3} - 1/\pi)}{\sqrt{(1-R_{\mathrm{lo}})(1+3R_{\mathrm{lo}})}}. \tag{53}$$

The expression for $\bar{c} = L/\overline{A}$ follows from $A_{\mathrm{eq}} = 4\pi^2/\sqrt{3}$ and $\overline{A}(R) = 2\pi^2\sqrt{(1-R)(1+3R)}$. Since $\sqrt{3} < 97/56$ and $\pi > 333/106$, the numerator exceeds $16732/32301$, and (53) is verified through this rational bound and a rational upper bound for the square root.

Lemma 9.2. *On a cell, $f_{R,s}(q) \le f_\rho(q) := \bigl(k_s(q)^2 - \rho^2\bigr)_+$ for $R_{\mathrm{lo}} \le R \le R_{\mathrm{hi}}$, $0 < s < 1$ and $-1 \le q \le 1$. Moreover $f_\rho(q) > 0$ exactly when $q > q_\rho(s) := (B - P/\rho)/(2s)$, and q_ρ increases on $0 < s < 1$. Finally $\overline{A}(R) \le \overline{A}(R_{\mathrm{lo}})$ on the cell.*

Proof. The function $(1-R)(1+3R)$ decreases on $[1/3, 1)$. Hence $\overline{A}$ decreases and $\bar{c}$ increases there, so that $\rho^2 < \bar{c}(R_{\mathrm{lo}}) \le \bar{c}(R)$ for $R \ge R_{\mathrm{lo}}$. Since k_s increases in q and $k_s(q_\rho(s)) = \rho$, the second assertion follows, and $q_\rho(s) = \frac{1+\rho^{-1}}{2}\, s - \frac{\rho^{-1}-1}{2s}$ is increasing because $\rho < 1$. □

Parametrization. We write $s = (1-x^2)/(1+x^2)$ with $0 < x < 1$; thus s decreases in x, and with $X = x^2$,

$$\begin{gathered} s = \frac{1-X}{1+X}, \qquad P = \frac{4X}{(1+X)^2}, \qquad q_\rho(s) = \frac{\rho(1+X^2) - 2X}{\rho(1-X^2)}, \\ B - 2sq = \frac{2\bigl[(1+X^2) - (1-X^2)q\bigr]}{(1+X)^2}. \end{gathered} \tag{54}$$

For an interval $[x_a, x_b] \subset (0,1)$ we use rational constants $\overline{R}$ and ω with

$$\begin{gathered} 0 < \overline{R} \le R_{\mathrm{hi}}, \qquad \overline{R} = R_{\mathrm{hi}} \ \text{ or } \ \sigma(\overline{R}) \ge s(x_a), \\ \omega > 0, \qquad \omega^2 \ge \overline{R}(1-\overline{R}), \end{gathered} \tag{55}$$

and we put $\widehat{d}(m) = \overline{R}m + \omega\sqrt{1-m^2}$.

Lemma 9.3. *Assume (55). If $R_{\mathrm{lo}} \le R \le R_{\mathrm{hi}}$, $x_a \le x \le x_b$ and $s(x) \ge \sigma(R)$, then $R \le \overline{R}$. If moreover $T > 0$ and $T^2 > \overline{R}^2 + \omega^2$, then $\widehat{d}(m) < T$ and*

$$\frac{1-R}{q - d_R(m)} \le \frac{1-\overline{R}}{q - \widehat{d}(m)} \qquad (T \le q \le m \le 1). \tag{56}$$

Proof. If $\overline{R} < R_{\mathrm{hi}}$ and $R > \overline{R}$, then $\sigma(R) > \sigma(\overline{R}) \ge s(x_a) \ge s(x)$, because σ increases on $[0, 13/16] \supset [0, R_*]$; this contradicts $s(x) \ge \sigma(R)$. Next, $\overline{R}^2 + \omega^2 \ge \overline{R}$, so $T > \sqrt{\overline{R}}$. By Cauchy–Schwarz, $d_{R'}(m) \le \sqrt{R'} < T \le q$ for $R \le R' \le \overline{R}$, and $d_{\overline{R}}(m) \le \widehat{d}(m) \le \sqrt{\overline{R}^2 + \omega^2} < T$. Lemma 7.3, applied along $[R, \overline{R}]$, gives $(1-R)/(q - d_R(m)) \le (1-\overline{R})/(q - d_{\overline{R}}(m))$, and the last fraction is at most $(1-\overline{R})/(q - \widehat{d}(m))$. □

Lemma 9.4 (Logarithmic bounds)**.** *For $0 \le u < 1$, $Y \ge 0$ and $w \ge w_0 > 0$,*

$$\log\frac{1+u}{1-u} \ge 2\Big(u + \frac{u^3}{3}\Big), \qquad \log(1+Y) \le Y,$$
$$\log\frac{w}{w_0} \ge 2\Big(v + \frac{v^3}{3}\Big), \qquad v = \frac{w-w_0}{w+w_0}.$$

Proof. The first and third inequalities follow from the series quoted before (32), since $w/w_0 = (1+v)/(1-v)$ with $0 \le v < 1$. The second is elementary. □

The certificate attaches to each box a rational number Θ, with denominator at most 10^{30}, which bounds a logarithm from above. An inequality $e^{\Theta} \ge \theta$ with rational $\theta > 0$ is verified exactly: for $\Theta \ge 0$ by $e^{\Theta} \ge \sum_{k<120} \Theta^k/k!$, and for $-1 < \Theta < 0$ by $e^{|\Theta|} \le \sum_{k<120} |\Theta|^k/k! + 2|\Theta|^{120}/120!$.

9.2. **Direct cells.**

Proposition 9.5. *Consider a cell, an interval $[x_a, x_b]$ and constants $\overline{R}, \omega$ with (55), and assume*

$$q_\rho(s(x_b)) > 0, \qquad q_\rho(s(x_b))^2 > \overline{R}^2 + \omega^2. \tag{57}$$

Let $R_{\mathrm{lo}} \le R \le R_{\mathrm{hi}}$, $x_a \le x \le x_b$ and $s = s(x) \ge \sigma(R)$. If $m \le q_\rho(s)$, then $J(r,s,p) = 0$. If $m > q_\rho(s)$, then

$$\frac{J(r,s,p)}{4\pi} \le \frac{1-\overline{R}}{2}\Big[A_0 \log\frac{m-\widehat{d}}{q_\rho - \widehat{d}} + K\log\frac{N}{V} + \frac{P^2}{D}\Big(\frac{1}{V} - \frac{1}{N}\Big)\Big], \tag{58}$$

where $q_\rho = q_\rho(s)$, $\widehat{d} = \widehat{d}(m)$, $D = B - 2s\widehat{d}$, $K = P^2/D^2$, $A_0 = K - \rho^2 < 0$, $N = P/\rho$ and $V = B - 2sm$.

Proof. By Lemmas 9.2 and 9.3, $q_\rho(s) \ge q_\rho(s(x_b)) > \sqrt{\overline{R}^2 + \omega^2} \ge \sqrt{\overline{R}} \ge \sqrt{R}$, and $f_{R,s} \le f_\rho = 0$ on $[-1, q_\rho]$. If $m \le q_\rho$, then $k_s(q)^2 \le \rho^2 < c(r)$ on the whole torus and $J = 0$. Otherwise Proposition 5.2, with $C = 0$ and $t = q_\rho$, Lemma 9.2, and (56) with $T = q_\rho$ give

$$\frac{J}{4\pi} \le \frac{1-R}{2}\int_{q_\rho}^{m} \frac{f_{R,s}(q)}{q - d_R(m)}\,dq \le \frac{1-\overline{R}}{2}\int_{q_\rho}^{m} \frac{k_s(q)^2 - \rho^2}{q - \widehat{d}(m)}\,dq;$$

the last integrand is nonnegative. Proposition 7.2, applied with $c = \rho^2$, $C = 0$, $T = q_\rho$ and d replaced by the constant $\widehat{d} < q_\rho$, evaluates the last integral; here $B - 2sq_\rho = P/\rho = N$, $E_0/(2s) = K$ and $F_0/(2s) = P^2/D$. Finally $k_s(\widehat{d}) < k_s(q_\rho) = \rho$, so $A_0 < 0$. □

Rational form. Choose a rational $\chi > 0$ with

$$\rho > x_b^2, \qquad \chi^2 \ge \frac{1-\rho x_b^2}{\rho - x_b^2}, \tag{59}$$

and put, for $0 \le z \le 1$,

$$y = \chi x z, \qquad Y = y^2, \qquad m = \frac{1-Y}{1+Y}, \qquad w = X + \chi^2 z^2,$$

so that $X^2 + Y = Xw$. Define

$$\ell = \overline{R}(1-Y) + 2\omega y, \qquad D_n = (1+X^2)(1+Y) - (1-X^2)\ell,$$
$$K_n = 4X^2(1+Y)^2, \qquad Q_n = \rho(1+X^2) - 2X, \qquad Q_d = \rho(1-X^2),$$
$$N_u = (1-Y)Q_d - (1+Y)Q_n, \qquad D_u = (1-Y)Q_d + (1+Y)Q_n - 2Q_d\ell.$$

Lemma 9.6. *Assume (59) and $x_a \le x \le x_b$. Every $m \in [q_\rho(s), 1]$ is attained by some $z \in [0,1]$. Moreover $\widehat{d} = \ell/(1+Y)$, $D = 2D_n/((1+X)^2(1+Y))$, $K = K_n/D_n^2$,*

$$\frac{m - q_\rho}{m + q_\rho - 2\widehat{d}} = \frac{N_u}{D_u}, \qquad \frac{N}{V} = \frac{1+Y}{\rho w},$$
$$\frac{P^2}{D}\Big(\frac{1}{V} - \frac{1}{N}\Big) = \frac{2X(1+Y)(1+Y-\rho w)}{D_n w}.$$

Proof. The map $z \mapsto m$ is continuous and decreasing, with $m = 1$ at $z = 0$. At $z = 1$, $m = (1-\chi^2 X)/(1+\chi^2 X)$, and by (54)

$$\frac{1-q_\rho}{1+q_\rho} = \frac{X(1-\rho X)}{\rho - X}.$$

Hence $m \le q_\rho$ at $z = 1$ if and only if $\chi^2 \ge (1-\rho X)/(\rho - X)$. The right-hand side increases in $X \in [0, \rho)$, its derivative being $(1-\rho^2)/(\rho - X)^2$, so (59) suffices. The identities follow from $\sqrt{1-m^2} = 2y/(1+Y)$, $q_\rho = Q_n/Q_d$, (54), and $B - 2sm = 4(X^2+Y)/((1+X)^2(1+Y))$. □

Proposition 9.7. *Assume the hypotheses of Proposition 9.5 and (59). Let $0 \le z_a < z_b \le 1$, $w_0 = x_a^2 + \chi^2 z_a^2$, and let Θ be rational with $e^\Theta \ge 1/(\rho w_0)$. With $\Xi = 3(w-w_0)(w+w_0)^2 + (w-w_0)^3$ put*

$$\mathcal{M} = 3D_n^2 D_u^3 (w+w_0)^3 w,$$
$$\mathcal{M}_1 = 2(K_n - \rho^2 D_n^2)(3N_u D_u^2 + N_u^3)(w+w_0)^3 w,$$
$$\mathcal{M}_2 = K_n\big(3(Y+\Theta)(w+w_0)^3 - 2\Xi\big)D_u^3 w,$$
$$\mathcal{M}_3 = 6X(1+Y)(1+Y-\rho w) D_n D_u^3 (w+w_0)^3,$$

and $\mathscr{F} = 2\mathcal{M} - (1-\overline{R})(\mathcal{M}_1 + \mathcal{M}_2 + \mathcal{M}_3)$, a polynomial in (x,z) with rational coefficients. If D_n, D_u and $\mathscr{F}$ are positive on the box $[x_a, x_b] \times [z_a, z_b]$, then $J(r,s,p) < 4\pi$ for every (R,s,p) as in Proposition 9.5 whose parameters (x,z) lie in this box.

Proof. We may assume $m > q_\rho$. Then $u = N_u/D_u \in [0,1)$, because $\widehat{d} < q_\rho \le m$, and $v = (w-w_0)/(w+w_0) \in [0,1)$ on the box. By Lemma 9.4 and

$A_0 < 0$,

$$A_0 \log \frac{m-\widehat{d}}{q_\rho - \widehat{d}} \le 2A_0\Big(u + \frac{u^3}{3}\Big),$$

$$\log \frac{N}{V} = \log(1+Y) - \log(\rho w_0) - \log \frac{w}{w_0} \le Y + \Theta - 2\Big(v + \frac{v^3}{3}\Big).$$

Insert these bounds into (58), use Lemma 9.6 and $K > 0$, and multiply by $2\mathcal{M} > 0$. Since $A_0 = (K_n - \rho^2 D_n^2)/D_n^2$ and $\Xi = (w+w_0)^3(3v+v^3)$, the three terms in the bracket of (58) are at most $\mathcal{M}_1/\mathcal{M}$, $\mathcal{M}_2/\mathcal{M}$ and $\mathcal{M}_3/\mathcal{M}$, respectively; hence

$$2\mathcal{M}\,\frac{J}{4\pi} \le (1-\overline{R})(\mathcal{M}_1+\mathcal{M}_2+\mathcal{M}_3) = 2\mathcal{M} - \mathscr{F} < 2\mathcal{M}.$$

□

9.3. **Quadratic cells.**

Lemma 9.8 (Quadratic majorant)**.** *Let $0 < \tau < 1$ and $b > 0$, let $\widehat{K} > 0$ be rational with $\widehat{K}^2\rho^2 \ge 32/27$, and assume*

$$q_\rho(s) < \tau, \qquad q_\rho(s) + b > 0, \qquad B + 2sb \ge \widehat{K}P. \tag{60}$$

Then $C := f_\rho(\tau)/(\tau+b)^2 > 0$, $f_\rho(q) \le C(q+b)^2$ for $-1 \le q \le \tau$, and

$$\psi(q) := k_s(q)^2 - \rho^2 - C(q+b)^2 \ge 0 \qquad (\tau \le q \le 1).$$

Proof. As in Subsection 7.4, for $q > q_\rho$, where $q + b > 0$, the derivative of $f_\rho(q)/(q+b)^2$ has the sign of $\rho^2 z^3 - 2P^2 z + P^2(B+2sb)$ with $z = B - 2sq$. Its minimum over $z \ge 0$ equals $P^2\big(B+2sb - \frac{4}{3}\sqrt{2/3}\,P/\rho\big) \ge P^2(B+2sb-\widehat{K}P) \ge 0$, because $\widehat{K}\rho \ge \frac{4}{3}\sqrt{2/3}$ by the hypotheses on $\widehat{K}$. Thus $f_\rho/(q+b)^2$ is nondecreasing on $(q_\rho, 1]$. Since $f_\rho = 0$ on $[-1, q_\rho]$ and $f_\rho(\tau) > 0$, all assertions follow. □

Put $a_R = \overline{A}(R)/(4\pi) = \frac{\pi}{2}\sqrt{(1-R)(1+3R)}$.

Proposition 9.9. *Consider a cell with a rational number $\bar{a} \ge a_{R_{\rm lo}}$, an interval $[x_a, x_b]$ with constants $\overline{R}, \omega$ satisfying (55), and constants τ, b, $\widehat{K}$ satisfying the hypotheses of Lemma 9.8 for every $s(x_b) \le s \le s(x_a)$, together with $\tau^2 > \overline{R}^2 + \omega^2$. Let $R_{\rm lo} \le R \le R_{\rm hi}$, $x_a \le x \le x_b$ and $s = s(x) \ge \sigma(R)$. Then*

$$\frac{J(r,s,p)}{4\pi} \le \bar{a}\Big(\frac{\overline{R}}{2} + b^2\Big)C + \frac{1-\overline{R}}{2}\,I(m), \tag{61}$$

where $I(m) = 0$ if $m \le \tau$, and otherwise, with $\widehat{d} = \widehat{d}(m)$, $D = B - 2s\widehat{d}$ and $K = P^2/D^2$,

$$I(m) = A_0' \log \frac{m-\widehat{d}}{\tau - \widehat{d}} + K \log \frac{B-2s\tau}{B-2sm} + \frac{P^2}{D}\Big(\frac{1}{B-2sm} - \frac{1}{B-2s\tau}\Big)$$
$$- C\Big(\frac{m^2-\tau^2}{2} + (\widehat{d}+2b)(m-\tau)\Big),$$

and $A_0' = K - \rho^2 - C(\widehat{d}+b)^2 \le 0$.

Proof. By Lemmas 9.2 and 9.8, $f_{R,s} \le f_\rho \le C(q+b)^2$ on $[-1,\tau]$, and $[f_{R,s} - C(q+b)^2]_+ \le \psi$ on $[\tau,1]$. By Lemma 9.3, $R \le \overline{R}$ and $\tau > \sqrt{\overline{R}} \ge \sqrt{R}$. Proposition 5.2, with $t=\tau$ and $\xi = -b$, together with $\overline{A}(R) \le \overline{A}(R_{\mathrm{lo}}) = 4\pi a_{R_{\mathrm{lo}}} \le 4\pi\bar{a}$ and (56) with $T=\tau$, gives (61) with $I(m) = \int_\tau^m \psi(q)/(q - \widehat{d}(m))\,dq$. Proposition 7.2, with $c=\rho^2$, $T=\tau$ and d replaced by the constant $\widehat{d} < \tau$, gives the closed form. Finally A_0' is the value at $q = \widehat{d} \in [0,\tau)$ of $k_s(q)^2 - \rho^2 - C(q+b)^2$, which is at most $f_\rho(\widehat{d}) - C(\widehat{d}+b)^2 \le 0$. □

Rational form. Choose $\tau = (1-H)/(1+H)$ with $H = \eta^2$ and a rational $\eta \in (0,1)$, and put, for $0 \le z \le 1$,

$$y = \eta z, \qquad Y = \eta^2 z^2, \qquad m = \frac{1-Y}{1+Y}, \qquad w = X^2 + Y.$$

Then $z \in [0,1]$ corresponds exactly to $\tau \le m \le 1$. With $\ell = \overline{R}(1-Y) + 2\omega\eta z$, with D_n and K_n given by the formulas preceding Lemma 9.6 for the present Y and ℓ, and with

$$N_u = H - Y, \qquad D_u = 1 - HY - (1+H)\ell, \qquad \ell_b = \ell + b(1+Y),$$
$$G = 1 - HY + (1+H)(\ell + 2b(1+Y)),$$
$$C_N = X^2(1+H)^2 - \rho^2(X^2+H)^2, \qquad C_D = (X^2+H)^2(\tau+b)^2,$$

one has $\widehat{d} = \ell/(1+Y)$, $D = 2D_n/((1+X)^2(1+Y))$, $K = K_n/D_n^2$, $C = C_N/C_D$, $\widehat{d}+b = \ell_b/(1+Y)$, $(m-\tau)/(m+\tau-2\widehat{d}) = N_u/D_u$, and

$$\frac{B-2s\tau}{B-2sm} = \frac{(X^2+H)(1+Y)}{(1+H)w},$$
$$\frac{P^2}{D}\Big(\frac{1}{B-2sm} - \frac{1}{B-2s\tau}\Big) = \frac{2X^2(1+Y)(H-Y)(1-X^2)}{D_n w(X^2+H)},$$
$$C\Big(\frac{m^2-\tau^2}{2} + (\widehat{d}+2b)(m-\tau)\Big) = \frac{2C_N(H-Y)G}{C_D(1+Y)^2(1+H)^2}.$$

These follow from (54), $k_s(\tau) = X(1+H)/(X^2+H)$, $m-\tau = 2(H-Y)/((1+H)(1+Y))$ and $m+\tau = 2(1-HY)/((1+H)(1+Y))$. In this notation the hypotheses (60) on $[x_a,x_b]$ read: $X(1+H) - \rho(X^2+H) > 0$, a concave function of X, at $X = x_a^2$ and $X = x_b^2$ (this is $C_N > 0$, that is, $q_\rho < \tau$); $\rho(1+X^2) - 2X + b\rho(1-X^2) > 0$ at $X = x_b^2$ (this is $q_\rho + b > 0$, as q_ρ decreases in X); and $(2-2b)X^2 - 4\widehat{K}X + 2 + 2b \ge 0$ for $x_a^2 \le X \le x_b^2$ (this is $B + 2sb \ge \widehat{K}P$).

Proposition 9.10. *Assume the hypotheses of Proposition 9.9. Let* $0 \le z_a < z_b \le 1$, $w_0 = x_a^4 + Hz_a^2$, *and let* Θ *be rational with* $e^\Theta \ge (x_b^4+H)/((1+H)w_0)$. *With* $\Pi = (w+w_0)^3$, $c_1 = (1+H)^2$ *and* $n_1 = 4X^2(1+Y)^4C_D - \rho^2 D_n^2(1+$

$Y)^2 C_D - C_N \ell_b^2 D_n^2$, *put*

$$\begin{aligned}
\mathcal{N} &= 3C_D D_n^2 (1+Y)^2 D_u^3 \,\Pi\, w(X^2+H) c_1,\\
\mathcal{N}_0 &= 3\bar{a}\big(\tfrac{\overline{R}}{2} + b^2\big) C_N D_n^2 (1+Y)^2 D_u^3 \,\Pi\, w(X^2+H) c_1,\\
\mathcal{N}_1 &= 2n_1 (3N_u D_u^2 + N_u^3) \,\Pi\, w(X^2+H) c_1,\\
\mathcal{N}_2 &= 4X^2 (1+Y)^4 C_D D_u^3 w(X^2+H) c_1 \big(3(Y+\Theta)\Pi - 2\Xi\big),\\
\mathcal{N}_3 &= 6X^2 (1+Y)^3 (H-Y)(1-X^2) C_D D_n D_u^3 \,\Pi\, c_1,\\
\mathcal{N}_4 &= 6C_N (H-Y)\, G\, D_n^2 D_u^3 \,\Pi\, w(X^2+H),
\end{aligned}$$

with $\Xi = 3(w-w_0)(w+w_0)^2 + (w-w_0)^3$ *as before, and put* $\mathscr{F} = 2\mathcal{N} - 2\mathcal{N}_0 - (1-\overline{R})(\mathcal{N}_1 + \mathcal{N}_2 + \mathcal{N}_3 - \mathcal{N}_4)$. *If* D_n, D_u *and* $\mathscr{F}$ *are positive on the box* $[x_a, x_b] \times [z_a, z_b]$, *then* $J(r,s,p) < 4\pi$ *for every* (R,s,p) *as in Proposition 9.9 such that either* $m \geq \tau$ *and* (x,z) *lies in the box, or* $m < \tau$ *and* $z_b = 1$.

Proof. Let first $m \geq \tau$. Then $u = N_u/D_u \in [0,1)$, since $\widehat{d} < \tau \leq m$, and $v = (w-w_0)/(w+w_0) \in [0,1)$. By Lemma 9.4 and $A_0' \leq 0$, $A_0' \log \frac{m-\widehat{d}}{\tau-\widehat{d}} \leq 2A_0'(u + u^3/3)$, and, since $X^2 \leq x_b^4$ and $w \geq w_0$,

$$\log \frac{B - 2s\tau}{B - 2sm} = \log(1+Y) + \log \frac{X^2+H}{(1+H)w_0} - \log \frac{w}{w_0} \leq Y + \Theta - 2\Big(v + \frac{v^3}{3}\Big).$$

We have $A_0' = n_1/(C_D D_n^2 (1+Y)^2)$. Inserting these bounds and the identities above into (61), using $K > 0$, and multiplying by $2\mathcal{N} > 0$, one obtains

$$2\mathcal{N}\,\frac{J}{4\pi} \leq 2\mathcal{N}_0 + (1-\overline{R})(\mathcal{N}_1 + \mathcal{N}_2 + \mathcal{N}_3 - \mathcal{N}_4) = 2\mathcal{N} - \mathscr{F} < 2\mathcal{N}.$$

If $m < \tau$, then $J/(4\pi) \leq \bar{a}(\overline{R}/2 + b^2)C$. At $z = 1$ the majorant just obtained reduces to this term plus $\frac{1-\overline{R}}{2} K(Y + \Theta - 2(v + v^3/3))$, which is nonnegative, being an upper bound for $\frac{1-\overline{R}}{2} K \log 1 = 0$. Hence $J/(4\pi) < 1$ also in this case. □

9.4. **The finite certificate and the proof of Theorem 9.1.**

Proposition 9.11 (Finite certificate)**.** *There are* 44 *cells,* 8 *direct and* 36 *quadratic, each with an interval of values of* x *and a finite set of boxes* $[x_a, x_b] \times [z_a, z_b]$ *in it,* 4439 *boxes in all, described in Appendix C, with the following properties.*

(i) *For every* $(R,s) \in \mathcal{D}_{\mathrm{hi}}$ *some cell has* R *in its weight interval and* x, *where* $s = s(x)$, *in its interval of values of* x.

(ii) *Each box carries rational constants* $\overline{R}, \omega$ *and* χ *(direct cells), respectively* $\overline{R}, \omega, \eta, b$ *(quadratic cells), together with* w_0 *and* Θ *as in Propositions 9.7 and 9.10. With* $[x_a, x_b]$ *the* x*-interval of the box, all hypotheses of Proposition 9.7, respectively of Proposition 9.10, hold; in particular* (53) *and* (55).

(iii) *The endpoints x_a, x_b of the boxes of a cell divide its interval of values of x into consecutive closed subintervals. For each such subinterval I, all boxes of the cell whose x-interval contains I carry the same constants $\overline{R}, \omega, \chi$, respectively $\overline{R}, \omega, \eta, b$, and their z-intervals cover $[0,1]$.*

(iv) *On every box all tensor Bernstein coefficients (64) of D_n, D_u and $\mathscr{F}$ are positive.*

Proof. All assertions are finite statements about rational numbers and polynomials with rational coefficients. They are verified in exact rational arithmetic, as described in Appendix C. □

Proof of Theorem 9.1. If $s \geq s_{\mathrm{top}}(R)$, the assertion is Theorem 8.1 or Corollary 8.3. Let $(R,s) \in \mathcal{D}_{\mathrm{hi}}$ and let p be a unit vector. Choose a cell as in Proposition 9.11(i) and write $s = s(x)$. Choose a subinterval I as in (iii) with $x \in I$; if x is a common endpoint of two subintervals, either one may be taken. Let $\overline{R}, \omega, \chi$, respectively $\overline{R}, \omega, \eta, b$, be the common constants of the boxes whose x-interval contains I; each of these boxes contains x in its x-interval. In a direct cell, if $m \leq q_\rho(s)$ then $J(r,s,p) = 0$ by Proposition 9.5; otherwise Lemma 9.6 gives $z \in [0,1]$ with $m = (1-\chi^2x^2z^2)/(1+\chi^2x^2z^2)$. In a quadratic cell, if $m \geq \tau$ let $z \in [0,1]$ be defined by $m = (1-\eta^2z^2)/(1+\eta^2z^2)$, and if $m < \tau$ let $z = 1$. By (iii) the point (x,z) lies in one of the boxes whose x-interval contains I. By (ii) and (iv), Proposition 9.7, respectively Proposition 9.10, applies to that box and gives $J(r,s,p) < 4\pi$. □

Remark 9.12. The certificate is a finite list of rational data; the verifying program rebuilds every polynomial from the formulas above with its own exact arithmetic. Theorem 9.1 is also verified by a second, independent program, which does not use Propositions 9.7 and 9.10: it rechecks parts (i)–(iii) of Proposition 9.11 and encloses the right-hand sides of (58) and (61), with the exact logarithms, in ball arithmetic on every box (Section C.4). For orientation only, and without use in the proof, the largest value of the right-hand sides of (58) and (61) at the corners and centres of the boxes is about 0.998 in the quadratic cells, attained for $81/200 \leq R \leq 41/100$ near $s = \sigma(R)$, and about 0.98 in the direct cells.

10. The certified product inequality and proof of the truncation theorem

One finite inequality, for the product majorant, covers the product region $7/20 \leq R \leq R_*$, $1/4 \leq s \leq \sigma(R)$. Its precise parameter domain is recorded here; the construction of the upper bounds, the arithmetic model, the complete verification records and the source-file identifiers are given in Appendices B and D and in the accompanying supplement.

Lemma 10.1 (Product inequality)**.** *Let* $R_* = 1936/2561$ *and* $\sigma(R) = (2 + 52R - 32R^2)/25$*. For every*

$$\frac{7}{20} \le R \le R_*, \qquad \frac{13}{100} \le s \le \sigma(R), \qquad 0 \le \alpha \le 1,$$

the product majorant $\mathcal{P}(R, s, \alpha)$ *of Proposition 5.1 satisfies*

$$\mathcal{P}(R, s, \alpha) < 4\pi.$$

Proof. The inequality is established by the finite verification of Section B.3. It uses on each parameter box one convex majorant whose average over one cosine variable is explicit, reduces the amplitudes of the box to two elliptic arcs by convexity, bounds the average over the other cosine variable by the upper chord rule, and evaluates all bounds in Arb ball arithmetic. The inequality is verified a second time, independently, by the interval certificate of Section B.4, which bounds both cosine averages by upper chord quadratures and the amplitudes by a circumscribed polygon, in outward-rounded binary64 interval arithmetic with exact rational checks of all transcendental constants. Each certificate covers the specified domain, as checked in exact rational arithmetic; the strict bounds and the reproducibility records are given in Appendix D. □

On three substrips of this domain, Appendix E checks the conclusion $J < 4\pi$ once more, by exact moments and rational Bernstein positivity and without interval or floating-point arithmetic; on part of these strips it proves $\mathcal{P} < 4\pi$ itself. This check is not used in the proof.

Proof of Theorem 2.2. The closed-domain ranges listed in the table of Section 2 cover all $1/3 \le R \le R_*$ and $0 \le s < 1$. Theorem 6.2 settles $s \le 1/4$ analytically. On $R \le 7/20$, Theorem 7.6 controls the full interval $0 \le s \le 19/20$. On $R \ge 7/20$, Lemma 10.1 and Proposition 5.1 control $1/4 \le s \le \sigma(R)$ (the lemma certifies the larger interval $13/100 \le s \le \sigma(R)$), and Theorem 9.1 controls $\sigma(R) \le s < 1$. Corollary 8.3 supplies the analytic bound for $s \ge 47/50$ in every weight. The domains overlap at their boundaries, so there is no uncovered parameter or limiting value.

The product certificate, the residual high-cap bound, the low-weight argument away from $s = 0$, and the large-center bound are strict. The small-center comparison is also strict away from the equilateral zero-center configuration: for $R > 1/3$ its area-envelope comparison is strict, while for $R = 1/3$ and $0 < t \le 4/17$ the comparison of Lemma 6.3 is strict: an exact simplification gives $1 - B(1/3, t) = 2t^2 N_5(t)/(9(2 - t)^3(1 - 2t)(5 + 2t)^3)$ with $N_5(t) = 844t^5 - 23756t^4 - 19549t^3 + 38870t^2 - 32700t + 9000$, and $N_5(t) \ge 9000 - 32700t - 19549t^3 - 23756t^4 > 0$ on $[0, 4/17]$. At $s = 0$,

$$J(r, 0) = (A(r) - L)_+ \le A_{\mathrm{eq}} - L = 4\pi,$$

with equality precisely at the equal-weight fundamental torus. There $s = 0$ indeed gives $J = 4\pi$. This proves the truncated-area theorem, including its equality case. □

11. The complementary moduli, with an exact endpoint

Let $0 \le a \le 1/2$ and $b \ge 44/25$. On the flat torus of modulus $a + ib$, use the embedding into S^3

$$\Psi_\rho(x,y) = \left(\sqrt{\rho}\, e^{2\pi i y/b}, \sqrt{1-\rho}\, e^{2\pi i(x-ay/b)}\right), \qquad \rho = 1 - \frac{1}{b^2 + 8/3} > \frac{2}{3}.$$

Its Dirichlet-energy and induced-area densities are both constant, with

$$E_0 = \frac{2\pi^2}{b}\{\rho + (a^2+b^2)(1-\rho)\}, \qquad A_0 = 4\pi^2\sqrt{\rho(1-\rho)}.$$

Although this map need not be conformal for the chosen source modulus, the two densities remain proportional after any target conformal transformation. The image of Ψ_ρ is that of Bryant's fundamental immersion [1, Section 3] for the rectangular modulus $i\sqrt{\rho/(1-\rho)}$, whose weights are $r = (\rho, 1-\rho, 0)$. Since $r_1 = \rho > 2/3$, this lies outside the Montiel–Ros range of [1, Theorem 2]. In this range the conformal volume is the value stated in [1, Remark 5]; its proof was added in the 2025 revision of [1] and relies on a computer-algebra (MAPLE) computation. The same value appears in the published paper [9, Lemma 2.3] for the rectangular tori of modulus $i\beta$ with $\beta > \sqrt{2}$; here $\beta = \sqrt{\rho/(1-\rho)}$, and $\beta > \sqrt{2}$ means $\rho > 2/3$. The corresponding maximization is carried out in [9, Lemma 2.4], from an inequality of [1] and a direct computation on the boundary of the parameter domain. For $r_3 = 0$ the conformal volume equals $8\pi^2/(3\sqrt{3}\sqrt{\rho}) = A_0 \cdot 2/(3\sqrt{3}\,\rho\sqrt{1-\rho})$. This value is the only computational input of the paper taken from the literature; it is used only for $b \ge 44/25$, where it also underlies Kang's reduction [9, Corollary 1.3]. A numerical check on the range used here, which is not part of the proof, is included in the supplement: for $44/25 \le b \le 10$ it locates the supremum of the conformal area at the direction of the larger circle and reproduces this value to about twenty digits. Therefore

$$\sup_M \mathcal{E}(M \circ \Psi_\rho) = E_0 \frac{2}{3\sqrt{3}\,\rho\sqrt{1-\rho}}.$$

Folding and the Rayleigh sum give $\lambda_2 \operatorname{Area} \le 4 \sup_M \mathcal{E}(M \circ \Psi_\rho)$, since each of the two piece energies is at most the full single-map supremum. Hence, with $B = b^2$,

$$\lambda_2 \operatorname{Area} \le \frac{16\pi^2}{3\sqrt{3}}\, H(B), \qquad H(B) = \frac{(2B + 23/12)\sqrt{(B+8/3)/B}}{B + 5/3}.$$

The logarithmic derivative is

$$\frac{H'(B)}{H(B)} = \frac{17/12}{(2B+23/12)(B+5/3)} - \frac{8/3}{2B(B+8/3)}.$$

After multiplication by the positive common denominator, its numerator is $-(5/2)B^2 - (58/9)B - 230/27$. Thus H decreases for $B > 0$. It remains to

bound the value at $B_0 = 1936/625$. At this point

$$\sqrt{\frac{B_0 + 8/3}{B_0}} = \sqrt{\frac{1351}{726}} < \frac{6821}{5000}.$$

The rational inequalities $333/106 < \pi < 22/7$ and $265/153 < \sqrt{3} < 97/56$ yield

$$\frac{16\pi^2}{3\sqrt{3}} H(B_0) < \frac{16(22/7)^2}{3(265/153)} \frac{2B_0 + 23/12}{B_0 + 5/3} \frac{6821}{5000} < \frac{707}{10},$$
$$C_* > \frac{8(333/106)^2}{97/56} + 8\frac{333}{106} > \frac{707}{10}.$$

The displayed endpoint comparisons are exact rational inequalities after applying the stated bounds for π and $\sqrt{3}$. A supplementary script provides an independent check (Appendix D). The exterior region thus has a uniform strict upper bound below C_*.

12. Sharpness, nonattainment, and the unique maximizing class

The preceding sections prove the strict upper bound for every smooth metric. For the lower bound, the standard conformal bubbling construction gives

$$\Lambda_2(T^2, \mathcal{C}) \geq \Lambda_1(T^2, \mathcal{C}) + 8\pi; \tag{62}$$

see [2, 12]. The equilateral embedding has area A_{eq} and its first positive eigenvalue is 2, by a direct Fourier computation. Consequently (62) gives $\Lambda_2(T_{\mathrm{eq}}, [g_{\mathrm{eq}}]) \geq 2A_{\mathrm{eq}} + 8\pi$. Equivalently, keep this flat torus and insert one unit round spherical bubble through conformal concentration. The total area tends to $A_{\mathrm{eq}} + 4\pi$, while $\lambda_1 \to 0$ and $\lambda_2 \to 2$. This proves sharpness and nonattainment by a smooth metric.

For completeness, we prove that no other fixed conformal class has the same supremum. For a fixed fundamental embedding define

$$V_2(r) = \sup_{v,w \in B^6} \int \max\{k_v(F_r)^2, k_w(F_r)^2\}\, dA_r.$$

At every interior pair of centers, the argument in Section 3 puts the integral defining $V_2(r)$ strictly below $A_{\mathrm{eq}} + 4\pi$; a further boundary argument is needed to conclude strictness of the supremum.

First, Theorem 2.2 itself implies

$$\limsup_{|v| \to 1} \int k_v(F_r)^2\, dA_r \leq 4\pi. \tag{63}$$

Indeed,

$$\int k_v^2\, dA_r = J(r, v) + \int \min\{k_v^2, L/A(r)\}\, dA_r.$$

For any sequence of centers tending to the boundary, first select a subsequence realizing the limsup and then one whose directions converge. The second

integrand tends to zero off the preimage of one point of the sphere. That preimage has area zero because F_r is an embedding. Dominated convergence proves (63).

Write $V_c(F_r) = \sup_{w\in B^6} \int k_w(F_r)^2\, dA_r$ for the conformal area of the fundamental embedding. Theorem 2.2 also controls this quantity. For every $w \in B^6$,

$$\int k_w^2\, dA_r = J(r,w) + \int \min\{k_w^2, L/A(r)\}\, dA_r \le J(r,w) + L.$$

If $R > 1/3$, then $J(r,w) < 4\pi$ for every w, so the integral is strictly smaller than $L + 4\pi = A_{\mathrm{eq}}$ at every interior centre. Along a maximizing sequence of centres, either a subsequence converges to an interior point, where the integral is continuous, or $|w| \to 1$, where (63) gives the bound $4\pi < A_{\mathrm{eq}}$. Hence

$$V_c(F_r) < A_{\mathrm{eq}} \qquad (R > 1/3),$$

without appeal to an explicit conformal-volume formula. Consequently, if one center tends to the boundary, the limsup of the two-center integral is at most $4\pi + V_c(F_r) < A_{\mathrm{eq}} + 4\pi$. If both tend to the boundary, it is at most $8\pi < A_{\mathrm{eq}} + 4\pi$. Compactness of $\overline{B}^6 \times \overline{B}^6$ now shows

$$V_2(r) < A_{\mathrm{eq}} + 4\pi \qquad (R > 1/3).$$

Otherwise a sequence approaching the claimed larger supremum would have either an interior limit, contradicting the interior strict bound, or a boundary limit, contradicting the preceding limsup bounds. Since $R = 1/3$ occurs only at the equilateral modulus, folding gives $\Lambda_2(T^2, \mathcal{C}) \le 2V_2(r) < C_*$ for every other class in $\mathcal{K}$. Section 11 covers every exterior class. This completes Theorem 2.1.

13. Concluding remarks

The inputs imported from the literature are uniformization, the spherical-cap folding lemma [9, Lemma 2.2] (see also [3, 14]), the conformal volume of product tori in S^3 used in Section 11 [1], [9, Lemmas 2.3 and 2.4] (for $r_1 > 2/3$ the proof in [1] relies on a MAPLE computation), and the conformal bubbling lower bound [2, 12]. The new ingredient is the sharp truncated-area estimate (6). A normal-curvature and normal-chord analysis controls the high caps, with direct analytic estimates in four weight-centre strips; the low-weight region is handled by quartic moment inequalities, monotonicity of the cap kernel, elementary logarithmic bounds, and rational Bernstein positivity, and the residual high-weight caps by the same cap kernel, logarithmic bounds and Bernstein positivity on finitely many explicit rational boxes. On the complementary compact product domain, the product majorant is established by validated computation. All remaining signs are analytic or exact rational polynomial comparisons. The only inequality certified by validated numerics is Lemma 10.1, which is verified twice, independently, in Arb ball arithmetic and in binary64 interval arithmetic; the exact high-cap

certificate of Proposition 9.11 is also checked independently in ball arithmetic. Their derivation and finite verifications are documented in the appendices and the accompanying source supplement. The certificates form part of the proof. No conclusion for higher eigenvalues is inferred.

Appendix A. Exact rational positivity certificates

A.1. **Small-center Bernstein comparisons.** All assertions here are over $\mathbb{Q}$; they follow by elementary polynomial expansion and are verified in exact rational arithmetic by `small_centre_certificates.py`. For a polynomial $P(u,v)=\sum a_{k\ell}u^k v^\ell$ of bidegree at most (n,m), its coefficients in the tensor Bernstein basis are

$$b_{ij}=\sum_{k=0}^{i}\sum_{\ell=0}^{j} a_{k\ell}\frac{\binom{i}{k}}{\binom{n}{k}}\frac{\binom{j}{\ell}}{\binom{m}{\ell}},\quad 0\le i\le n,\quad 0\le j\le m. \tag{64}$$

The basis functions are nonnegative and sum to one, hence $P(u,v)\ge \min b_{ij}$ on $[0,1]^2$. Under restriction to an affine subrectangle one applies the same formula after the affine substitution. This defines all certificates below without dependence on a symbolic algebra package.

$u=17t/4$	$v=(h+1)/2$	lower bound for least Bernstein coefficient
$[0,1/2]$	$[0,1]$	>187
$[1/2,3/4]$	$[0,1/4]$	>51
$[1/2,1]$	$[1/4,1/2]$	>24
$[1/2,1]$	$[1/2,1]$	>265
$[3/4,1]$	$[0,1/8]$	>19
$[3/4,1]$	$[1/8,1/4]$	>2

Table 2. Exact lower bounds, using (64) of bidegree $(7,4)$, for the Bernstein coefficients of $P=2D(t)(H_t(h)-1/2)$. The six rectangles form an exact partition of the unit square.

Polynomial and normalized rectangle	Bidegree	Zeros	Least positive coefficient
$D(t)h_2(t)$, $u=17t/4\in[0,1]$	7	2	>31
$D(t)h_3(t)$, same	7	3	>11
$D(t)h_4(t)$, same	7	4	>7
P_A, $u=17t/4$, $R=1/3+7v/24$	$(7,2)$	4	$>1/2$
P_B, $u=17t/4$, $R=5/8+v/24$	$(7,3)$	0	$>1/3$

Table 3. Exact rational Bernstein coefficient bounds on full unit intervals/rectangles. The polynomials P_A, P_B and D are defined in the proof of Lemma 6.3.

For an independent arithmetical check, the exact minimum *positive* coefficients of P_A and the minimum coefficient of P_B are respectively

$$\frac{17052549075}{26261675072} > \frac{1}{2}, \qquad \frac{882755069353}{2256862701500} > \frac{1}{3}.$$

The four zero coefficients of P_A correspond to its boundary equality at $t = 0, R = 1/3$. For the one-variable Dh_j certificates, the exact least positive Bernstein coefficients are

$$\frac{64000}{2023}, \qquad \frac{409600}{34391}, \qquad \frac{4096000}{584647} \quad (j = 2, 3, 4).$$

These fractions and Tables 2–3 provide short, finite and hand-reproducible rational positivity certificates. They are not numerical sampling of a continuum.

A.2. **Quartic Hermite and moment-envelope identities.** Let $I_1 = [4/17, 10/29]$, $I_2 = [10/29, 680/1889]$. For either $I = [t_0, t_1]$, divide it into two halves $I_i = [t_0 + i(t_1 - t_0)/2, t_0 + (i + 1)(t_1 - t_0)/2]$, $i = 0, 1$, and divide $[-1, 1]$ into eight intervals $J_j = [-1 + j/4, -1 + (j + 1)/4]$, $0 \le j < 8$. Define the bivariate polynomials

$$P_{1,1}(t, h) = D(t)\left[H_t(h) + \frac{(1-h)^2}{17} - \frac{9}{20}\right],$$
$$P_{1,2}(t, h) = D(t)\left[H_t(h) + \frac{(1-h)^2}{14} - \frac{9}{20}\right].$$

These have bidegree at most $(7, 4)$. The following table gives *strict integer lower bounds* for the least of their 40 Bernstein coefficients on each rectangle $I_i \times J_j$; the bounds follow by substituting the rational endpoint data in (64).

	i	$j=0$	1	2	3	4	5	6	7
$P_{1,1}$	0	114	47	40	54	100	178	328	629
	1	129	28	2	6	36	90	219	552
$P_{1,2}$	0	215	34	4	6	32	81	205	541
	1	230	34	0	2	25	70	191	529

Every entry is strictly smaller than the actual least coefficient. For the entry written 0 in the last row, the exact minimum is

$$\frac{453066687288041190235175}{480630948788577613399122 4} > \frac{1}{12} > 0.$$

Thus every Bernstein coefficient on the specified rectangles is strictly positive.

For the moment envelopes, introduce

$$P_{2,1}(t, R) = D(t)\left[\frac{93}{100} - B(R, t)\right], \quad P_{2,2}(t, R) = D(t)\left[\frac{229}{250} - B(R, t)\right].$$

On the full rectangles $I_1 \times [1/3, 7/20]$ and $I_2 \times [1/3, 7/20]$, respectively, these have bidegree at most $(7, 2)$. Their least Bernstein coefficients are,

respectively,

$$\frac{426653190}{410338673} > 1, \qquad \frac{23681895118301658281116}{85826955140817430964129} > \frac{1}{4}.$$

Finally $D(t)h_j(t)$, $j = 2, 3, 4$, are one-variable polynomials of degree at most seven. Their least Bernstein coefficients on I_1 all exceed 127, and those on I_2 all exceed 97. The direct verification uses the one-variable version of (64). These exact comparisons establish every polynomial-sign assertion used in the proof of Theorem 7.1.

A.3. **The intermediate-centre rational sign.**

Proof of Lemma 7.4. Clearing the denominators in (34), using the following *specified positive* integer denominator,

$$\begin{aligned}\mathcal{D}_{\mathrm{mid}} = {} & 111284280(1+y^2)^2(5s^2-6s+5)^2(5y^2-32y+15)^3 \\ & \times \big((1-s)^2+(1+s)^2y^2\big)\big(5s^2-8s+5+(5s^2+2s+5)y^2\big)^3 \\ & \times \big(50s^2y^2+50s^2+35sy^2-96sy-35s+50y^2+50\big)^2,\end{aligned}$$

one finds that $\mathcal{N}_{\mathrm{mid}} := \mathcal{D}_{\mathrm{mid}}(1 - W_{\mathrm{mid}})$ is an integer polynomial of bidegree $(16, 22)$. Every displayed factor of $\mathcal{D}_{\mathrm{mid}}$ is strictly positive on the stated rectangle. The last factor is a positive multiple of $B - 2sd$.

For completeness the following table gives strict integer lower bounds for the least tensor Bernstein coefficient of $\mathcal{N}_{\mathrm{mid}}$ on each listed rational rectangle; the conversion is the binomial identity (64), applied with bidegree $(16, 22)$.

s-interval	y-interval	least coefficient greater than
$[17/40, 117/200]$	$[0, 1/2]$	1045937920126
$[117/200, 149/200]$	$[0, 1/4]$	40254425419694
$[117/200, 149/200]$	$[1/4, 1/2]$	1488390323358

All entries follow by expanding the explicitly factored rational expression (34) and applying (64); in particular no floating-point evaluation is used. Thus $\mathcal{N}_{\mathrm{mid}} > 0$ and $W_{\mathrm{mid}} < 1$ on the full rectangle. □

A.4. **The large-intermediate-centre rational sign.**

Proof of Lemma 7.5. The denominator can be chosen as the integer polynomial

$$\mathcal{D}_{\mathrm{end}} = -72F_1F_2^3F_3^2F_4,$$

where

$$\begin{aligned}F_1 &= x^4z^2 - 4x^2z^2 + x^2 + 4z^2,\\ F_2 &= x^4z^2 + 2x^2z^2 + x^2 - 8z^2 - 6,\\ F_3 &= 50x^6z^2 - 135x^4z^2 + 50x^4 + 96x^3z + 135x^2z^2 - 65x^2 - 96xz + 65,\\ F_4 &= 125x^6z^2 - 220x^4z^2 + 125x^4 + 192x^3z \\ &\qquad + 70x^2z^2 - 280x^2 - 192xz + 130.\end{aligned}$$

The polynomial $\mathcal{N}_{\mathrm{end}} := \mathcal{D}_{\mathrm{end}}(1 - W_{\mathrm{end}})$ has bidegree $(34, 14)$ and integer coefficients. On the full rectangle the least Bernstein coefficient of $\mathcal{D}_{\mathrm{end}}$, with this bidegree, is greater than $102300857 > 0$. For $\mathcal{N}_{\mathrm{end}}$, splitting both coordinate intervals into halves yields the following *strict integer lower bounds* for the least Bernstein coefficients (using (64)):

x-interval	z-interval	least coefficient greater than
$[1/5, 141/400]$	$[0, 1/2]$	1611848
$[1/5, 141/400]$	$[1/2, 1]$	4699163158
$[141/400, 101/200]$	$[0, 1/2]$	14479899
$[141/400, 101/200]$	$[1/2, 1]$	102060289

Thus $\mathcal{N}_{\mathrm{end}}, \mathcal{D}_{\mathrm{end}} > 0$ throughout this larger rectangle, and hence $W_{\mathrm{end}} < 1$. □

Appendix B. The product inequality: upper quadratures and certified bounds

The product region used here is

$$\frac{7}{20} \le R \le \frac{1936}{2561}, \qquad \frac{13}{100} \le s \le \sigma(R), \qquad \sigma(R) = \frac{2 + 52R - 32R^2}{25}. \tag{65}$$

The complementary high-weight parameter region is controlled by Theorem 9.1, while low-weight caps are covered by Theorem 7.6. The inequality on this region is established by the verification in ball arithmetic of Section B.3, and verified a second time, independently, by the interval certificate of Section B.4. Both use the upper chord rule of Section B.1. The completed execution records are collected in Appendix D.

B.1. **The upper chord rule.** Let $-1 = x_0 < x_1 < \cdots < x_N = 1$. For a convex function on $[-1, 1]$, the piecewise affine interpolant at these nodes lies above the function. Integrating the interpolant against the arcsine law $dx/(\pi\sqrt{1 - x^2})$, which is the law of $\cos u$ for a uniform angle u, gives a positive atomic upper rule. On $[x_j, x_{j+1}]$ the law has mass and first moment

$$\mu_j = \frac{\arcsin x_{j+1} - \arcsin x_j}{\pi}, \qquad \nu_j = \frac{\sqrt{1 - x_j^2} - \sqrt{1 - x_{j+1}^2}}{\pi},$$

and its contributions to the weights of x_j and x_{j+1} are $(x_{j+1}\mu_j - \nu_j)/(x_{j+1} - x_j)$ and $(\nu_j - x_j\mu_j)/(x_{j+1} - x_j)$; both are nonnegative, because $\nu_j/\mu_j \in [x_j, x_{j+1}]$. For the Chebyshev nodes $x_j = -\cos(j\pi/N)$ all masses equal $1/N$. No quadrature error estimate is inferred from convergence.

B.2. **An exact angular representation.** The product upper function also admits an exact reduction from a double integral to a single integral. Put

$$a = \sqrt{R}\,\alpha, \quad b = \sqrt{1 - R}\sqrt{1 - \alpha^2}, \quad P = 1 - s^2,\ B = 1 + s^2,\ \nu = \frac{P}{\sqrt{c(R)}}.$$

For fixed u, set $z = B - 2sa\cos u$ and $\beta = 2sb$. The positivity of $B - 2s(a+b) \geq (1-s)^2$ implies $z > \beta$. If $\beta > 0$ define $\vartheta \in [0, \pi]$ by

$$\vartheta = \begin{cases} 0, & z - \beta \geq \nu, \\ \pi, & z + \beta \leq \nu, \\ \arccos((z-\nu)/\beta), & \text{otherwise.} \end{cases}$$

Introduce

$$I_1(\vartheta; z, \beta) = \frac{2}{\sqrt{z^2 - \beta^2}} \arctan\left(\sqrt{\frac{z+\beta}{z-\beta}} \tan\frac{\vartheta}{2} \right),$$
$$I_2(\vartheta; z, \beta) = \frac{z I_1(\vartheta; z, \beta) + \beta \sin\vartheta/(z - \beta\cos\vartheta)}{z^2 - \beta^2}.$$

Interpret the expressions continuously at $\vartheta = \pi$; for $\beta = 0$ use $I_2 = \vartheta/z^2$. Direct integration of the cosine variable gives

$$\frac{1}{\pi}\int_0^\pi \Big(\frac{P^2}{(z - \beta\cos w)^2} - c(R)\Big)_+ dw = \frac{1}{\pi}\big(P^2 I_2(\vartheta; z, \beta) - c(R)\vartheta\big).$$

It follows that

Proposition B.1. *The product majorant of Proposition 5.1 satisfies the exact identity*

$$\mathcal{P}(R, s, \alpha) = \frac{\overline{A}(R)}{\pi^2} \int_0^\pi \big[P^2 I_2(\vartheta; z, \beta) - c(R)\vartheta\big]\, du.$$

The verification of Section B.3 applies the same primitive to a majorant that is uniform on parameter boxes; the interval certificate of Section B.4 does not use it.

B.3. **The verification in ball arithmetic.** This verification uses a single convex majorant of the integrand on each parameter box, integrates it over the second cosine variable with the primitive of Section B.2, reduces the amplitudes of a whole box to two elliptic arcs by convexity, and evaluates every bound in the ball arithmetic of Arb.

A majorant uniform on a box. For $0 < s < 1$ put $q_s = 2s/(1+s^2)$, so that $k_s(q_s)^2 = (1 - q_s^2)^{-1}$. Since

$$\partial_s k_s(q) = \frac{2\big((1+s^2)q - 2s\big)}{(1 + s^2 - 2sq)^2}$$

and q_s increases with s, for fixed q the function $s \mapsto k_s(q)$ increases while $q_s < q$ and decreases while $q_s > q$.

Lemma B.2. *Let $0 < s_0 < s_1 < 1$, $q_i = q_{s_i}$ and $v_i = (1 - q_i^2)^{-1}$, and let ℓ be the affine function with $\ell(q_0) = v_0$ and $\ell(q_1) = v_1$. Define F on $(-\infty, 1/q_1)$ by*

$$F = k_{s_0}^2 \text{ on } (-\infty, q_0], \qquad F = \ell \text{ on } [q_0, q_1], \qquad F = k_{s_1}^2 \text{ on } [q_1, 1/q_1).$$

Then F is continuous, convex and nondecreasing, and $k_s(q)^2 \le F(q)$ for $s_0 \le s \le s_1$ and $q < 1/q_1$.

Proof. For $s \le s_1$ the function k_s^2 is convex and increasing on $(-\infty, 1/q_s) \supset (-\infty, 1/q_1)$. By the monotonicity in s, the function $M(q) = \max_{s_0 \le s \le s_1} k_s(q)^2$ equals $k_{s_0}(q)^2$ for $q \le q_0$, $(1-q^2)^{-1}$ for $q_0 \le q \le q_1$, and $k_{s_1}(q)^2$ for $q_1 \le q < 1/q_1$. As a supremum of convex functions, M is convex, and ℓ is its chord over $[q_0, q_1]$. Hence $M \ge \ell$ outside $[q_0, q_1]$ and $M \le \ell$ on $[q_0, q_1]$, so that $F = \max(M, \ell)$ is convex and dominates M. Its three pieces are nondecreasing, since $0 < q_0 < q_1$ gives $v_0 < v_1$. □

Parameter boxes. Consider a box $[R_0, R_1] \times [s_0, s_1]$ with $7/20 \le R_0 < R_1 \le R_*$. Since $(1-R)(1+3R)$ decreases for $R > 1/3$, the function $\overline{A}$ is decreasing and $\bar{c}$ is increasing on $[7/20, R_*]$, and $\bar{c}(R_*) < 1$. Fix c and A with $0 < c \le \bar{c}(R_0)$ and $A \ge \overline{A}(R_0)$; then $c < 1 \le v_0$. Let F be the function of Lemma B.2 and $F_c = (F - c)_+$. Then $f_{R,s}(q) \le F_c(q)$ and $\overline{A}(R) \le A$ for $R_0 \le R \le R_1$, $s_0 \le s \le s_1$ and $|q| \le 1$. Put

$$\Phi(a,b) = \frac{1}{\pi^2} \int_0^\pi \int_0^\pi F_c(a\cos u + b \cos w)\, du\, dw \qquad (|a| + |b| < 1/q_1).$$

Since $\sqrt{R}\alpha + \sqrt{1-R}\sqrt{1-\alpha^2} \le 1 < 1/q_1$ by the Cauchy–Schwarz inequality, the majorant of Proposition 5.1 satisfies

$$\mathcal{P}(R, s, \alpha) \le A\, \Phi\big(\sqrt{R}\alpha, \sqrt{1-R}\sqrt{1-\alpha^2}\big) \tag{66}$$

for $R_0 \le R \le R_1$, $s_0 \le s \le s_1$ and $0 \le \alpha \le 1$. The function Φ is convex, as an average of convex functions of (a, b), and it is even in each variable because $\cos u$ and $-\cos u$ have the same distribution. Hence Φ is nondecreasing in $a \ge 0$ and in $b \ge 0$.

Amplitude arcs. For $0 < R < 1$ let E_R be the arc

$$\theta \mapsto (\sqrt{R}\sin\theta, \sqrt{1-R}\cos\theta), \qquad 0 \le \theta \le \pi/2.$$

It consists of the amplitude pairs in (66), with $\alpha = \sin\theta$, and it touches the line $a + b = 1$ at $(R, 1-R)$, where $\sin\theta = \sqrt{R}$. Let E_R^- and E_R^+ be its subarcs with $\sin\theta \le \sqrt{R}$ and $\sin\theta \ge \sqrt{R}$, respectively.

Lemma B.3. *Let $0 < R_0 \le R \le R_1 < 1$. Every point of E_R is dominated coordinatewise by a point of the convex hull of $E_{R_0}^- \cup E_{R_1}^+$. Consequently*

$$\sup_{E_R} \Phi \le \max\Big(\sup_{E_{R_0}^-} \Phi,\ \sup_{E_{R_1}^+} \Phi\Big).$$

Proof. The arc E_R is the graph of $e_R(a) = \sqrt{(1-R)(1-a^2/R)}$ over $[0, \sqrt{R}]$, and

$$e_{R'}(a)^2 - e_R(a)^2 = (R - R')\Big(1 - \frac{a^2}{RR'}\Big).$$

The subarc $E_{R_0}^-$ is the graph of e_{R_0} over $[0, R_0]$, and $E_{R_1}^+$ is that of e_{R_1} over $[R_1, \sqrt{R_1}]$. If $a \le R_0$, then $a^2 \le R_0 R$, so $e_R(a) \le e_{R_0}(a)$. If $a \ge R_1$,

then $a^2 \ge R_1 R$, so $e_R(a) \le e_{R_1}(a)$. If $R_0 \le a \le R_1$, then $e_R(a) \le 1-a$ by the Cauchy–Schwarz inequality, and $(a, 1-a)$ lies on the segment from $(R_0, 1-R_0) \in E_{R_0}^-$ to $(R_1, 1-R_1) \in E_{R_1}^+$. The convex hull lies in $\{a, b \ge 0,\ a+b \le 1\}$, so the second assertion follows from the convexity and the monotonicity of Φ. □

Pieces of an arc. With $t = \tan(\theta/2)$ one has $(\sin\theta, \cos\theta) = \big(2t/(1+t^2), (1-t^2)/(1+t^2)\big)$, which is rational for rational t. The subarcs E_R^- and E_R^+ correspond to $0 \le t \le t_*(R)$ and $t_*(R) \le t \le 1$, where $t_*(R) = \sqrt{R}/(1+\sqrt{1-R})$. Let $0 \le t_0 < t_1 \le 1$ correspond to $\theta_0 < \theta_1$. On the unit circle, the arc from θ_0 to θ_1 is dominated by the corner $(\sin\theta_1, \cos\theta_0)$, and it is contained in the triangle with the vertices $(\sin\theta_i, \cos\theta_i)$ and

$$\frac{1}{\sin(\theta_1-\theta_0)}(\cos\theta_0 - \cos\theta_1,\ \sin\theta_1 - \sin\theta_0),$$

the intersection of the tangent lines at its endpoints. The map $(x, y) \mapsto (\sqrt{R}x, \sqrt{1-R}\,y)$ preserves both properties. Hence, on the corresponding piece of E_R, the function Φ is bounded by its value at the image of the corner, and also by its maximum at the images of the three vertices of the triangle, provided these points satisfy $a + b < 1/q_1$.

The second cosine variable. Let $b > 0$ and $|y| + b < 1/q_1$. The number $q_c = (1 + s_0^2 - (1-s_0^2)c^{-1/2})/(2s_0)$ satisfies $k_{s_0}(q_c)^2 = c$ and $q_c < q_0$, because $v_0 > c$. Hence F_c vanishes on $(-\infty, q_c]$ and equals $F - c > 0$ on $(q_c, 1/q_1)$. With $\operatorname{clip}(x) = \min\{1, \max\{-1, x\}\}$ put

$$\omega_i = \arccos\operatorname{clip}\Big(\frac{q_i - y}{b}\Big) \quad (i = 0, 1), \qquad \omega_c = \arccos\operatorname{clip}\Big(\frac{q_c - y}{b}\Big).$$

Since $w \mapsto y + b\cos w$ decreases on $[0, \pi]$, the integrand $F_c(y + b\cos w)$ equals $k_{s_1}^2 - c$, $\ell - c$, $k_{s_0}^2 - c$ and 0 on the consecutive intervals with endpoints $0 \le \omega_1 \le \omega_0 \le \omega_c \le \pi$. Put $P_i = 1 - s_i^2$, $z_i = 1 + s_i^2 - 2s_i y$ and $\beta_i = 2s_i b$; then $z_i > \beta_i > 0$, because $y + b < 1/q_1 \le 1/q_i$. The function I_2 of Section B.2 gives $\int_0^\omega k_{s_i}(y + b\cos w)^2\, dw = P_i^2 I_2(\omega; z_i, \beta_i)$. Therefore, with ℓ' the slope of ℓ, the average $\mathcal{G}(y, b) = \pi^{-1}\int_0^\pi F_c(y + b\cos w)\, dw$ is

(67)
$$\begin{aligned}\pi\,\mathcal{G}(y,b) = {} & P_1^2 I_2(\omega_1; z_1, \beta_1) - c\,\omega_1 + (\ell(y) - c)(\omega_0 - \omega_1) + \ell' b\,(\sin\omega_0 - \sin\omega_1) \\ & + P_0^2\big(I_2(\omega_c; z_0, \beta_0) - I_2(\omega_0; z_0, \beta_0)\big) - c\,(\omega_c - \omega_0).\end{aligned}$$

For $b = 0$ we have $\mathcal{G}(y, 0) = F_c(y)$.

The first cosine variable. For $a, b \ge 0$ with $a + b < 1/q_1$, the function $x \mapsto \mathcal{G}(ax, b)$ is convex on $[-1, 1]$. For nodes $-1 = x_0 < x_1 < \cdots < x_N = 1$, replacing it by its chords as in Section B.1 gives

$$\Phi(a, b) = \frac{1}{\pi}\int_0^\pi \mathcal{G}(a\cos u, b)\, du \le \sum_{j=0}^{N} W_j\, \mathcal{G}(a x_j, b),$$

where $W_j \geq 0$ are the weights of the upper chord rule of Section B.1 for these nodes.

The certificate. The certificate lists 5400 boxes with rational endpoints. For each box it partitions an interval $[0, t_L]$ with $t_L > t_*(R_0)$, for $E^-_{R_0}$, and an interval $[t_R, 1]$ with $t_R < t_*(R_1)$, for $E^+_{R_1}$; altogether there are 30051 pieces with dyadic endpoints. Each piece is marked as a corner or a triangle and carries one of six node sets, $N \in \{16, 32, 64, 128, 256, 512\}$, whose interior nodes are dyadic rationals with denominator 2^{24} close to $-\cos(j\pi/N)$, the middle node being 0. The verifier checks the following obligations.

(i) The boxes lie in $7/20 \leq R \leq R_*$, $0 < s < 1$, and they cover the domain (65). As σ is increasing on $[7/20, R_*]$, it suffices that over each of the 203 slabs between consecutive R-endpoints of boxes, the s-intervals of the boxes containing the slab cover $[13/100, \sigma(\rho)]$, where ρ is the right end of the slab. This is checked in exact rational arithmetic.

(ii) The pieces of each partition are consecutive and contained in $[0, 1]$, and the inequalities $t_L > t_*(R_0)$ and $t_R < t_*(R_1)$ hold. The node lists increase strictly from -1 to 1.

(iii) $0 < c < v_0$, and every corner or triangle vertex (a, b) satisfies $1 + s_1^2 - 2s_1(a + b) > 0$, that is, $a + b < 1/q_1$.

(iv) At every such vertex, $A \sum_j W_j \mathcal{G}(ax_j, b) < 4\pi$, with $\mathcal{G}$ given by (67).

These obligations imply Lemma 10.1. Indeed, by (i) every admissible (R, s) lies in a box, and by (66) and Lemma B.3 it suffices to show $A\,\Phi < 4\pi$ on $E^-_{R_0}$ and on $E^+_{R_1}$. By (ii) these subarcs are covered by the pieces; by (iii) and the paragraph on pieces of an arc, Φ is bounded on each piece by its values at the vertices of the piece; and at each vertex $\Phi(a, b) \leq \sum_j W_j \mathcal{G}(ax_j, b)$, so that (iv) gives $A\,\Phi(a, b) < 4\pi$.

The computation uses the ball arithmetic of Arb, as included in FLINT 3.6.0, through python-flint 0.9.0 at a working precision of 96 bits. Every real quantity is represented by a ball that contains it: c and A are the lower and upper endpoints of balls containing $\bar{c}(R_0)$ and $\overline{A}(R_0)$, the clipping in ω_0, ω_1, ω_c is applied to both endpoints of the balls containing the quotients, and an inequality is accepted only if it holds for all points of the balls involved. Arb computes with its own arbitrary-precision arithmetic and rigorous error bounds, so this verification does not use the binary64 model of Section B.4. All obligations hold; the largest certified vertex bound is $12.566357268 < 4\pi$. The certificate was found by a floating-point search, which plays no role in its verification. In the supplement folder the verification is run by

```
python3 reproduce.py --product-ball
```

and takes about one minute on two processor cores. Two programs in the folder `diagnostics`, which are not part of the proof, compare (67) with numerical quadrature of the defining integral (agreement to 10^{-26}), and

check that the verifier rejects corrupted certificates: a missing box, a lowered top box, an enlarged box, an arc partition that stops short of $t_*(R_0)$ or leaves $[0,1]$, a gap between pieces, a vertex beyond the pole, a nonmonotone node list, and a threshold slightly below the largest bound of a box.

B.4. **An independent interval certificate.** Lemma 10.1 is verified a second time by a program that shares no code or data with Section B.3 and uses outward-rounded binary64 interval arithmetic. It applies the upper chord rule of Section B.1, with Chebyshev nodes, to each of the two cosine variables, which gives a tensor upper bound, and it treats the amplitudes as follows.

The product average is also jointly convex in its two amplitudes. Replace the quarter unit circle by its circumscribed polygon with the axis vertices and the tangent-intersection vertices

$$\sec\frac{\pi}{4M}\left(\cos\frac{(j+1/2)\pi}{2M},\sin\frac{(j+1/2)\pi}{2M}\right),\qquad 0\le j<M.$$

After scaling its coordinates by $\sqrt{R},\sqrt{1-R}$, the maximum at these $M+2$ vertices bounds the amplitude supremum in Proposition 5.1. Positivity of every denominator on the enlarged polygon is explicitly checked.

The implementation uses $M=256$. The hat rule is successively refined through the orders $N=32$, 64, 128, 256, and 512. Each accepted box bounds *all* (R,s) it contains. For a fixed quadrature atom, its height has the form $A\sqrt{R}+B\sqrt{1-R}$. Its maximum over an R interval occurs at an endpoint or, when $A,B>0$, at $R=A^2/(A^2+B^2)$, where its value is $\sqrt{A^2+B^2}$. The maximum of $k_s(q)^2$ over an s interval is likewise at an endpoint or at its unique critical radius; at the latter point its value is $(1-q^2)^{-1}$.

Constants, trigonometric nodes, positive hat weights, and polygon vertices are enclosed by `mpmath.iv` at 70 decimal digits and converted outward to IEEE754 binary64. Basic operations and square roots are rounded outward using `nextafter`. Positive sums with n terms are increased by $1/(1-n2^{-53})$. The actual binary64 bounds generated in this way are independently checked by exact rational arithmetic: a 32-term alternating Machin formula encloses π, 24-term alternating Taylor polynomials enclose all sine and cosine values, and an integer square encloses $\sqrt{3}$. This check verifies all 258 polygon-vertex intervals, every quadrature node, all 351173 tensor weights, the scalar constants, and the 115 distinct area-envelope bounds used by accepted boxes. Thus the proof does not assume the correctness of the transcendental outputs of `mpmath.iv`. It retains the explicit assumption of correctly rounded IEEE754 basic arithmetic and square root. No tolerance-based equality or unvalidated mesh maximum is accepted. A defensive branch includes the critical-height candidate whenever the lower bound for its squared norm is nonpositive, including the exactly zero quadrature atom.

The main run examined 3106 boxes and accepted 1530 boxes, with no unresolved box. An independent exact rational sweep through the 115 vertical

slabs determined by their endpoints verifies that these boxes cover the entire curved domain. A separate 9-box run, with 5 accepted boxes, covers the tiny interval between 13/100 and its binary64 literal; thus (65) has exactly the rational endpoints displayed above.

The largest accepted main upper bound is

$$12.566370563416791 < 12.56637061435917 < 4\pi.$$

The boundary-strip upper bound is 12.540953041914735. Every accepted main box is evaluated a second time, independently of the search, by a replay program that calls the same upper-bound routine, including the defensive branch; every box is accepted again. The replay record, the exact coverage checker, the source code and the SHA-256 checksums are part of the supplement. In the supplement folder, the reproduction driver runs the product replay, the endpoint strip, the exact constant checks and the coverage check:

```
python3 reproduce.py --product
```

The driver creates a fresh working directory with the relative paths expected by the scripts.

Product-certificate identifiers. The main certificate read by the replay and the numerical producer have SHA-256 digests

```
product_certificate_largeR.json:
1ff9f59f70686cb71ea48e4ce7effe6ce404789498579e2028b9f182cb879069
product_interval_certificate.py:
606b8650fe9faa263511006166fc493954bc7fdf49f1a44bb85c56484c9ed73c
```

The replay evaluates every box of this certificate again and writes the record `product_certificate_largeR_rechecked.json`. That record also stores its running time, so its digest differs from run to run. The record of the reference run, the summary `product_certificate_summary.json` and the independent constant check `product_constants_exact_audit.json` are included in the supplement.

Appendix C. The residual high-cap certificate

This appendix describes the finite certificate of Proposition 9.11 and its two verifications. The certificate consists of rational data only; the first verification uses exact rational arithmetic throughout, and the second, independent one is described in Section C.4.

C.1. **Cells, bands and boxes.** Each of the 44 cells is stored as a file in the folder `highcap_certificate` of the supplement. All numbers are exact rationals written as quotients of integers. A direct cell records R_{lo}, R_{hi}, ρ and an interval $[s_{\mathrm{lo}}, s_{\mathrm{hi}}]$ of centre radii; a quadratic cell records R_{lo}, R_{hi}, ρ, $\widehat{K}$, $\bar{a}$ and an interval $[x_{\mathrm{lo}}, x_{\mathrm{hi}}]$ with $s(x_{\mathrm{hi}}) \le \sigma(R_{\mathrm{lo}})$. Every box records x_a, x_b, z_a, z_b, the constants $\overline{R}$, ω and χ (direct cells) or $\overline{R}$, ω, η, b (quadratic cells), and w_0, Θ. Boxes with common constants form a *band*.

Direct cell	ρ	centre radii	bands	boxes
$7/20 \le R \le 19/50$	$6697/10^4$	$s(37/100) \le s \le 9/10$	24	211
$19/50 \le R \le 41/100$	$1341/2000$	$s(179/500) \le s \le 9/10$	22	195
$41/100 \le R \le 11/25$	$6719/10^4$	$s(173/500) \le s \le 9/10$	20	179
$11/25 \le R \le 47/100$	$337/500$	$s(167/500) \le s \le 9/10$	18	163
$47/100 \le R \le 1/2$	$6769/10^4$	$s(161/500) \le s \le 9/10$	16	147
$1/2 \le R \le 53/100$	$1361/2000$	$s(311/1000) \le s \le 23/25$	18	171
$53/100 \le R \le 3/5$	$137/200$	$\sigma(53/100) \le s \le 23/25$	19	178
$3/5 \le R \le R_*$	$139/200$	$\sigma(3/5) \le s \le 47/50$	16	163

Each quadratic cell has a weight interval of length $1/200$. The quadratic cells lying under one direct cell share the left endpoint x_{lo}, which is the right endpoint of the x-interval of that direct cell:

Weights	x_{lo}	range of ρ	cells	bands	boxes
$7/20 \le R \le 19/50$	$37/100$	$[6697, 6703]/10^4$	6	28	825
$19/50 \le R \le 41/100$	$179/500$	$[6705, 6716]/10^4$	6	28	711
$41/100 \le R \le 11/25$	$173/500$	$[6719, 6736]/10^4$	6	27	567
$11/25 \le R \le 47/100$	$167/500$	$[6740, 6763]/10^4$	6	27	442
$47/100 \le R \le 1/2$	$161/500$	$[6769, 6799]/10^4$	6	27	311
$1/2 \le R \le 53/100$	$311/1000$	$[6805, 6842]/10^4$	6	22	176

In every cell ρ is a rational number with at most four decimal digits slightly below $\sqrt{\overline{c}(R_{\mathrm{lo}})}$, and in every quadratic cell $\widehat{K}$ and $\bar{a}$ are rationals slightly above $\frac{4}{3}\sqrt{2/3}/\rho$ and $a_{R_{\mathrm{lo}}}$. The constants Θ have denominators at most 10^{30}. In direct cells $\mathscr{F}$ has bidegree $(38, 20)$ in (x, z) and D_n, D_u have bidegree $(6, 2)$; in quadratic cells $\mathscr{F}$ has bidegree $(36, 24)$, D_n bidegree $(4, 2)$ and D_u bidegree $(0, 2)$. The boxes and the band constants were found by an adaptive subdivision search; only the verification below is part of the proof.

C.2. **Verification obligations.** The program `highcap_exact_verify.py` reads the 44 files and checks the following statements, in exact rational arithmetic.

(a) *Cell constants.* $7/20 \le R_{\mathrm{lo}} < R_{\mathrm{hi}} \le R_*$, $0 < \rho < 1$, and (53), through $2(56/97 - 106/333) > \rho^2 U$ for a rational $U \ge \sqrt{(1 - R_{\mathrm{lo}})(1 + 3R_{\mathrm{lo}})}$. In quadratic cells, $\widehat{K} > 0$, $\widehat{K}^2\rho^2 \ge 32/27$ and $\bar{a}^2 \ge (\pi_+/2)^2(1 - R_{\mathrm{lo}})(1 + 3R_{\mathrm{lo}})$, where $\pi_+ > \pi$ is a rational upper bound obtained from Machin's formula with alternating-series remainders.

(b) *Box constants.* For every box, (55) with its own x_a; in direct cells (59) and (57) with its own x_b; in quadratic cells $0 < \eta < 1$, $b > 0$, $\tau^2 > \overline{R}^2 + \omega^2$, the three conditions equivalent to (60) stated before Proposition 9.10, where the quadratic inequality in X is checked at both endpoints and, when it lies inside, at the vertex.

(c) *Logarithmic constants.* $w_0 = x_a^2 + \chi^2 z_a^2$, respectively $w_0 = x_a^4 + \eta^2 z_a^2$, and $e^{\Theta} \ge 1/(\rho w_0)$, respectively $e^{\Theta} \ge (x_b^4 + \eta^2)/((1 + \eta^2)w_0)$, by the exponential series as described after Lemma 9.4.

(d) *Polynomial signs.* The polynomials D_n, D_u and $\mathscr{F}$ are expanded in the monomial basis from the formulas of Section 9; each variable is substituted affinely, $x = x_a + (x_b - x_a)t$ and $z = z_a + (z_b - z_a)t'$, and all tensor Bernstein coefficients (64) on $[0,1]^2$ are computed and found positive. A missing monomial counts as a zero coefficient, so the test can only fail conservatively.

(e) *Bands.* Let $x_0 < x_1$ be consecutive points among all endpoints x_a, x_b of the boxes of a cell. All boxes of the cell whose x-interval contains $[x_0, x_1]$ carry the same band constants, and their z-intervals cover $[0,1]$ without gaps.

(f) *Cells.* In a direct cell the x-intervals of the boxes cover an interval $[x_-, x_+]$ with $s(x_-) \geq s_{\mathrm{hi}}$ and $s(x_+) \leq s_{\mathrm{lo}}$; in a quadratic cell they cover exactly $[x_{\mathrm{lo}}, x_{\mathrm{hi}}]$.

(g) *Coverage of $\mathcal{D}_{\mathrm{hi}}$.* Let $7/20 = \varrho_0 < \cdots < \varrho_N = R_*$ be all endpoints of weight intervals of cells together with $1/2$ and $3/5$. For each $[\varrho_{j-1}, \varrho_j]$ the intervals of centre radii of the cells whose weight intervals contain it, namely $[s_{\mathrm{lo}}, s_{\mathrm{hi}}]$ for direct cells and $[\sigma(R_{\mathrm{lo}}), s(x_{\mathrm{lo}})]$ for quadratic cells, cover $[\sigma(\varrho_{j-1}), s_{\mathrm{top}}]$, where s_{top} is the largest value of $s_{\mathrm{top}}(R)$ on that interval. Since σ increases, this covers every $(R,s) \in \mathcal{D}_{\mathrm{hi}}$.

Items (a)–(c) and (e)–(g) verify parts (i)–(iii) of Proposition 9.11, and item (d) verifies part (iv).

C.3. **Arithmetic and execution.** All computations use the exact rational type `Fraction` of the Python standard library. If the optional package `python-flint` is installed, the Bernstein conversion uses its exact rational type `fmpq` for speed; the outcome does not depend on this choice. No floating-point number enters any assertion. The command

```
python3 reproduce.py --high-cap
```

runs the verification of all 44 cells, in parallel processes when available, and prints `PASS` only after every obligation above has been checked. With `python-flint` it takes about twenty minutes on two processor cores.

Two further programs in the folder `diagnostics` are not part of the proof. The first evaluates, with sixty significant digits, the closed forms of Propositions 9.5 and 9.9 at the corners and centres of all boxes, compares them with numerical quadrature of the defining integrals (agreement to 10^{-25}), checks that the logarithmic majorant dominates them and is smaller than 1, and compares that majorant with $1 - \mathscr{F}/(2\mathcal{M})$, respectively $1 - \mathscr{F}/(2\mathcal{N})$, for the polynomials built by the verifier (agreement to 10^{-40}). The second checks that the verifier rejects corrupted certificates: a missing box, a threshold ρ that is too large, constants $\bar{a}$ or Θ that are too small, a modified τ, χ or $\overline{R}$, inconsistent band constants, an overstated range of centre radii, and a bulk term enlarged by one per cent in the cell where the majorant is largest.

C.4. **A second verification in ball arithmetic.** The program `highcap_ball_verify.py` verifies Theorem 9.1 independently of the verification above. It shares no code with it and uses neither the polynomials D_n, D_u, $\mathscr{F}$ of Propositions 9.7 and 9.10 nor the logarithmic series bounds and the constants w_0, Θ. It reads the same cells and boxes and checks the following statements.

- (a′) The cell and box constants satisfy the hypotheses of Lemmas 9.2, 9.3 and 9.8 and of Propositions 9.5 and 9.9, including (59) for the parametrization of Lemma 9.6: rational conditions are checked exactly, and the conditions involving π and $\sqrt{3}$ with Arb balls. Conditions on an interval of centre radii are reduced to its endpoints through the monotonicity of q_ρ (Lemma 9.2) and of $B+2sb-\widehat{K}P = (1+\widehat{K})s^2+2bs+1-\widehat{K}$ for $s>0$.
- (b′) The band and coverage statements (e)–(g) of Section C, with separate code.
- (c′) On every box $[x_a,x_b]\times[z_a,z_b]$, the right-hand side of (58) in direct cells, or of (61) in quadratic cells, written as a function of (x,z) through the parametrizations of Section 9 and with the exact logarithms, is enclosed in ball arithmetic on sub-boxes obtained by bisection, until each enclosure lies below 1. In a direct cell a sub-box on which $m\le q_\rho(s)$ holds throughout is discarded, because $J=0$ there by Proposition 9.5; in a quadratic cell the value at $z=1$ also covers the case $m<\tau$, because $I(\tau)=0$.

By Propositions 9.5 and 9.9, statements (a′)–(c′) imply Theorem 9.1. The computation uses Arb at 96-bit precision, as described in Appendix D.3; the 4439 boxes are split into 679475 sub-boxes, and every check passes. A program in the folder `diagnostics` checks that this verifier rejects corrupted certificates, among them a missing box, a threshold ρ that is too large, a constant $\bar a$ below $a_{R_{\mathrm{lo}}}$, inadmissible constants $\overline{R}$ or χ, a negative constant $\widehat{K}$, an overstated range of centre radii, a missing cell, and a constant $\bar a$ enlarged by five per cent in one quadratic cell. The command

```
python3 reproduce.py --high-cap-ball
```

runs it in about ten seconds on two processor cores.

Appendix D. Certificate obligations, arithmetic model, and reproducibility

D.1. **Finite proof obligations.** The only input certified by validated numerics is the product inequality

$$\mathcal{P}(R,s,\alpha)<4\pi \qquad \Big(\frac{7}{20}\le R\le R_*,\quad \frac{13}{100}\le s\le \sigma(R),\quad 0\le\alpha\le 1\Big)$$

on the entire closed parameter set; it is an inequality for the full real domain, not for samples of a mesh. It is established by the verification in ball arithmetic of Section B.3, which bounds every parameter box through a

convex majorant with an explicit cosine average and an exact covering of the amplitude arcs. It is verified a second time by the interval certificate of Section B.4, which uses a positive upper quadrature and a circumscribed polygon for amplitude directions and accepts a box only after strict control of its entire range, or reduction to a justified maximizing face. The two programs share no code or data, both certificates cover the whole domain, as checked in exact rational arithmetic, and each of them establishes Lemma 10.1 on its own. The strips of Theorem E.1 lie in this domain; there Appendix E gives a third, exact, check of the resulting bound $J < 4\pi$, and of the product inequality itself on part of them.

The low-weight region and the residual high caps of Theorem 9.1 have no obligation certified by validated numerics: the quantities in Sections 7 and 9 are converted to the explicit rational polynomials specified there, and their signs follow from the Bernstein basis and exact rational comparisons. The supplementary rational checkers supply machine-readable expansions of these polynomial identities. For the residual high caps, the exact verification described in Appendix C is part of the proof, and the verification in ball arithmetic of Section C.4 is an independent second check.

D.2. **Completed finite verification records.** The verifications in ball arithmetic of Sections B.3 and C.4 were run with Python 3.13.18 and python-flint 0.9.0 (FLINT 3.6.0); the certificate of Section B.3 was produced by a floating-point search with NumPy 2.5.3, which is not part of the proof. The interval certificate of Section B.4 was produced with Python 3.12.14, NumPy 2.3.5 and mpmath 1.3.0, with independent rational checks of its transcendental bounds; the replay of every accepted box and the exact audits recorded in the supplement were obtained with Python 3.13.18, NumPy 2.5.3 and mpmath 1.3.0. The accepted boxes and maximal strict upper bounds are:

Domain	Evaluated boxes	Accepted leaves	Certified upper bound
Product, ball arithmetic	5400	5400	$J < 12.566357268$
Product, interval, main	3106	1530	$J < 12.566370564$
Product, interval, endpoint strip	9	5	$J < 12.540953042$

The table records upward-rounded display bounds. The exact rational lower bound for 4π exceeds 12.566370614. Both product coverage checks are exact over the curved parameter domain. The residual high-cap certificate consists of 44 cells with 4439 boxes; on every box all Bernstein coefficients of the polynomials of Section 9 are positive, the coverage of $\mathcal{D}_{\mathrm{hi}}$ is checked exactly (Appendix C), and the second verification encloses the closed-form majorants below 1 on 679475 sub-boxes (Section C.4). The low-weight caps are treated by the rational identities of Section 7.

D.3. **Validated arithmetic and coverage.** The verifications in ball arithmetic use Arb [8], as included in FLINT 3.6.0 [4], through python-flint 0.9.0 [24], at a working precision of 96 bits: every operation, including square roots, logarithms and inverse trigonometric functions, returns a ball

containing the exact result, and an inequality is accepted only if it holds on the whole balls. These verifications do not depend on a floating-point model. The interval certificate bounds circular averages by positive upper chord quadratures and controls the amplitude quarter-circle by an external convex polygon. No numerical mesh maximum is used. Its enclosures assume IEEE-754 binary64 arithmetic with correctly rounded basic operations and square roots; each elementary operation is enlarged by an adjacent representable number. Its trigonometric and quadrature constants, enclosed with mpmath [18], are checked by exact rational bounds based on Machin's formula, Taylor polynomials and integer square bounds. NumPy [6] is used by the interval certificate and by the searches that produced the certificates, and SymPy [16] by the second check of the product strips of Appendix E. Every domain coverage is checked in exact rational arithmetic, and the exact verification of the residual high caps uses exact rational arithmetic only.

D.4. **Source integrity and execution.** The supplement is the folder `Pigazzini_KLO_Supplement` that accompanies this article; in the arXiv version of the article it is distributed as ancillary files. Its manifest contains SHA-256 digests of every included file except the manifest itself. The principal source identifiers are

```
product_ball_verify.py:
   c51433da7aee06f255fc4a4a0a8dce48aed9c086fa86530fc007191338f64ffc

   product_ball_certificate.json:
   ada644ca8f798ee0e965be75dcd85131884f681e3bebef6eee943c6e6fec6314

   product_interval_certificate.py:
   606b8650fe9faa263511006166fc493954bc7fdf49f1a44bb85c56484c9ed73c

   highcap_exact_verify.py:
   f3b9b6136e618862d1b9a7e8cfa7dfeaa2ef35f05a665e9b074d6c73030d239f

   highcap_ball_verify.py:
   289baa191551cb62b2b308e9a409ee4cebd35684558850261c1366c566149737
```

In the supplement folder, the verification commands are

```
python3 reproduce.py --verify-files
python3 reproduce.py --rational
python3 reproduce.py --product-ball
python3 reproduce.py --product
python3 reproduce.py --high-cap
python3 reproduce.py --high-cap-ball
```

The reproducer creates a fresh working directory for every run and uses no checkpoint. Full success means that both product certificates are accepted without unresolved boxes, that the obligations of Appendix C hold in both verifications, and that all recorded rational inequalities and domain coverage checks pass. The certificate code and data accompany this article as part of the proof. The programs were written with the help of AI tools (see the Statements and Declarations). The proof depends only on what these programs check, not on how they were written: every comparison is an

exact rational inequality or is made in validated ball or interval arithmetic, each of the two main computer-assisted steps is verified by two independent programs, and the negative tests in the folder `diagnostics` confirm that perturbed certificates are rejected.

Remark D.1 (Size of the margins). In the verification in ball arithmetic of Section B.3, whose boxes were refined until their bounds were below 4π by about 10^{-5}, the smallest margin is $1.33 \cdot 10^{-5}$. The boxes of the interval certificate are stopped as soon as their outward upper bounds are strictly below 4π, so that its smallest leaf margins may be of order 10^{-8}. These margins do not measure the intrinsic strength of the geometric estimates, and the certified bounds in Section 10 hold on the full continuous domains independently of numerical optimization. For orientation only, and without use in the proof, a floating-point maximization gives $\sup \mathcal{P} \approx 12.518$ on the product region, compared with $4\pi \approx 12.566$. In the high-cap certificate every comparison is an exact rational inequality; sampled values of its majorant are recorded in the remark following the proof of Theorem 9.1. The scale of the bounds in the exact check of Appendix E is discussed in Sections E.2 and E.3.

Appendix E. An exact rational check on product strips

Lemma 10.1 covers the whole product domain and, through Proposition 5.1, gives $J < 4\pi$ there. This appendix proves $J < 4\pi$ on three substrips of that domain by a different method, exact moments and rational Bernstein positivity, which uses no interval or floating-point arithmetic; on part of these strips it also proves the product bound $\mathcal{P} < 4\pi$ itself. It is an independent check on these strips and is not used in the proof of Theorem 2.2.

E.1. **Statement and the higher-order mechanism.** Throughout this appendix, $R = r_1$ is the largest weight, $t = s/(1+s^2)$, and

$$f_t(q) = \frac{1-4t^2}{(1-2tq)^2}, \qquad Q = \sqrt{R}\,\alpha\cos u + \sqrt{1-R}\sqrt{1-\alpha^2}\cos w,$$

where u, w are independent uniform angles and $0 \le \alpha \le 1$. The majorant is precisely

$$\mathcal{P}(R,s,\alpha) = \overline{A}(R)\mathbb{E}\big(f_t(Q) - \bar{c}(R)\big)_+, \qquad \bar{c}(R) = L/\overline{A}(R).$$

Theorem E.1 (Rational-algebraic product bounds)**.** *For every fundamental torus whose largest weight R and centre radius s lie in one of the following regions, and every unit direction p, the strict inequality $J(r,s,p) < 4\pi$ holds:*

$$\begin{aligned} &\frac{7}{20} \le R \le R_*, && \frac{1}{4} \le s \le \frac{3}{10};\\ &\frac{7}{20} \le R \le \frac{2}{5}, && \frac{3}{10} \le s \le \frac{7}{20};\\ &\frac{9}{20} \le R \le R_*, && \frac{3}{10} \le s \le \frac{1}{2}. \end{aligned}$$

In the last region the stronger inequality

$$\mathcal{P}(R,s,\alpha) < 4\pi \qquad (0 \le \alpha \le 1)$$

holds. The first region admits this stronger product bound for $R \ge 9/20$ *as well.*

The first two regions follow from quartic interpolation, the three-frequency moments and, at larger R, the two-cosine fourth moment; the exact rational comparisons appear in Section E.2. We describe here the common higher-order mechanism for $3/10 \le s \le 1/2$.

Let $V = \{v_1, \dots, v_k\} \subset (-1,1)$ be distinct rational numbers and put $p_t = 1/(2t) > 1$ and $W_V(q) = (q-1)\prod_{v\in V}(q-v)^2$. Define

$$H_{V,t}(q) = f_t(q)\left[1 - \frac{W_V(q)}{W_V(p_t)}\left(1 + (p_t - q)\frac{W_V'(p_t)}{W_V(p_t)}\right)\right]. \tag{68}$$

Lemma E.2. *For* $0 < t < 1/2$, $H_{V,t}$ *is a polynomial in* q *of degree at most* $2k$, *satisfying* $H_{V,t}(q) \ge f_t(q)$ *for every* $q \in [-1,1]$.

Proof. In (68), the numerator before division by $(1-2tq)^2$ has a double zero at $q = p_t$, hence is divisible by $(1-2tq)^2$. Its quotient has degree at most $2k$. For $q \le 1$, $W_V(q) \le 0$, whereas $W_V(p_t) > 0$ and

$$\frac{W_V'(p_t)}{W_V(p_t)} = \frac{1}{p_t - 1} + 2\sum_{v\in V}\frac{1}{p_t - v} > 0.$$

The identity for $f_t - H_{V,t}$ obtained from (68) is therefore nonpositive. □

With $x = \alpha^2$, the even moments are explicit:

$$M_{2j}(R,x) = \mathbb{E}Q^{2j} = \sum_{i=0}^{j} \frac{\binom{2j}{2i}\binom{2i}{i}\binom{2j-2i}{j-i}}{4^j}(Rx)^i((1-R)(1-x))^{j-i}. \tag{69}$$

All odd moments vanish. Consequently, every polynomial $H_{V,t}$ can be integrated exactly against the two-cosine distribution. The choices

$$V = \left\{-\frac{4}{5}, -\frac{2}{5}, 0, \frac{2}{5}, \frac{4}{5}\right\} \quad \left(\frac{3}{10} \le s \le \frac{9}{20}\right)$$

and

$$V = \left\{-\frac{9}{10}, -\frac{3}{5}, -\frac{3}{10}, \frac{3}{10}, \frac{3}{5}, \frac{9}{10}\right\} \quad \left(\frac{9}{20} \le s \le \frac{1}{2}\right)$$

lead to polynomial bounds of degrees ten and twelve. A nonnegative quadratic correction $\gamma(t,R)(1-q)^2$ makes each polynomial dominate the positive truncation level. Using (69), this reduces the global inequality to two explicit, strictly positive rational polynomials on fixed compact boxes; their exact definitions, comparisons and rational Bernstein data are in Section E.3.

Proof of Theorem E.1. The quartic comparisons of Section E.2 cover the first two strips. In the last strip, Lemma E.2 and the exact even moments, combined with the rational positivity lemmas of Section E.3, yield $\mathcal{P}(R,s,\alpha) < 4\pi$ uniformly for $0 \le \alpha \le 1$. Proposition 5.1 then gives $J(r,s,p) < 4\pi$. □

E.2. **Quartic product strips.**

E.2.1. *Quartic Hermite majorants and rational comparisons.* Throughout this subsection, write $c(R) = L/\overline{A}(R)$. Set $t = s/(1+s^2)$ and $f_t(h) = (1-4t^2)/(1-2th)^2$. At $x = -1/5$ and $y = 1/4$ put $d = y - x$ and

$$\begin{aligned} U_2 &= \frac{f_t(y) - f_t(x) - f_t'(x)d}{d^2}, \\ U_3 &= \frac{f_t'(y) - f_t'(x) - 2U_2 d}{d^2}, \\ U_4 &= \frac{N_4}{(1-x)^2(1-y)^2}, \\ N_4 &= f_t(1) - f_t(x) - f_t'(x)(1-x) - U_2(1-x)^2 \\ &\quad - U_3(1-x)^2(1-y). \end{aligned}$$

Define the quartic

$$\begin{aligned} H_t(h) &= f_t(x) + f_t'(x)(h-x) + U_2(h-x)^2 \\ &\quad + U_3(h-x)^2(h-y) + U_4(h-x)^2(h-y)^2 \\ &= \sum_{j=0}^{4} h_j(t) h^j. \end{aligned} \tag{70}$$

The fifth derivative of f_t is positive for $0 < t < 1/2$. Its Hermite remainder at double nodes x, y and the simple node 1 gives

$$f_t(h) \le H_t(h) \quad (-1 \le h \le 1). \tag{71}$$

Introduce the positive polynomial

$$D(t) = (2-t)^3(1-2t)(5+2t)^3.$$

The expressions $d_j(t) := D(t)h_j(t)$ are degree-≤ 7 polynomials in $\mathbb{Q}[t]$. The finite sign verifications below are made using the exact Bernstein identity: for a polynomial P of bidegree at most (n, m), after affine transformation of a rectangle to $[0,1]^2$,

$$\beta_{ij} = \sum_{k=0}^{i} \sum_{\ell=0}^{j} \frac{\binom{i}{k}\binom{j}{\ell}}{\binom{n}{k}\binom{m}{\ell}} a_{k\ell}, \qquad P(U,V) = \sum_{k,\ell} a_{k\ell} U^k V^\ell. \tag{72}$$

Because the Bernstein basis is nonnegative and sums to one, $P \ge \min \beta_{ij}$ on the rectangle. All quantities below are rational; no floating-point inequalities are invoked.

Lemma E.3 (Finite exact comparisons)**.** *For $4/17 \le t \le 140/449$ one has $d_2, d_3, d_4 > 0$, and for $4/17 \le t \le 30/109$ the same positivity holds. Furthermore:*

(a) *For $4/17 \le t \le 140/449$ and $-1 \le h \le 1$,*

$$H_t(h) + \frac{1}{40}(1-h)^2 > \frac{23}{50}, \qquad h_0 + \frac{1}{5}h_2 + \frac{1}{10}h_3 + \frac{1}{10}h_4 < \frac{969}{1000}.$$

(b) *For* $4/17 \le t \le 30/109$ *and* $-1 \le h \le 1$,

$$H_t(h) > \frac{23}{50}, \qquad h_0 + \frac{9}{40}h_2 + \frac{9}{80}h_3 + \frac{81}{640}h_4 < \frac{1999}{2000}.$$

(c) *For* $4/17 \le t \le 30/109$ *and* $-1 \le h \le 1$,

$$H_t(h) + \frac{1}{200}(1-h)^2 > \frac{47}{100}.$$

(d) *For* $4/17 \le t \le 30/109$, $1/2 \le R \le R_*$ *and* $-1 \le h \le 1$, *with*

$$\gamma(R) = \frac{R}{4} - \frac{3}{25}, \qquad c_{\mathrm{lin}}(R) = \frac{47}{100} + \frac{R-1/2}{2},$$

one has $H_t(h) + \gamma(R)(1-h)^2 > c_{\mathrm{lin}}(R)$.

The following table describes exact lower bounds for the Bernstein coefficients of the cleared rational polynomials; a positive integer in the final column is a strict lower bound unless the entry is a fraction.

Cleared difference	*Rational partition*	*Lower bound*
(a) $D(H_t + (1-h)^2/40 - 23/50)$	*Two equal* t*-halves; eight equal* h*-intervals, with* $[-1/2, -1/4]$ *split once more in the upper* t*-half*	> 1
(a) $D(969/1000 - B_{2/5})$	*Full* t*-interval*	> 1
(b) $D(H_t - 23/50)$	*Two equal* t*-halves; eight equal* h*-intervals*	> 1
(b) $D(1999/2000 - B_{9/20})$	*Full* t*-interval*	> 0
(c) $D(H_t + (1-h)^2/200 - 47/100)$	*Six* h*-intervals specified below*	> 1
(d) $D(H_t + \gamma(R)(1-h)^2 - c_{\mathrm{lin}}(R))$	*Same six* h*-intervals; verify at* $R = 1/2$ *and* $R = R_*$	> 1

The six h*-intervals in (c)–(d) have endpoints* $-1, -1/2, -3/8, -1/4, 0, 1/2, 1$.

Here $B_R = h_0 + (h_2/2 + h_3/4)R + (5h_4/8)R^2$, *and in (a) and (b) the last entries mean* $B_{2/5}$ *and* $B_{9/20}$ *respectively. In (a) the last coefficient is* $h_4/10$ *since* $(5/8)(2/5)^2 = 1/10$. *In (b) the last coefficient is* $(5/8)(9/20)^2 = 81/640$. *Formula (72), (70) and the listed rational subdivisions specify each finite comparison without an unspecified numerical search.*

E.2.2. *Uniform quartic estimates for smaller weights.* The Fourier moments of the original three-mode height function $q = p \cdot F_r$ satisfy, when $R \le 2/3$,

$$\mathbb{E}q = 0, \quad \mathbb{E}q^2 \le R/2, \quad |\mathbb{E}q^3| \le R/4, \quad \mathbb{E}q^4 \le 5R^2/8. \tag{73}$$

If $Q_\gamma(h) = H_t(h) + \gamma(1-h)^2 \ge c(R)$, then (71) yields

$$\big(f_t(h) - c(R)\big)_+ \le H_t(h) + \gamma(1-h)^2 - c(R).$$

The right-hand side is everywhere nonnegative, so $A(r) \le \overline{A}(R)$ and (73) give

$$J(r,s,p) \le \overline{A}(R)\,(B_R + \gamma(1 + R/2)) - L. \tag{74}$$

Both $c(R)$ and B_R are increasing in $R \geq 1/3$, because $\overline{A}(R)$ decreases and $h_2, h_3, h_4 > 0$. Elementary rational bounds $\sqrt{3} > 265/153$, $\pi < 22/7$ and $\sqrt{517}/20 > 113/100$ imply

$$c(R) \leq c(9/20) < \frac{30220}{65879} < \frac{23}{50} \quad (1/3 \leq R \leq 9/20).$$

For $7/20 \leq R \leq 2/5$ and $1/4 \leq s \leq 7/20$, choose $\gamma = 1/40$. Lemma E.3(a) gives

$$B_R + \gamma(1 + R/2) < \frac{969}{1000} + \frac{3}{100} = \frac{999}{1000}.$$

Consequently $J < \frac{999}{1000}\overline{A}(R) - L < 4\pi$. For $7/20 \leq R \leq 9/20$, $1/4 \leq s \leq 3/10$, choose $\gamma = 0$. Lemma E.3(b) gives

$$J < \frac{1999}{2000}\overline{A}(R) - L < 4\pi.$$

These are bounds for the original three-mode height distribution; no product certificate is used.

E.2.3. *The exact fourth-moment bound.* Let $1/2 \leq R \leq R_*$ for the moment, and retain the two-cosine random variable $Q = a\cos u + b\cos w$ with $a^2 = R\alpha^2$ and $b^2 = (1-R)(1-\alpha^2)$. Its odd moments vanish and

$$\mathbb{E}Q^2 = \frac{a^2 + b^2}{2}, \qquad \mathbb{E}Q^4 = \frac{3}{8}(a^4 + b^4) + \frac{3}{2}a^2b^2. \tag{75}$$

Maximising the quartic expression in $x = \alpha^2 \in [0,1]$ gives, throughout $9/20 \leq R \leq R_*$,

$$\mathbb{E}Q^4 \leq M_4(R) := \begin{cases} \dfrac{9R^2(1-R)^2}{8(6R(1-R)-1)}, & 9/20 \leq R \leq 2/3, \\ \dfrac{3R^2}{8}, & 2/3 \leq R \leq R_*. \end{cases} \tag{76}$$

Indeed $\mathbb{E}Q^4$ is quadratic in x, with coefficient $\frac{3}{8}(6R^2 - 6R + 1)$ and vertex $x = (R-1)(3R-1)/(6R^2-6R+1)$, which lies in $[0,1]$ up to $R = 2/3$; thereafter the maximum occurs at $x = 1$. Also $\mathbb{E}Q^2 \leq (1-R)/2$ when $R \leq 1/2$ and $\mathbb{E}Q^2 \leq R/2$ when $R \geq 1/2$.

Lemma E.4 (Two-cosine rational inequalities)**.** *For $4/17 \leq t \leq 30/109$ the following strict inequalities hold:*

$$h_0 + \frac{1-R}{2}h_2 + M_4(R)h_4 + \frac{1}{200}\left(1 + \frac{1-R}{2}\right) < 1 + \frac{u}{2} + \frac{3u^2}{8}, \tag{77}$$

$$h_0 + \frac{R}{2}h_2 + M_4(R)h_4 + \gamma(R)\left(1 + \frac{R}{2}\right) < 1 + \frac{u}{2} + \frac{3u^2}{8}. \tag{78}$$

The first inequality holds for $9/20 \leq R \leq 1/2$, and the second for $1/2 \leq R \leq R_*$; here $u = \frac{9}{4}(R - \frac{1}{3})^2$. After multiplying by $D(t)$ and, for $R \leq 2/3$, by the positive denominator $6R(1-R) - 1$, these become rational polynomial positivity statements. Their tensor Bernstein coefficients have the following strict rational lower bounds:

R-interval	*Bidegree* (t, R)	*Least coefficient* $>$
$[9/20, 1/2]$	$(7, 6)$	2
$[1/2, 2/3]$	$(7, 6)$	4
$[2/3, R_*]$	$(7, 4)$	12

All three comparisons use the full t-interval $[4/17, 30/109]$ *and the full corresponding R-interval, with no subdivision. They are determined solely by* (72) *and* (70).

E.2.4. *Quartic two-cosine bounds for larger weights.* Since

$$\frac{A_{\mathrm{eq}}}{\overline{A}(R)} = (1-u)^{-1/2} \geq 1 + \frac{u}{2} + \frac{3u^2}{8}, \qquad u = \frac{9}{4}\left(R - \frac{1}{3}\right)^2 < 1,$$

Lemma E.4 implies the required strict area comparison.

For $9/20 \leq R \leq 1/2$, the truncation threshold satisfies $c(R) < 47/100$. Indeed c is increasing, $\sqrt{5} > 223/100$ and the bounds on $\sqrt{3}, \pi$ above give

$$c(1/2) < \frac{1511}{2915}\frac{200}{223} < \frac{47}{100}.$$

Thus Lemma E.3(c), with $\gamma = 1/200$, ensures that $H_t(h) + \gamma(1-h)^2 - c(R) \geq 0$ everywhere.

For $1/2 \leq R \leq R_*$, $c(R)$ is convex: it is a positive multiple of $(1 + 2R - 3R^2)^{-1/2}$, whose second derivative is strictly positive. Its endpoint bounds are

$$c(1/2) < 47/100, \qquad c(R_*) < \frac{1511}{2915}\frac{8}{7} < \frac{47}{100} + \frac{R_* - 1/2}{2};$$

the second follows because $(1 - R_*)(1 + 3R_*) > 49/64$. Convexity therefore gives $c(R) < c_{\mathrm{lin}}(R)$ throughout. Lemma E.3(d) proves that $H_t + \gamma(R)(1 - h)^2 - c(R) > 0$ everywhere.

For either range, by the vanishing of the odd moments in (75), the positivity of h_2, h_4, and the pointwise bounds just proved,

$$\begin{aligned}\mathcal{P}(R, s, \alpha) &\leq \overline{A}(R)\left[\mathbb{E}H_t(Q) + \gamma(1 + \mathbb{E}Q^2) - c(R)\right] \\ &\leq \overline{A}(R)\left[h_0 + h_2\, V_2(R) + h_4 M_4(R) + \gamma(1 + V_2(R))\right] - L < 4\pi,\end{aligned}$$

where $V_2(R) = (1 - R)/2$ for $R \leq 1/2$ and $R/2$ for $R \geq 1/2$. The final strict inequality uses Lemma E.4. The product-majorant reduction then yields $J(r, s, p) \leq \sup_\alpha \mathcal{P}(R, s, \alpha) < 4\pi$. Together with the low-weight ranges, this proves Theorem E.1.

Size of the quartic gaps. The gaps certified in the quartic strips are explicit. The bounds above give $J < \frac{999}{1000}\overline{A}(R) - L$ for $R \leq 2/5$, $s \leq 7/20$, and $J < \frac{1999}{2000}\overline{A}(R) - L$ for $R \leq 9/20$, $s \leq 3/10$, that is, at least $A_{\mathrm{eq}}/1000$ and $A_{\mathrm{eq}}/2000$ below 4π, about 0.18% and 0.09% of 4π. They are small because the truncated area is close to 4π near the equality configuration $R = 1/3$, $s = 0$ of Theorem 2.2: for orientation only, and without use in the proof, a floating-point evaluation of the product majorant gives $\sup \mathcal{P} \approx 12.40$ on the

first strip of Theorem E.1 and $\sup \mathcal{P} \approx 12.45$ on the second, about 1% below $4\pi \approx 12.566$. All comparisons are exact rational inequalities, so the size of the gaps affects neither their validity nor their reproducibility.

E.3. **Higher-order two-cosine bounds.** Retain Q, t, f_t, $H_{V,t}$, and M_{2j} from Section E.1. Write $H_{V,t}(q) = \sum_{j=0}^{2k} h_{V,j}(t) q^j$ and set

$$P_V(t) = (1-2t) \prod_{v \in V} (1-2tv)^2, \qquad E_V(t) = P_V(t)^2. \tag{79}$$

Then $E_V(t) > 0$ and $E_V(t) h_{V,j}(t)$ is in $\mathbb{Q}[t]$. Let $u(R) = \frac{9}{4}(R - \frac{1}{3})^2$ and

$$B_K(R) = \sum_{j=0}^{K} \binom{2j}{j} 4^{-j} u(R)^j \le (1-u(R))^{-1/2} = \frac{A_{\mathrm{eq}}}{\overline{A}(R)}. \tag{80}$$

for an integer truncation order $K \ge 0$, chosen independently of $k = |V|$. If $\hat{c}(R) \ge c(R) := L/\overline{A}(R)$ and $\gamma(t,R) \ge 0$, it suffices to prove on the stated parameter boxes

$$S(t,R,q) := H_{V,t}(q) + \gamma(t,R)(1-q)^2 - \hat{c}(R) > 0, \tag{81}$$

$$T(t,R,x) := B_K(R) - \sum_{j=0}^{k} h_{V,2j}(t) M_{2j}(R,x) - \gamma(t,R)(1 + M_2(R,x)) > 0. \tag{82}$$

These inequalities are required for all $-1 \le q \le 1$ and $0 \le x \le 1$.

Indeed Lemma E.2, $\gamma \ge 0$, and $S > 0$ imply

$$\big(f_t(q) - c(R)\big)_+ \le H_{V,t}(q) + \gamma(1-q)^2 - c(R).$$

The exact even moments then give

$$\begin{aligned} \mathcal{P}(R,s,\alpha) &\le \overline{A}(R)\Big(\sum_{j=0}^{k} h_{V,2j}(t) M_{2j}(R,\alpha^2) + \gamma(1+M_2) - c(R) \Big) \\ &< \overline{A}(R) B_K(R) - L \le A_{\mathrm{eq}} - L = 4\pi. \end{aligned}$$

The polynomials checked below are $E_V S$ and $E_V T$; all comparisons are over $\mathbb{Q}$.

E.3.1. *Decic Hermite comparisons.* Take

$$V_{10} = \left\{ -\tfrac{4}{5}, -\tfrac{2}{5}, 0, \tfrac{2}{5}, \tfrac{4}{5} \right\}, \qquad \frac{30}{109} \le t \le \frac{180}{481} \quad \left(\frac{3}{10} \le s \le \frac{9}{20} \right).$$

Set $d = t - 30/109$, $e = R - 9/20$, and define

$$\gamma_{10} = \frac{13}{250} + \frac{2}{5} d + \frac{12}{125} e + \frac{21}{20} de + \frac{11}{4} d^2, \qquad \hat{c}_{10}(R) = \frac{9}{20} + \frac{R - 7/20}{3}. \tag{83}$$

Then $\gamma_{10} \ge 0$, and $\hat{c}_{10}(R) \ge c(R)$. To justify the latter inequality, observe that

$$c(R) = 2\left(\frac{1}{\sqrt{3}} - \frac{1}{\pi} \right) \left[(1-R)(1+3R) \right]^{-1/2}$$

is convex on $[9/20, R_*]$. Its endpoint values are bounded strictly by the affine function $\hat{c}_{10}$ using

$$\sqrt{3} > \frac{265}{153}, \quad \pi < \frac{22}{7}, \quad \sqrt{517} > \frac{227}{10}, \quad \sqrt{\frac{5230625}{6558721}} > \frac{89}{100}.$$

In particular $c(9/20) < 60440/132341 < 29/60$ and $c(R_*) < 30220/51887 < 1499/2561$. The relevant numerator polynomials are

$$S_{10}^* = E_{V_{10}} S, \qquad T_{10}^* = E_{V_{10}} T \quad \text{with } \hat{c} = \hat{c}_{10},\ \gamma = \gamma_{10},\ k = 5,\ K = 4.$$

Their degrees in (t, R, q) and (t, R, x) are at most $(21, 1, 10)$ and $(21, 8, 5)$ respectively. The exact rational calculations specified in Section E.3.3 give $S_{10}^*, T_{10}^* > 0$.

E.3.2. *Degree-twelve Hermite comparisons.* Take

$$V_{12} = \left\{-\tfrac{9}{10}, -\tfrac{3}{5}, -\tfrac{3}{10}, \tfrac{3}{10}, \tfrac{3}{5}, \tfrac{9}{10}\right\}, \qquad \frac{180}{481} \le t \le \frac{2}{5} \quad \left(\frac{9}{20} \le s \le \frac{1}{2}\right).$$

With $d = t - 180/481$ and $e = R - 9/20$ put

$$\gamma_{12} = \frac{101}{1000} + d + \frac{6}{25}e + 2de + 10d^2. \tag{84}$$

For the truncation level choose the continuous piecewise affine function

$$\hat{c}_{12}(R) = \begin{cases} \dfrac{457}{1000} + \dfrac{34}{150}\left(R - \dfrac{9}{20}\right), & \tfrac{9}{20} \le R \le \tfrac{3}{5}, \\[2ex] \dfrac{491}{1000} + \dfrac{\frac{583}{1000} - \frac{491}{1000}}{R_* - \frac{3}{5}}\left(R - \dfrac{3}{5}\right), & \tfrac{3}{5} \le R \le R_*. \end{cases} \tag{85}$$

The endpoint rational estimates

$$c(9/20) < 457/1000, \qquad c(3/5) < 491/1000, \qquad c(R_*) < 583/1000$$

follow from the bounds of the preceding section and $\sqrt{28/25} > 1057/1000$. Convexity of c gives $c(R) < \hat{c}_{12}(R)$ throughout the two intervals. Now let

$$S_{12}^* = E_{V_{12}} S, \qquad T_{12}^* = E_{V_{12}} T, \quad \hat{c} = \hat{c}_{12},\ \gamma = \gamma_{12},\ k = K = 6.$$

These are polynomial on each affine branch. The degrees are at most $(28, 1, 12)$ in (t, R, q) and $(28, 12, 6)$ in (t, R, x). Their positivity on the stated domains follows from the explicit finite comparisons below.

E.3.3. *Rational positivity certificates for the higher-order product bounds.* For a polynomial $F(U_1, \dots, U_m) = \sum_{\boldsymbol{\ell}} a_{\boldsymbol{\ell}} U^{\boldsymbol{\ell}}$ of multidegree at most $\boldsymbol{n}$, its tensor Bernstein coefficients are

$$\beta_{\boldsymbol{i}} = \sum_{\boldsymbol{\ell} \le \boldsymbol{i}} a_{\boldsymbol{\ell}} \prod_{j=1}^{m} \frac{\binom{i_j}{\ell_j}}{\binom{n_j}{\ell_j}}. \tag{86}$$

On $[0,1]^m$ one has $F \ge \min \beta_{\boldsymbol{i}}$. For any rational box we apply the affine substitution to $[0,1]^m$. Every entry in the following table is a strict lower bound for *every* Bernstein coefficient of the specified polynomial on the specified boxes:

Polynomial	Boxes / intervals	Strict lower bound
S_{10}^*	$R = 9/20, R_*$; $q \in [-1,-1/2], [-1/2,0], [0,1]$; full t-strip	10^{-5}
T_{10}^*	$R \in [9/20, R_m], [R_m, R_*]$; $x \in [0,1/2], [1/2,1]$; full t-strip	10^{-5}
S_{12}^*	$R = 9/20, R_*$; $q \in [-1,-1/2], [-1/2,-1/4], [-1/4,0], [0,1]$; full t-strip	10^{-7}
S_{12}^*	$R = 3/5$; $q \in [-1,-1/2], [-1/2,0], [0,1]$; full t-strip	10^{-7}
T_{12}^*	$(R,x) \in [9/20, R_*] \times [0,1/2]$, or $[9/20, R_m] \times [1/2,1]$, or $[R_m, R_*] \times [1/2,1]$; full t-strip	10^{-7}

where $R_m = (9/20 + R_*)/2 = 61769/102440$. Because S_{10}^* is affine in R, positivity at the two stated endpoints proves it throughout the whole R-interval. Likewise, on each branch of (85), S_{12}^* is affine in R; the three endpoint checks suffice.

Scale of the listed bounds. The bounds in the table refer to the cleared polynomials $E_V S$ and $E_V T$, and the factor E_V is small on these strips: $7\cdot10^{-3} < E_{V_{10}}(t) < 8\cdot10^{-2}$ on the decic strip and $5\cdot10^{-4} < E_{V_{12}}(t) < 2\cdot10^{-3}$ on the degree-twelve strip. Rounded down, the exact least coefficients are $2.47 \cdot 10^{-5}$ for S_{10}^*, $6.12 \cdot 10^{-5}$ for T_{10}^*, $8.28 \cdot 10^{-7}$ for S_{12}^* and $1.72 \cdot 10^{-6}$ for T_{12}^*. For orientation only, and without use in the proof, a floating-point evaluation gives $\min S \approx 7.0 \cdot 10^{-3}$ and $\min T \approx 1.4 \cdot 10^{-2}$ on the decic strip, and $\min S \approx 1.4 \cdot 10^{-3}$ and $\min T \approx 9.7 \cdot 10^{-3}$ on the degree-twelve strip. The resulting upper bounds for $\mathcal{P}$ lie below 4π by at least 2.5% and 1.4% of 4π, respectively, whereas $\sup \mathcal{P} \approx 10.96$ on the whole region $9/20 \le R \le R_*$, $3/10 \le s \le 1/2$. The smallest relative margin occurs in the pointwise condition $S > 0$: the coefficient γ is taken close to its least admissible value, because it also enters T through the term $\gamma(1 + M_2)$. All comparisons are exact rational inequalities, so the size of these numbers affects neither their validity nor their reproducibility.

Each polynomial is explicitly determined by (68)–(80), (83) and (84)–(85); there is no unspecified polynomial or numerical extremum. In particular, the listed rational boxes comprise six pointwise and four moment boxes for the decic estimate, and eleven pointwise and three moment boxes for the degree-twelve estimate. Formula (86) proves all required signs. The supplementary programs `verify_exact_rational.py` (degrees ten and twelve) and `verify_quartic_product_rational_only.py` (the quartic comparisons of Section E.2) reconstruct the interpolants and coefficients directly from these formulae, evaluating every coefficient in $\mathbb{Q}$ using Python's standard-library integer arithmetic and `fractions.Fraction`. They require no symbolic algebra package, interval arithmetic package, floating-point operations or numerical optimizer, and they are run by the rational checks of the reproducer (Appendix D). A second, independent program, `independent_product_strip_check.py`, builds the same polynomials with SymPy from

the Newton form of the quartic interpolant and from the closed formula (68), checks the Hermite interpolation conditions, and recomputes all Bernstein coefficients with a separate routine; it confirms every bound in the tables above, the exact minima quoted in this appendix and the stated range of E_V. This check is a finite exact rational-algebraic certificate. All asserted Bernstein coefficient inequalities are verified in exact rational arithmetic by the programs described above, and their execution records are part of the supplement (Appendix D).

Statements and Declarations

Conflict of interest. The author declares no conflict of interest.

Data and code availability. No external experimental or observational datasets were used in this study. All computational certificates, verification scripts, and supporting files required for the computer-assisted parts of the proof are included in the supplementary archive `Pigazzini_KLO_Supplement` accompanying this article, which is also distributed with the arXiv version of the article as ancillary files (see also Zenodo: https://doi.org/10.5281/zenodo.24473074). The archive contains the exact rational certificates, the validated numerical verification programs, reproducibility instructions, reference logs and SHA-256 file checksums. The computational procedures and software requirements are documented in Appendix D.

Funding. The author received no funding from any organization for the submitted work.

Use of AI tools. AI assistants (Claude, Anthropic; GPT, OpenAI) were used for the computer-assisted part of this work: to write and test the verification programs, to generate the certificates and to draft parts of the appendices that describe them. They were also used for help with editing and revising the text. The mathematical results, the strategy of the proof and the analytic arguments in the body of the paper are the author's. The validity of the computer-assisted steps does not depend on these tools: the certificates are checked by the open-source programs described in Appendix D, in exact rational or validated arithmetic, and each of the two main computer-assisted steps is verified by two independent programs. The author takes full responsibility for the content of this article.

References

[1] R. L. Bryant, *On the conformal volume of* 2*-tori*, preprint, arXiv:1507.01485 (2015); the second version (2025) adds the proof of the value stated in Remark 5.

[2] B. Colbois and A. El Soufi, *Extremal eigenvalues of the Laplacian in a conformal class of metrics: the 'conformal spectrum'*, Ann. Global Anal. Geom. **24** (2003), no. 4, 337–349.

[3] M. Eddaoudi and A. Girouard, *Upper bounds for the second nonzero eigenvalue of the Laplacian via folding and conformal volume*, preprint, arXiv:2501.08761 (2025).

[4] The FLINT team, *FLINT: Fast Library for Number Theory*, version 3.6.0, https://flintlib.org.
[5] A. Girouard, N. Nadirashvili, and I. Polterovich, *Maximization of the second positive Neumann eigenvalue for planar domains*, J. Differential Geom. **83** (2009), no. 3, 637–661.
[6] C. R. Harris et al., *Array programming with NumPy*, Nature **585** (2020), 357–362; doi:10.1038/s41586-020-2649-2.
[7] J. Hersch, *Quatre propriétés isopérimétriques de membranes sphériques homogènes*, C. R. Acad. Sci. Paris Sér. A–B **270** (1970), A1645–A1648.
[8] F. Johansson, *Arb: efficient arbitrary-precision midpoint-radius interval arithmetic*, IEEE Trans. Comput. **66** (2017), no. 8, 1281–1292; doi:10.1109/TC.2017.2690633.
[9] F. Kang, *An improved upper bound for the second eigenvalue on tori*, Differential Geom. Appl. **104** (2026), 102428; doi:10.1016/j.difgeo.2026.102428; arXiv:2506.05846 (statement numbers as in version 3, 2026).
[10] C.-Y. Kao, R. Lai, and B. Osting, *Maximization of Laplace–Beltrami eigenvalues on closed Riemannian surfaces*, ESAIM Control Optim. Calc. Var. **23** (2017), no. 2, 685–720; doi:10.1051/cocv/2016008.
[11] M. Karpukhin, *Index of minimal spheres and isoperimetric eigenvalue inequalities*, Invent. Math. **223** (2021), no. 1, 335–377; doi:10.1007/s00222-020-00992-5.
[12] M. Karpukhin, N. Nadirashvili, A. V. Penskoi, and I. Polterovich, *Conformally maximal metrics for Laplace eigenvalues on surfaces*, Surveys in Differential Geometry **24** (2019), 205–256; doi:10.4310/SDG.2019.v24.n1.a6.
[13] M. Karpukhin, N. Nadirashvili, A. V. Penskoi, and I. Polterovich, *An isoperimetric inequality for Laplace eigenvalues on the sphere*, J. Differential Geom. **118** (2021), no. 2, 313–333; doi:10.4310/jdg/1622743142.
[14] M. Karpukhin and D. Stern, *Min-max harmonic maps and a new characterization of conformal eigenvalues*, J. Eur. Math. Soc. **26** (2024), no. 11, 4071–4129; doi:10.4171/JEMS/1401.
[15] P. Li and S.-T. Yau, *A new conformal invariant and its applications to the Willmore conjecture and the first eigenvalue of compact surfaces*, Invent. Math. **69** (1982), 269–291; doi:10.1007/BF01399507.
[16] A. Meurer et al., *SymPy: symbolic computing in Python*, PeerJ Comput. Sci. **3** (2017), e103; doi:10.7717/peerj-cs.103.
[17] S. Montiel and A. Ros, *Minimal immersions of surfaces by the first eigenfunctions and conformal area*, Invent. Math. **83** (1986), 153–166.
[18] The mpmath development team, *mpmath: a Python library for arbitrary-precision floating-point arithmetic*, version 1.3.0 (2023), https://mpmath.org.
[19] N. Nadirashvili, *Berger's isoperimetric problem and minimal immersions of surfaces*, Geom. Funct. Anal. **6** (1996), no. 5, 877–897; doi:10.1007/BF02246788.
[20] N. Nadirashvili, *Isoperimetric inequality for the second eigenvalue of a sphere*, J. Differential Geom. **61** (2002), no. 2, 335–340; doi:10.4310/jdg/1090351388.
[21] N. Nadirashvili and A. V. Penskoi, *An isoperimetric inequality for the second non-zero eigenvalue of the Laplacian on the projective plane*, Geom. Funct. Anal. **28** (2018), no. 5, 1368–1393; doi:10.1007/s00039-018-0458-7.
[22] R. Petrides, *Existence and regularity of maximal metrics for the first Laplace eigenvalue on surfaces*, Geom. Funct. Anal. **24** (2014), no. 4, 1336–1376; arXiv:1310.4697.
[23] R. Petrides, *Maximization of the second conformal eigenvalue of spheres*, Proc. Amer. Math. Soc. **142** (2014), no. 7, 2385–2394.
[24] python-flint, *Python bindings for FLINT*, version 0.9.0, https://github.com/flintlib/python-flint.